Daytime Raman Lidar measurements

Ilya Serikov

Max Planck Institute for Meteorology, Hamburg

Lidar signal and skylight background

Atmospheric response:

$$P(r) = E_0 f_L Q(r) K \frac{A}{r^2} \frac{c\tau}{2} \beta_\pi(r) \exp\left(-2\int_0^r \alpha(x)\,dx\right)$$

Sky background:

$$P_{BGR} = E_\nu K A \Delta\Omega \Delta\nu f_L \tau$$

Signal to background:

$$\frac{P}{P_{BGR}} \sim \frac{E_0 \beta_\pi}{\Delta\Omega \Delta\nu}$$

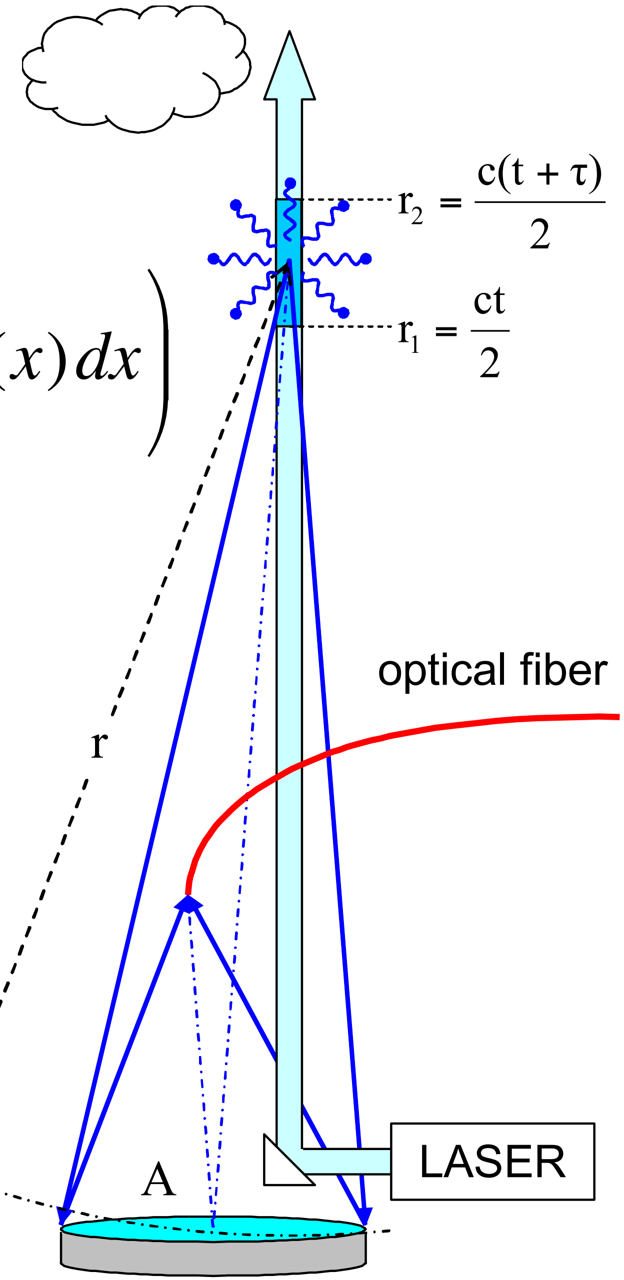

E_0 laser pulse energy

f_L pulse repetition rate

K total throughput

A receiving telescope area

τ time bin length

$Q(r)$ overlap function

E_ν sky brightness density

$\beta_\pi(r)$ backscatter coefficient

$\alpha(r)$ extinction coefficient

$\Delta\nu$ spectral passband

$\Delta\Omega$ solid angle of “field-of-view”

Atmospheric response

$$\beta_\pi = \left[\frac{d\sigma}{d\Omega}\right]_\pi \cdot N$$

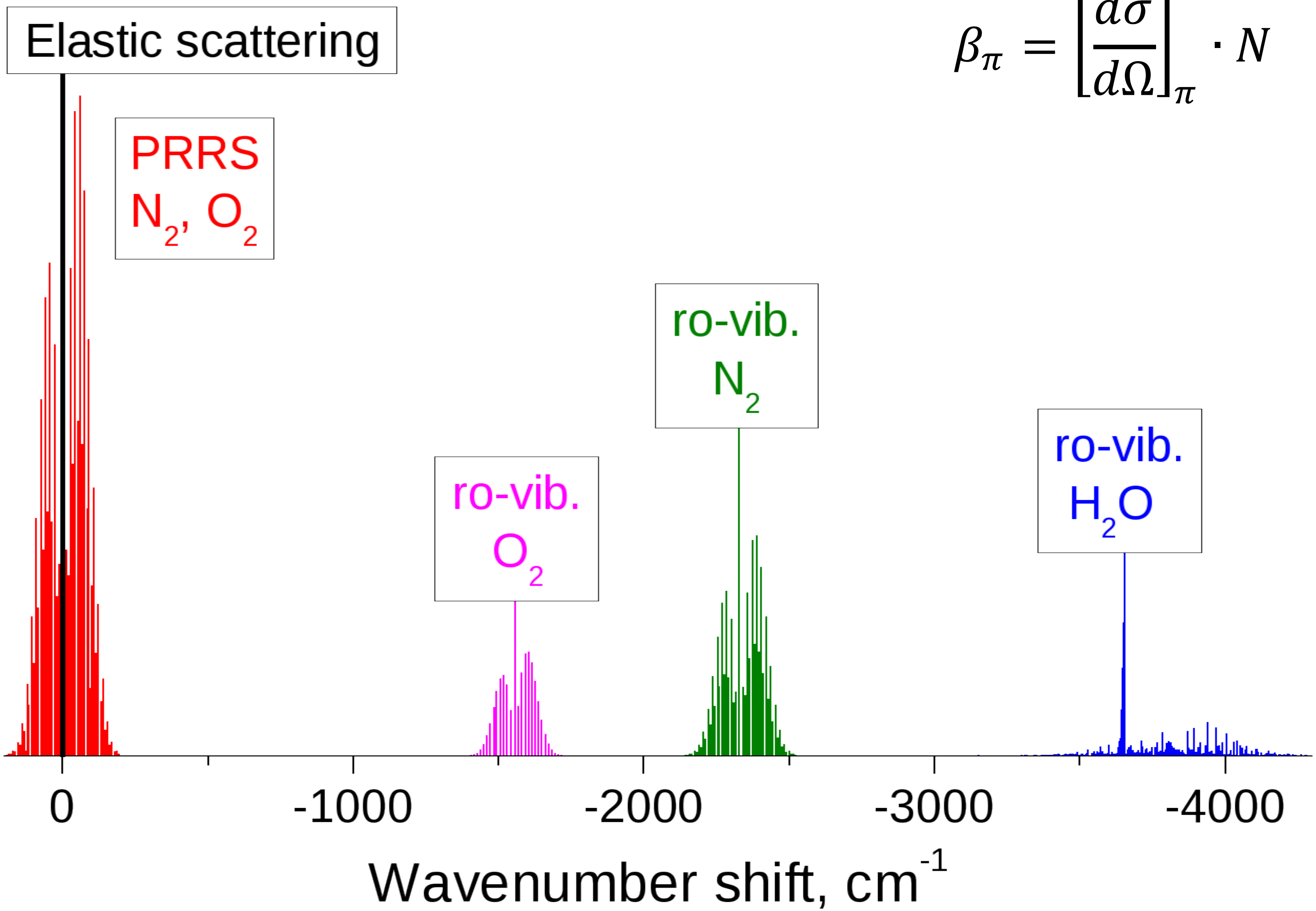

Pure rotational Raman spectra of N_2 and O_2

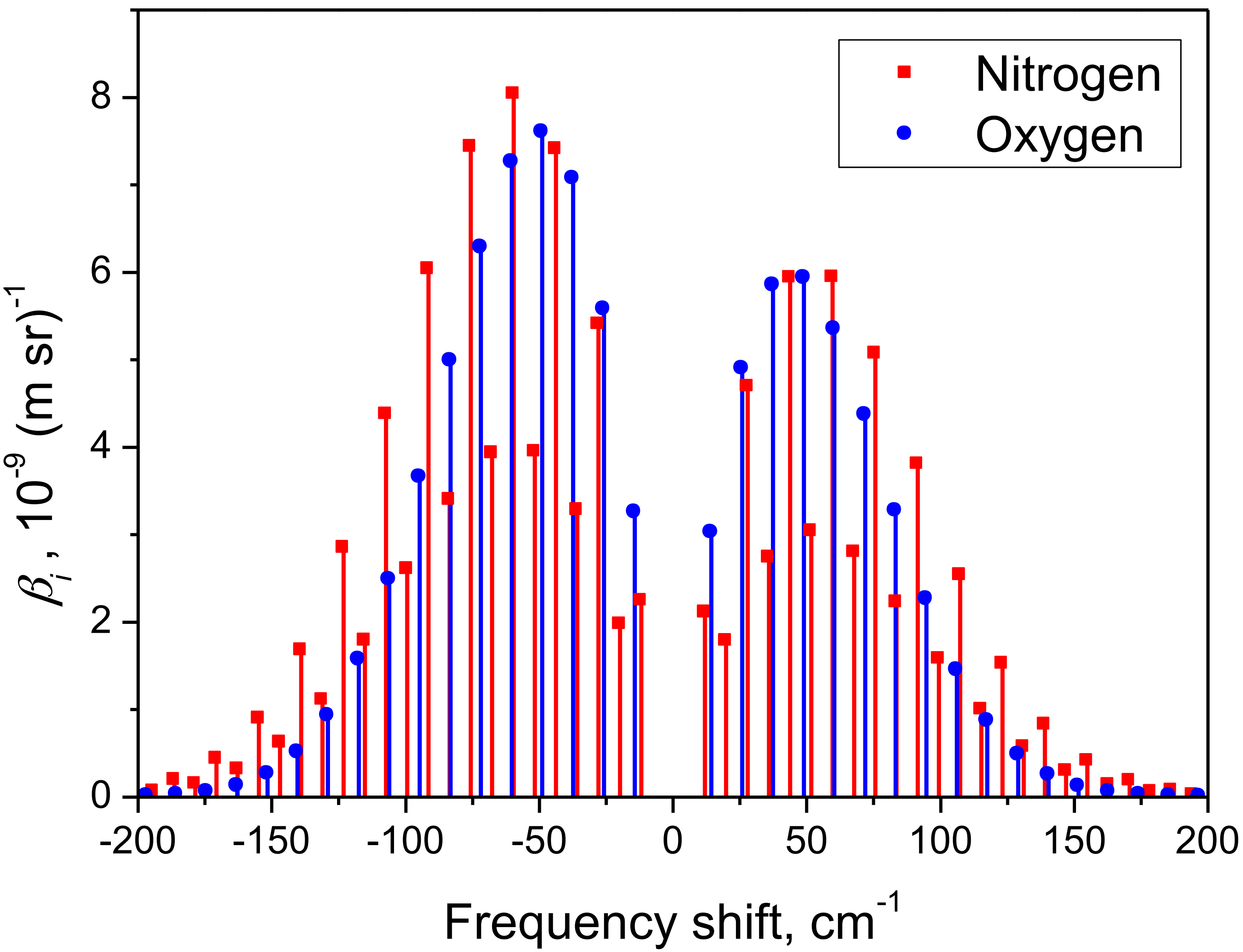

Example for air mixture at 1 atm and 273 K. Excitation at 355 nm.

Scattering efficiency @532nm

$$\frac{\left[\frac{d\sigma}{d\Omega}\right]_{\pi}^{PRRS\ N_2,\ J=6}}{\left[\frac{d\sigma}{d\Omega}\right]_{\pi}^{vib}} \cong 1.9\ @273K$$

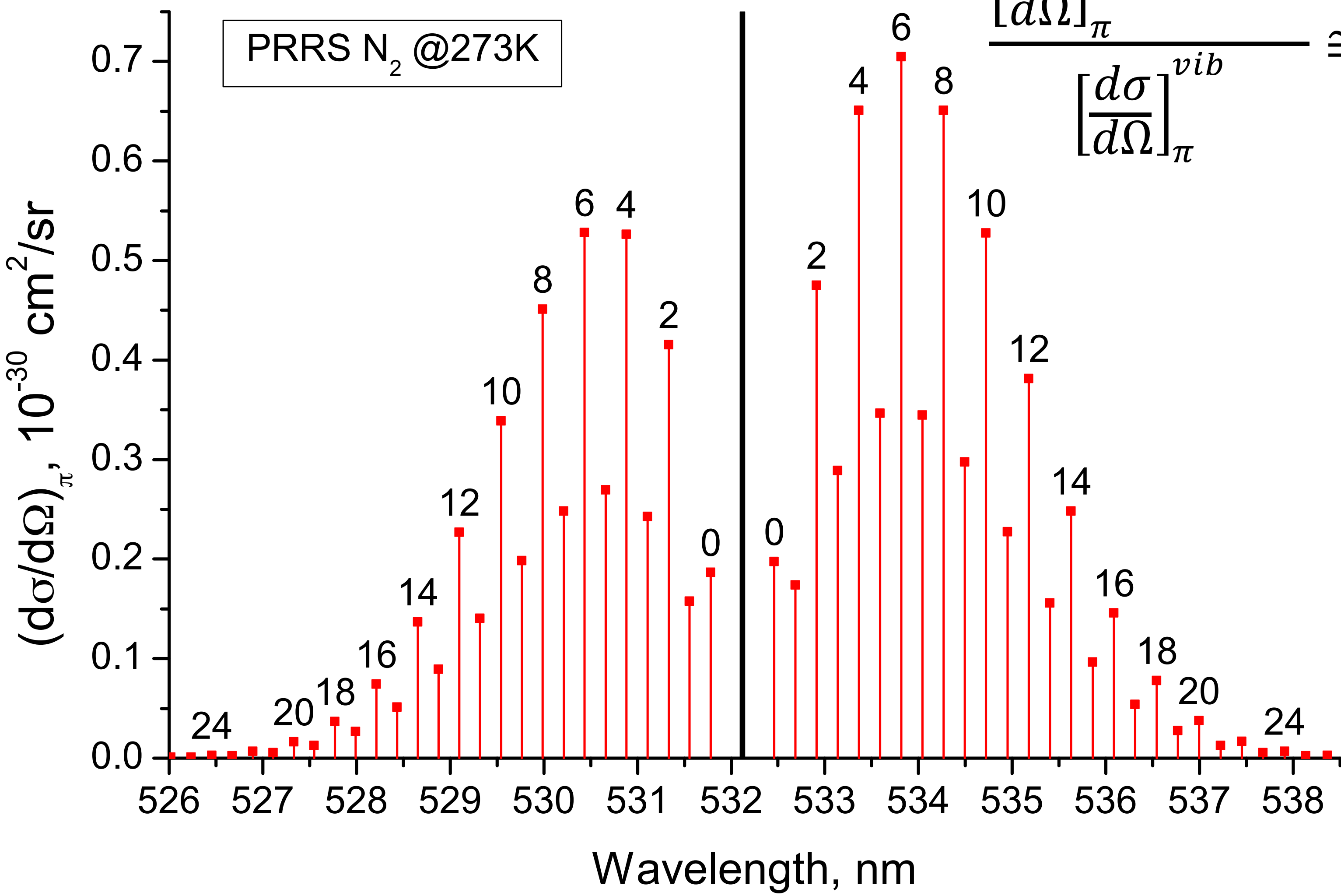

Scattering efficiency

$$\frac{\left[\frac{d\sigma}{d\Omega}\right]_{\pi}^{PRRS\ N_2,\ J=6}}{\left[\frac{d\sigma}{d\Omega}\right]_{\pi}^{vib}} \cong 1.9\ @273K$$

$$N_{lines}^{eff} = \frac{1}{n_{N_2}\left[\frac{d\sigma}{d\Omega}\right]_{\pi}^{vib}}\left(n_{N_2}\sum_{\forall J}^{N_2}\left[\frac{d\sigma}{d\Omega}\right]_{\pi}^{J} + n_{O_2}\sum_{\forall J}^{O_2}\left[\frac{d\sigma}{d\Omega}\right]_{\pi}^{J}\right) \cong 48\ @273K$$

$$\frac{1}{\left[\frac{d\sigma}{d\Omega}\right]_{\pi}^{vib}}\sum_{\forall J}^{N_2}\left[\frac{d\sigma}{d\Omega}\right]_{\pi}^{J} \cong 28\ @273K \qquad \frac{n_{O_2}}{n_{N_2}\left[\frac{d\sigma}{d\Omega}\right]_{\pi}^{vib}}\sum_{\forall J}^{O_2}\left[\frac{d\sigma}{d\Omega}\right]_{\pi}^{J} \cong 20\ @273K$$

PRRS, temperature sensitivity

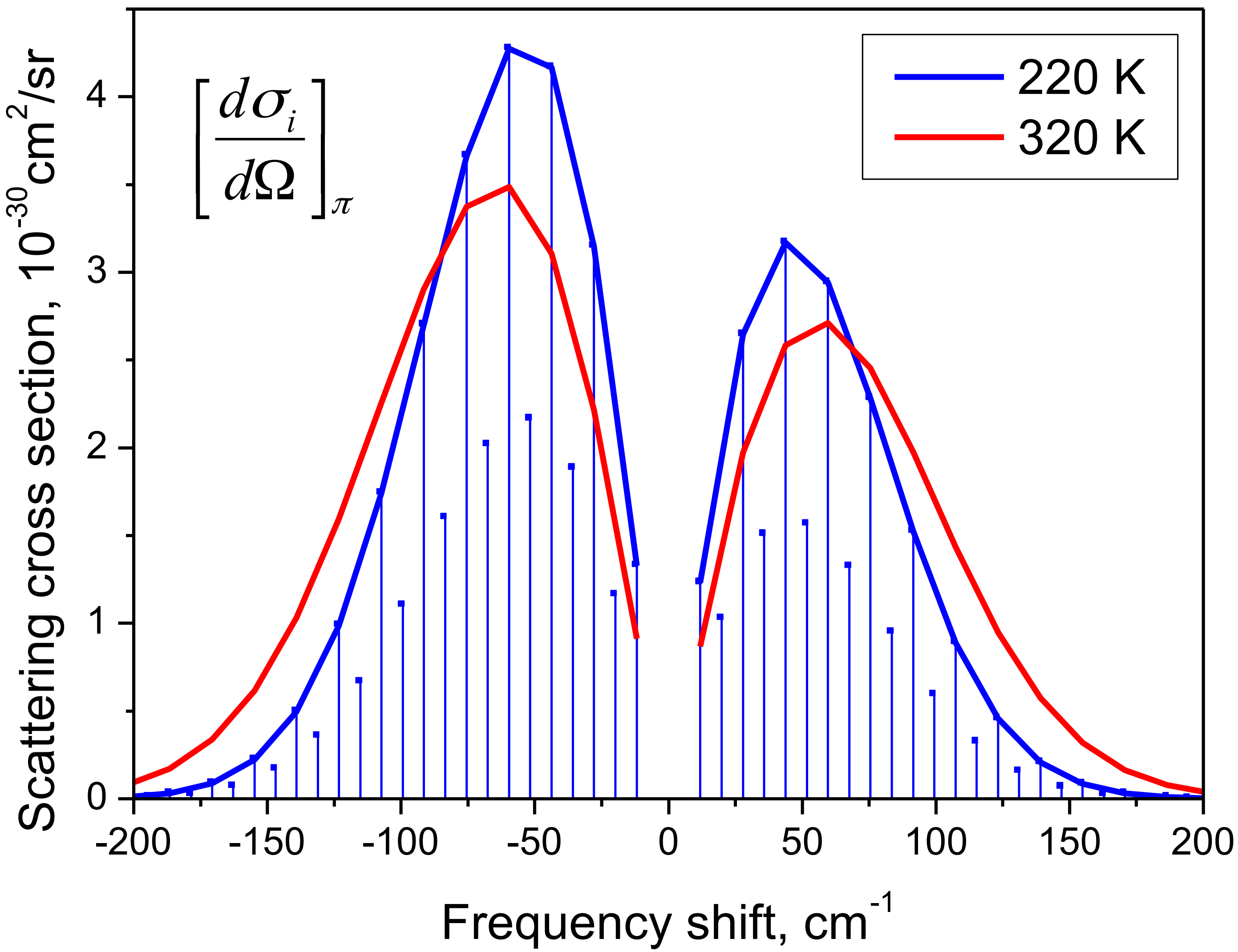

Envelops of PRRS of nitrogen for 220 and 320 K. Excitation at 355 nm.

PRRS, temperature sensitivity

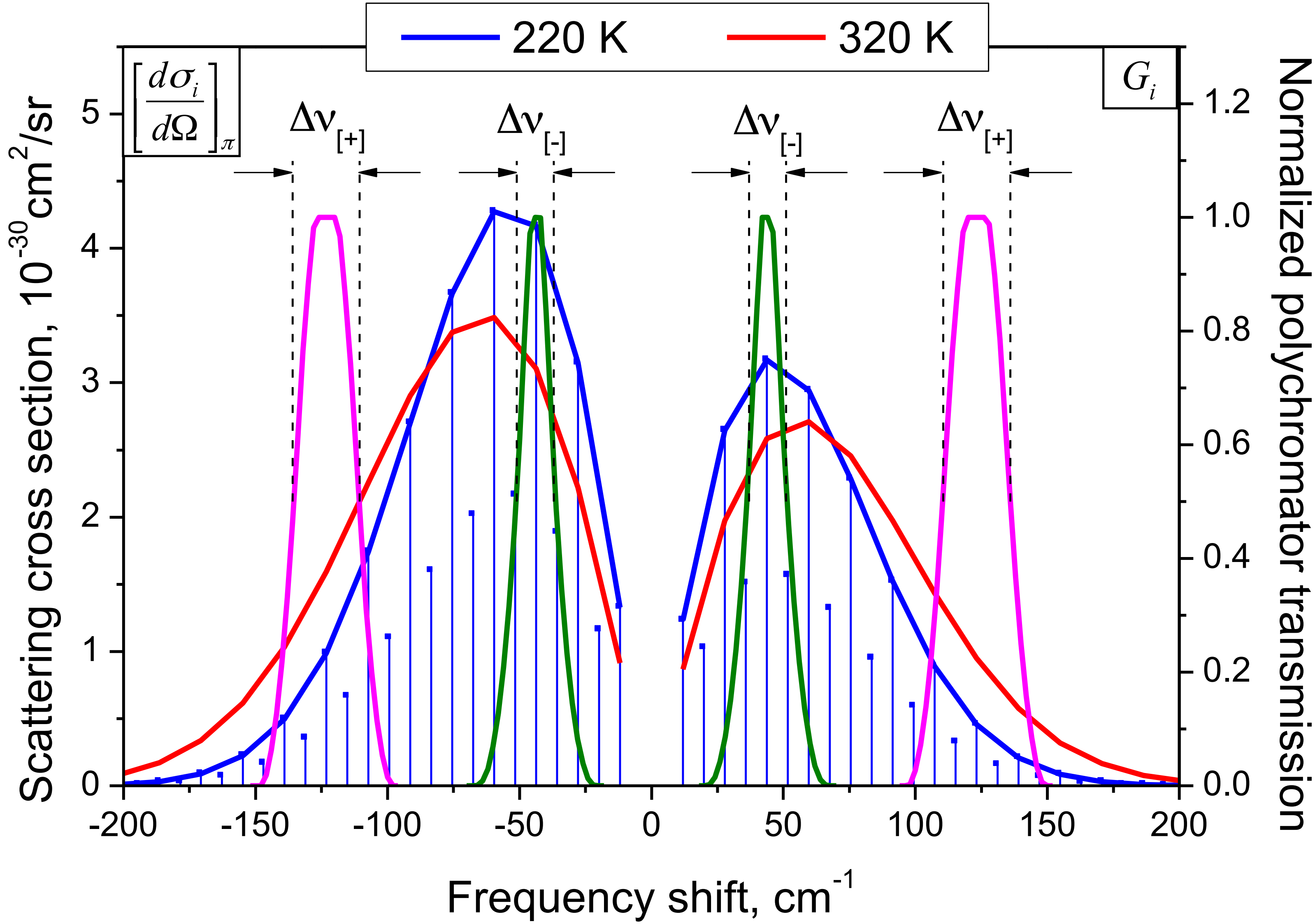

Envelops of PRRS of nitrogen for 220 and 320 K. Excitation at 355 nm.

PRRS signal ratio

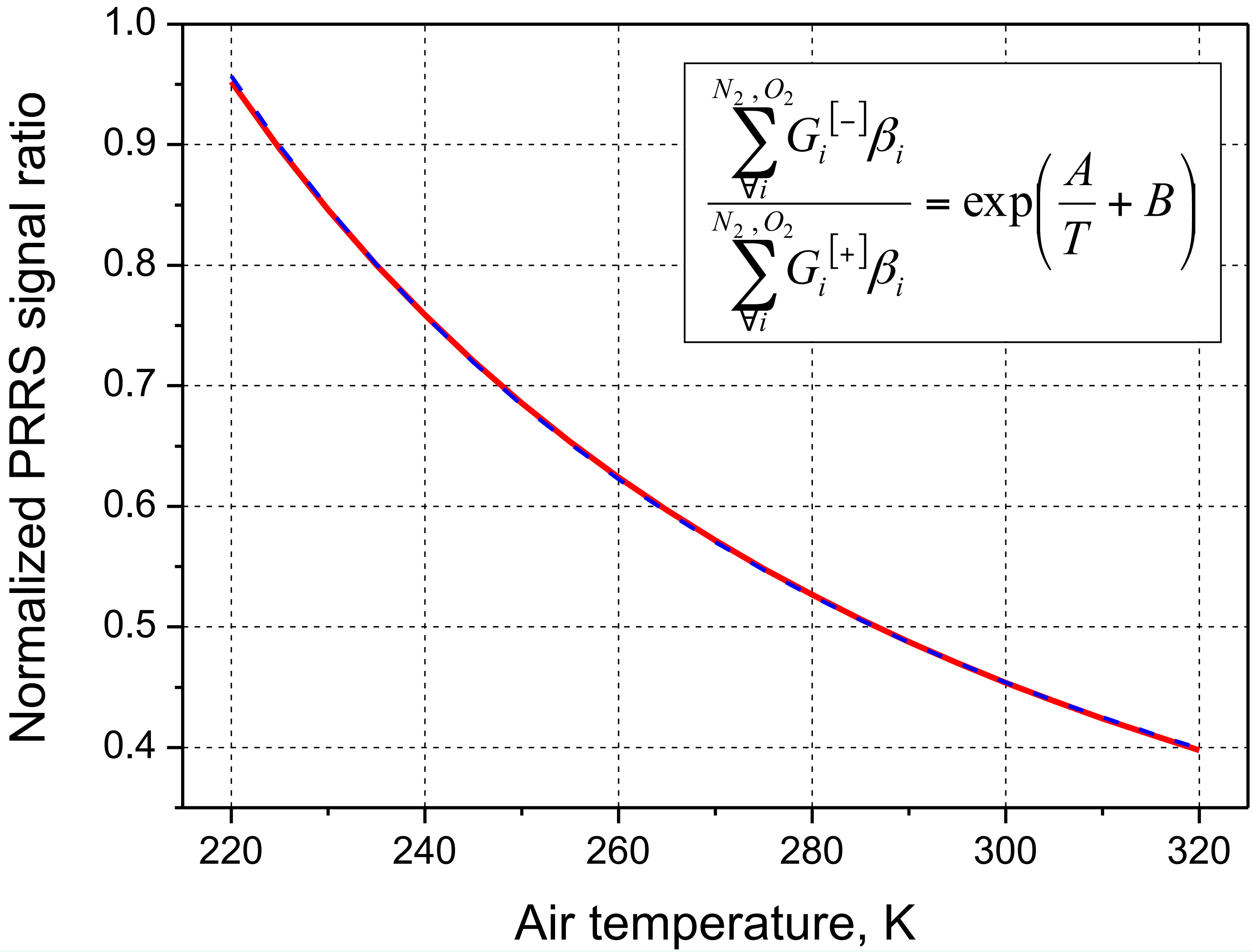

355 nm

Isolating "temperature-insensitive" lines with interference filters

$$N_{lines}^{eff} = \frac{1}{n_{N_2}\left[\frac{d\sigma}{d\Omega}\right]_{\pi}^{vib}} \left(n_{N_2} \sum_{\forall J}^{N_2} G_J \left[\frac{d\sigma}{d\Omega}\right]_{\pi}^{J} + n_{O_2} \sum_{\forall J}^{O_2} G_J \left[\frac{d\sigma}{d\Omega}\right]_{\pi}^{J} \right) \cong 16 \ @273K$$

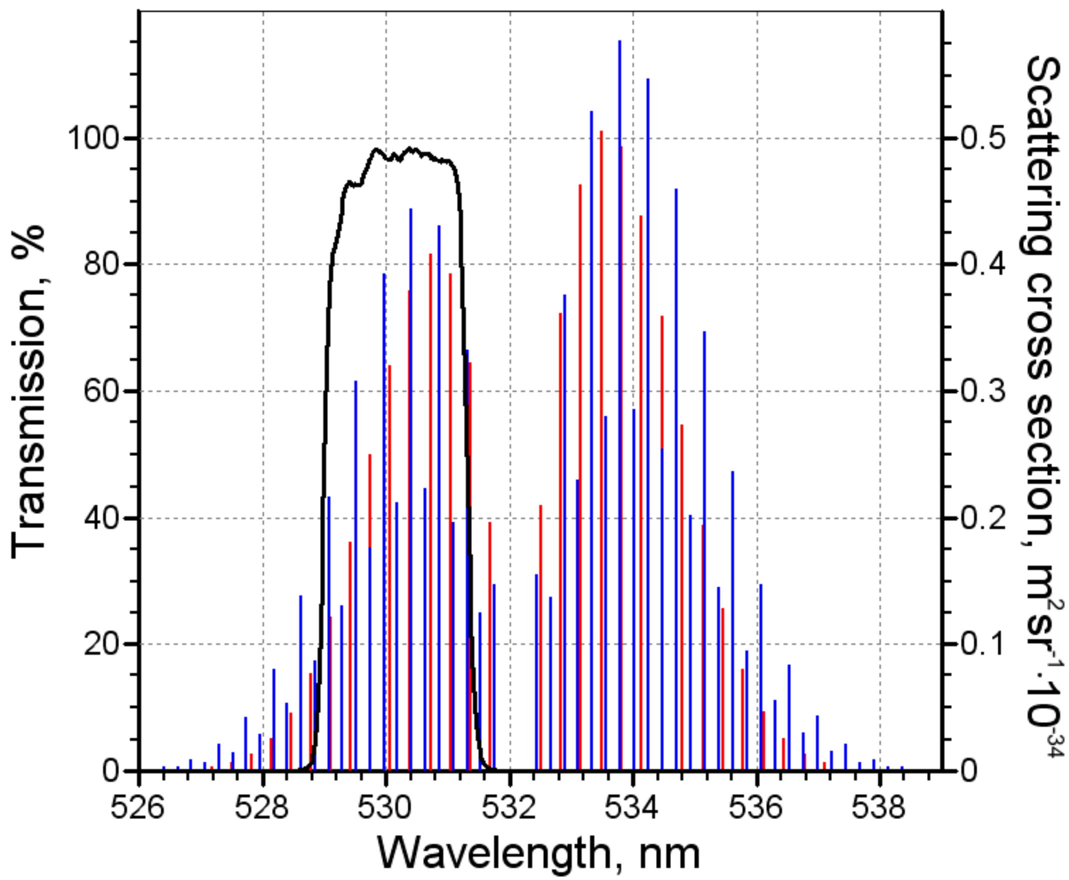

"PRRS of N_2 (blue) and O_2(red) @T=300 K and the interference filter transmission" after Veselovskii et al. "Use of rotational Raman measurements in multiwavelength aerosol lidar for Evaluation of particle backscattering and extinction", Atmos. Meas. Tech., 8, 4111–4122, 2015

Isolating "temperature-insensitive" lines with interference filters

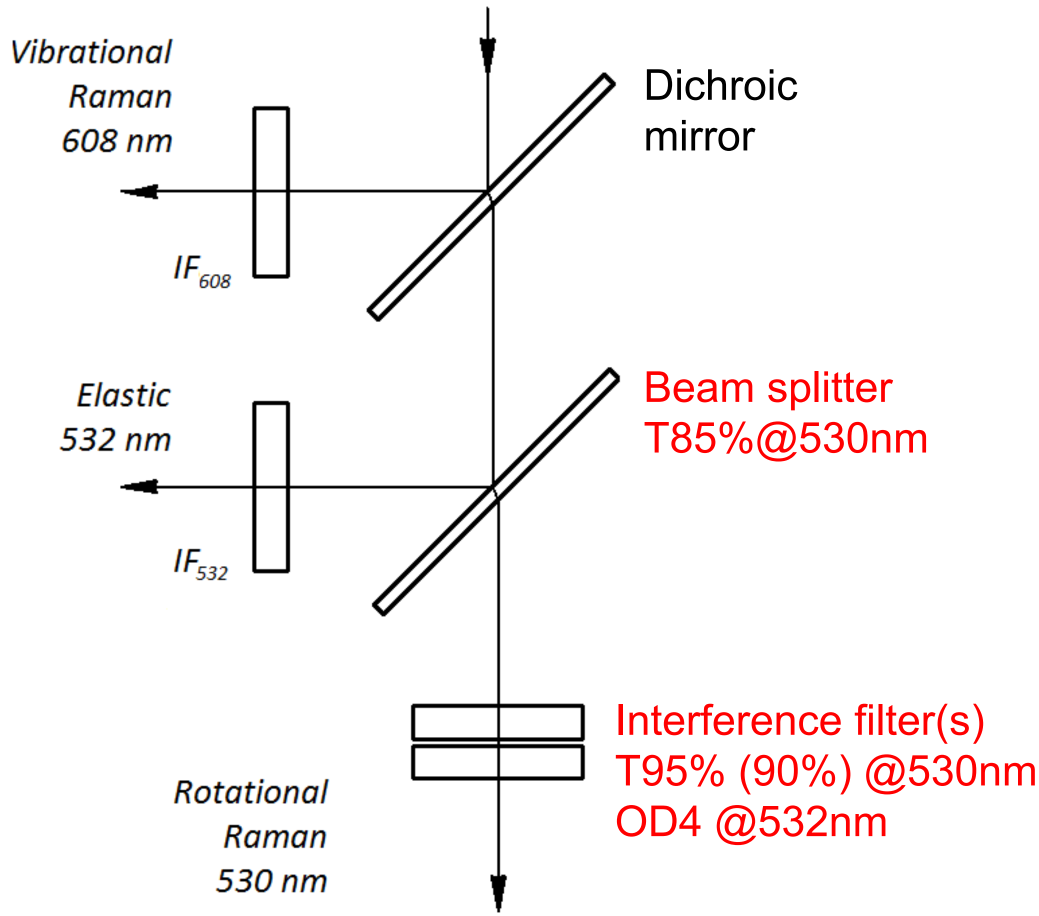

T78% (69%)
OD8@532nm $\longrightarrow$ $N_{lines}^{eff} = 12.4\ (11)$

after Veselovskii et al. "Use of rotational Raman measurements in multiwavelength aerosol lidar for Evaluation of particle backscattering and extinction", Atmos. Meas. Tech., 8, 4111–4122, 2015

Isolating “temperature-sensitive” lines with interference filters

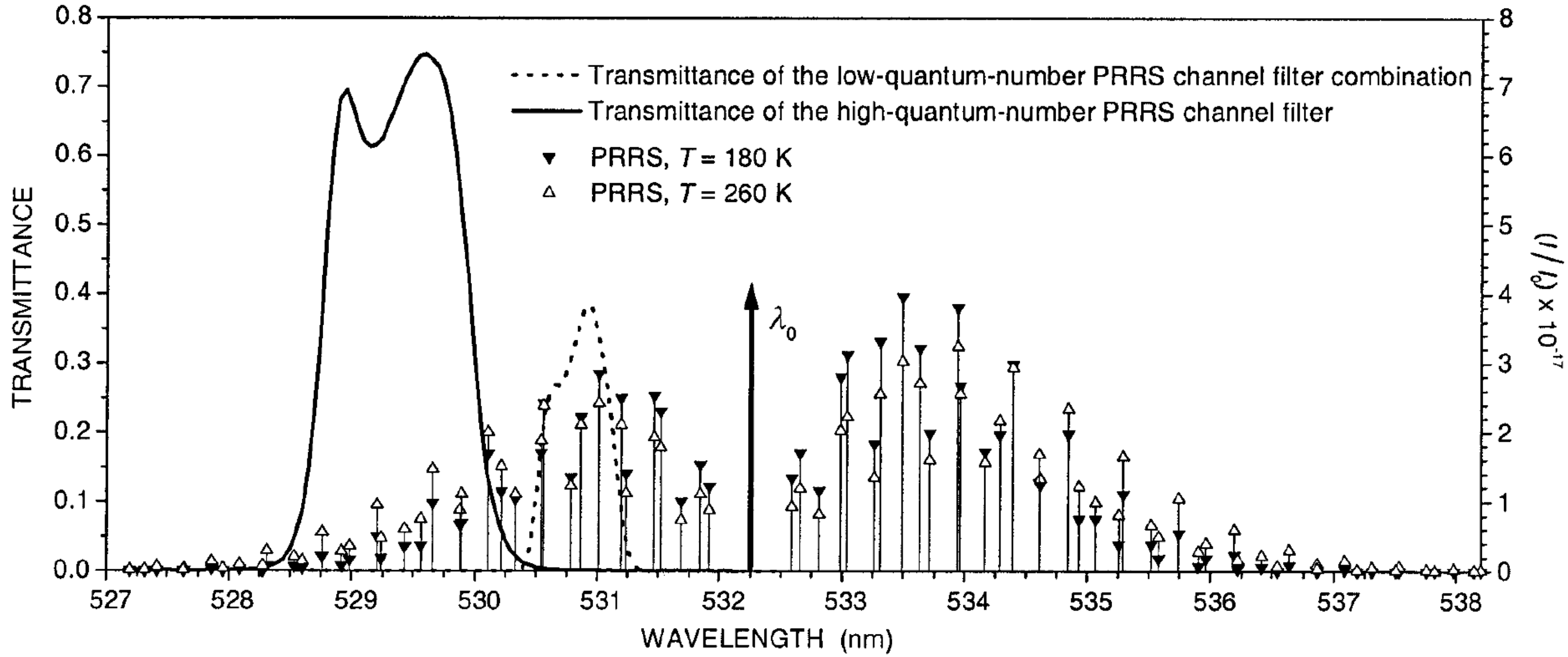

“Scaled intensity of the PRR signal and transmittances of employed interference filters”

after Behrendt and Reichardt, “Atmospheric temperature profiling in the presence of clouds with a pure rotational Raman lidar by use of an interference-filter-based polychromator” App. Opt., Vol. 39, No. 9, 1372-1378, 2000

Isolating "temperature-sensitive" lines with interference filters

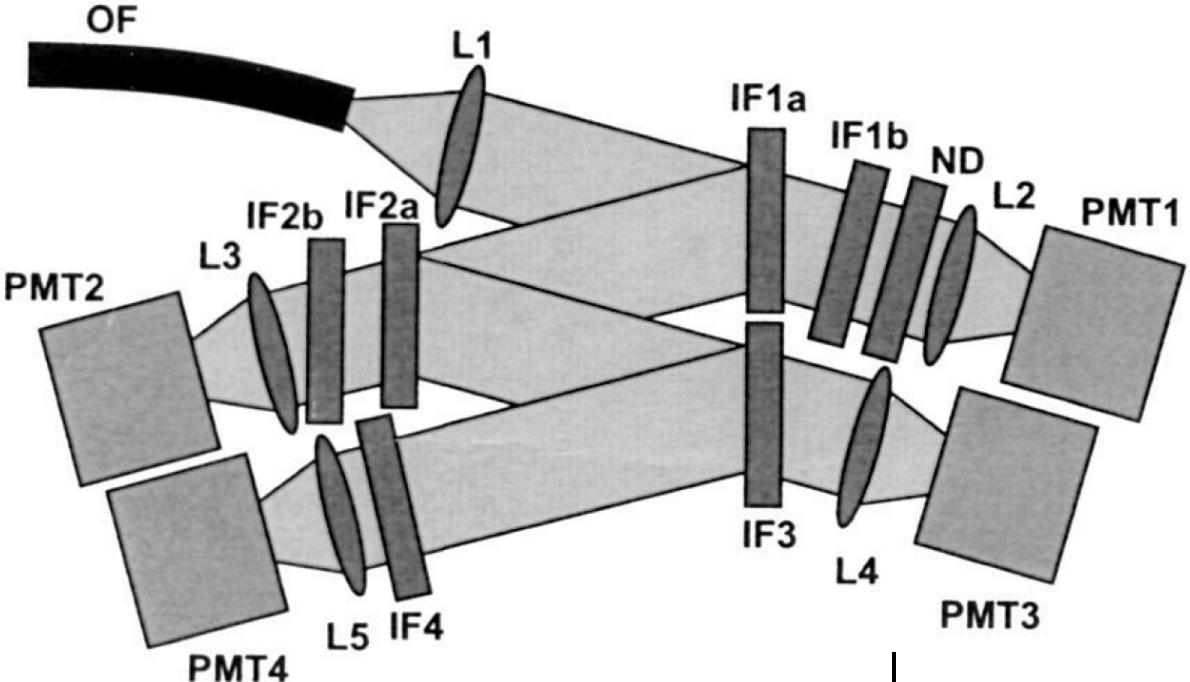

Elastic (PMT1)	$n_{[-]}$ (PMT2)	$n_{[+]}$ (PMT3)
$T_{IF1a} \cdot T_{IF1b}$	$R_{IF1a} \cdot T_{IF2a} \cdot T_{IF2b}$	$R_{IF1a} \cdot R_{IF2a} \cdot T_{IF3}$
62%	36% ≥OD7@532nm	68% ≥OD7@532nm

after Behrendt and Reichardt, "Atmospheric temperature profiling in the presence of clouds with a pure rotational Raman lidar by use of an interference-filter-based polychromator" App. Opt., Vol. 39, No. 9, 1372-1378, 2000

Improved transmission of interference filters (as of 2004)

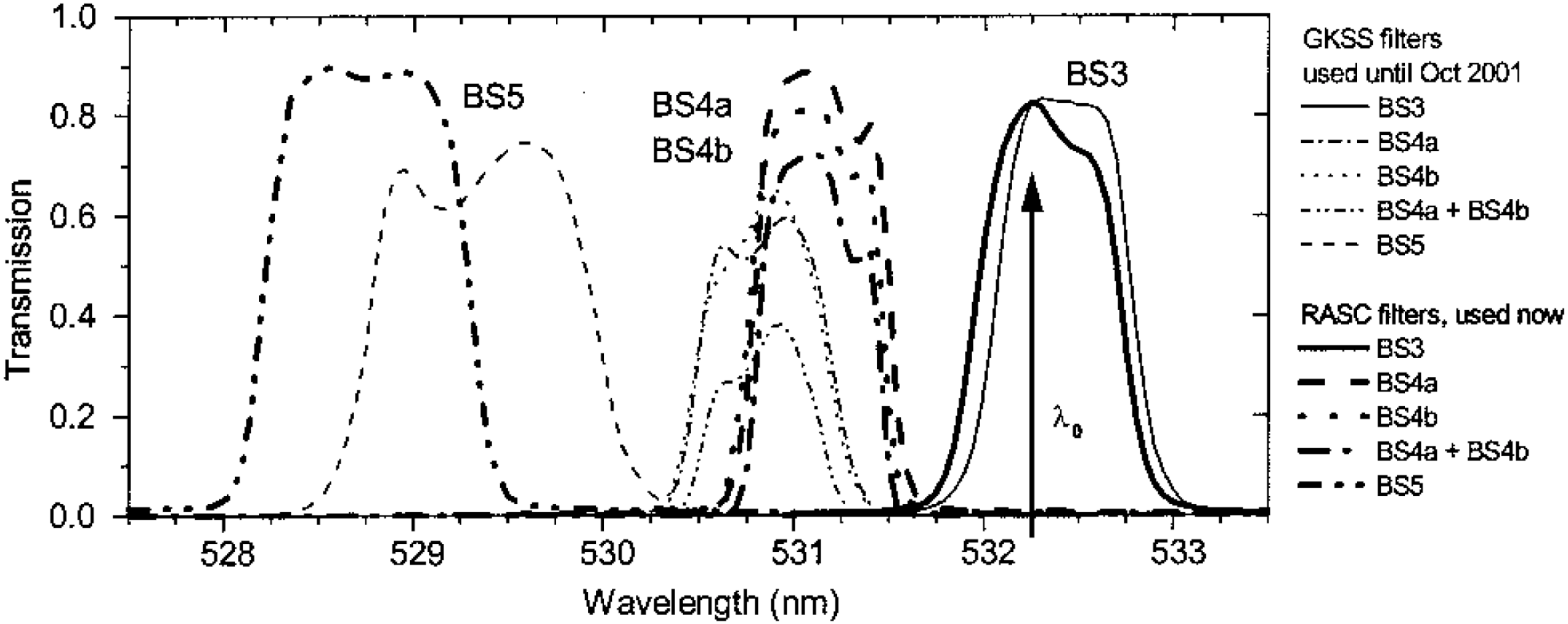

Elastic	$n_{[-]}$	$n_{[+]}$
T_{BS3}	$R_{BS3} \cdot T_{BS4a} \cdot T_{BS4b}$	$R_{BS3} \cdot R_{BS4a} \cdot T_{BS5}$
82%	68% ≥OD7@532nm	80% ≥OD7@532nm

after Behrendt et al., "Combined temperature lidar for measurements in the troposphere, stratosphere, and mesosphere", App. Opt., Vol. 43, No. 14, 2930-2939, 2004

Isolating "temperature-sensitive" lines with diffraction gratings

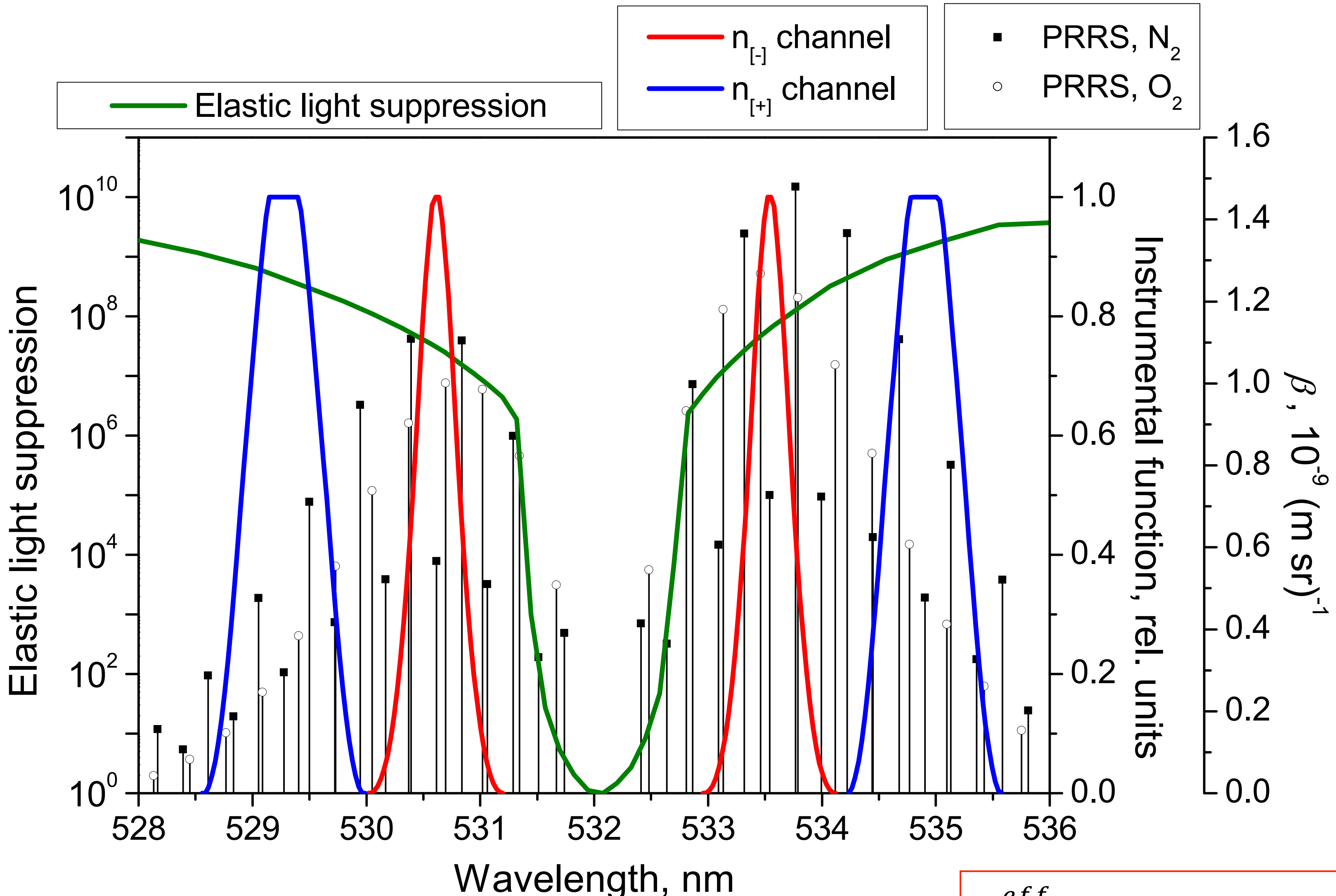

$$N_{lines}^{eff} = 15 \div 20 \;\; @273K$$

Diffraction grating polychromator

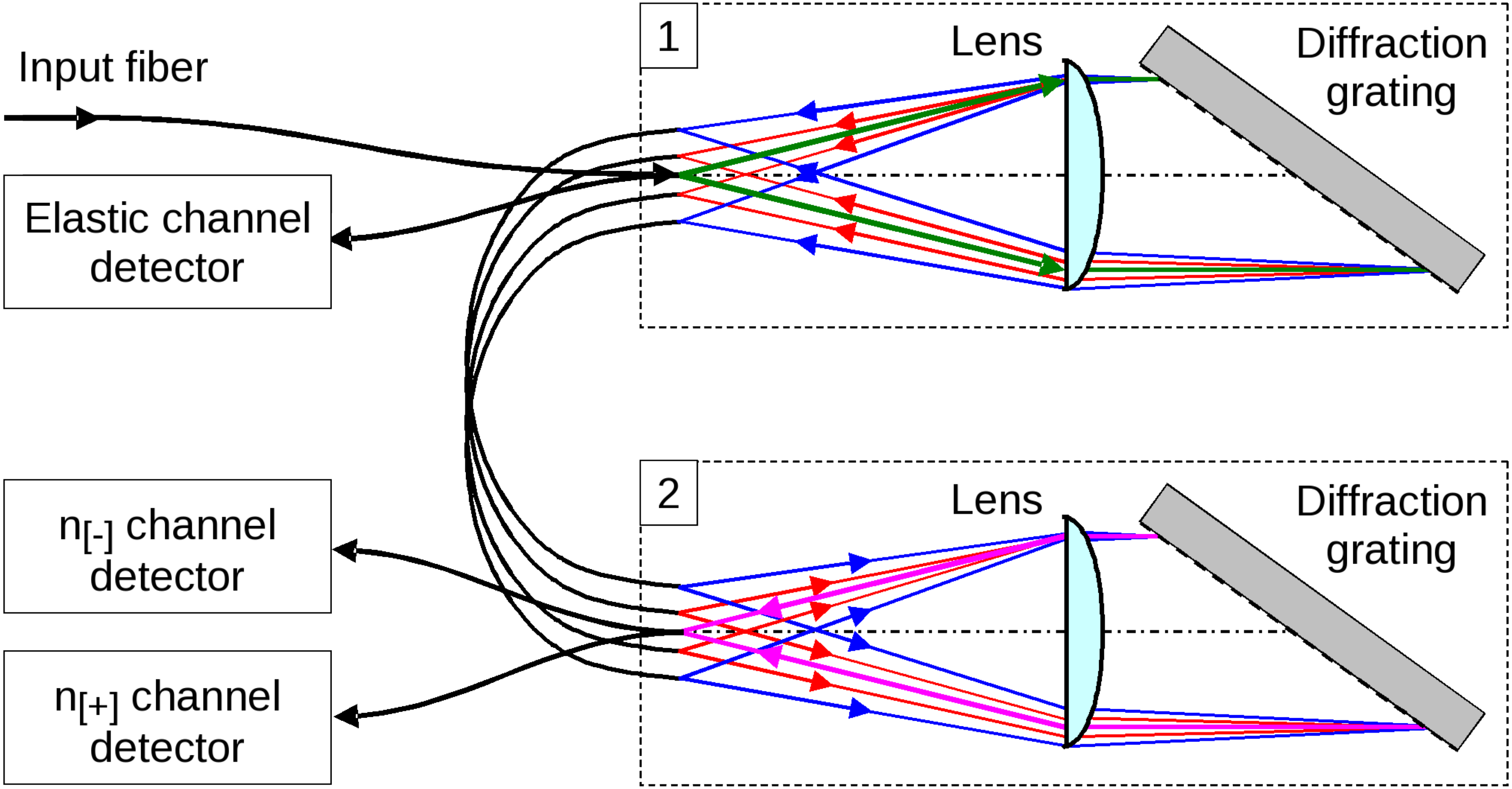

* $n_{[+]}$ and $n_{[-]}$ refer to the PRRS lines with positive and negative temperature dependence

Input / output “slits” (fibers) arrangement

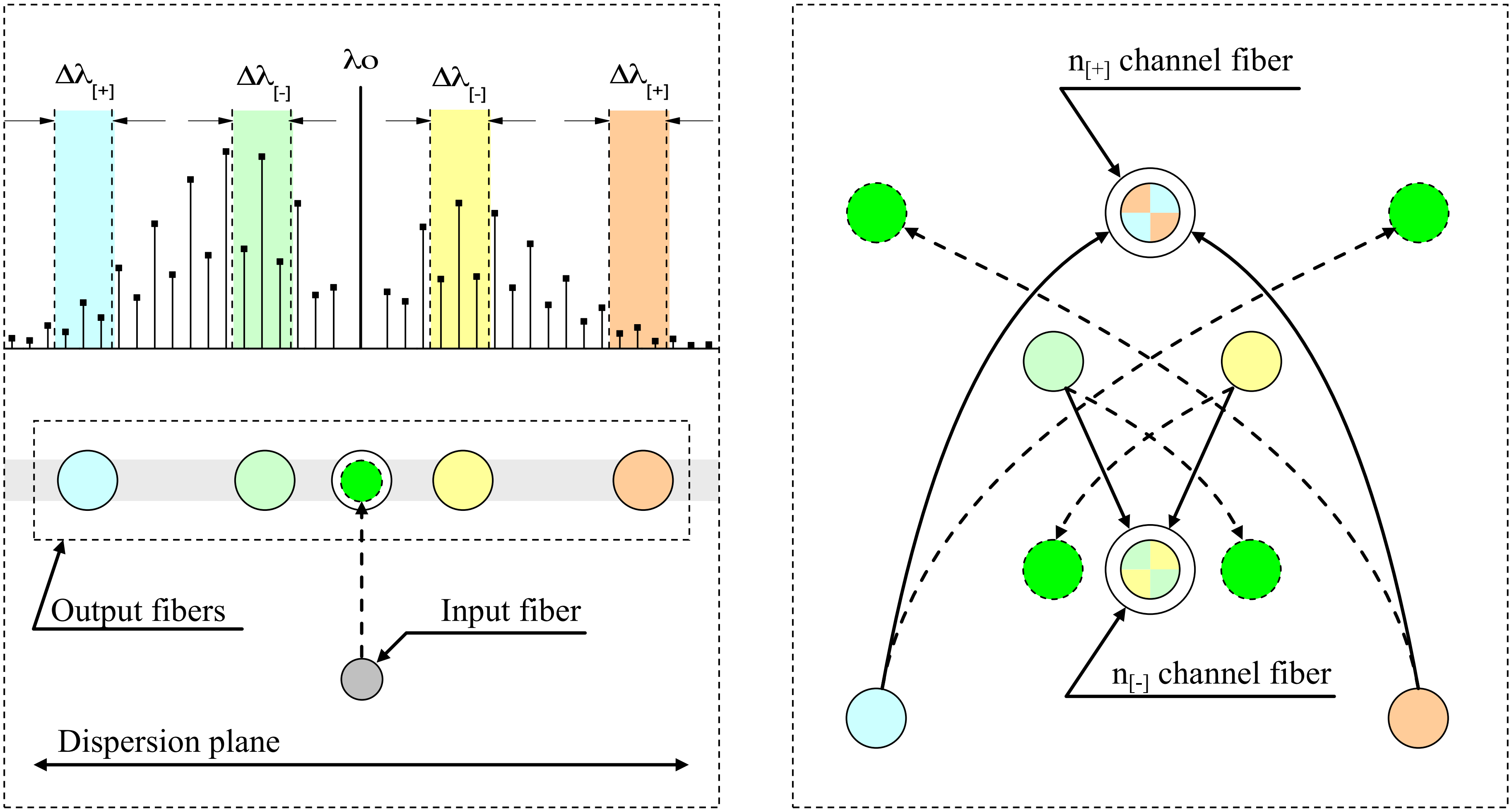

first unit

second unit

Single telescope configuration.

Diffraction grating efficiency (Richardson Gratings Lab)

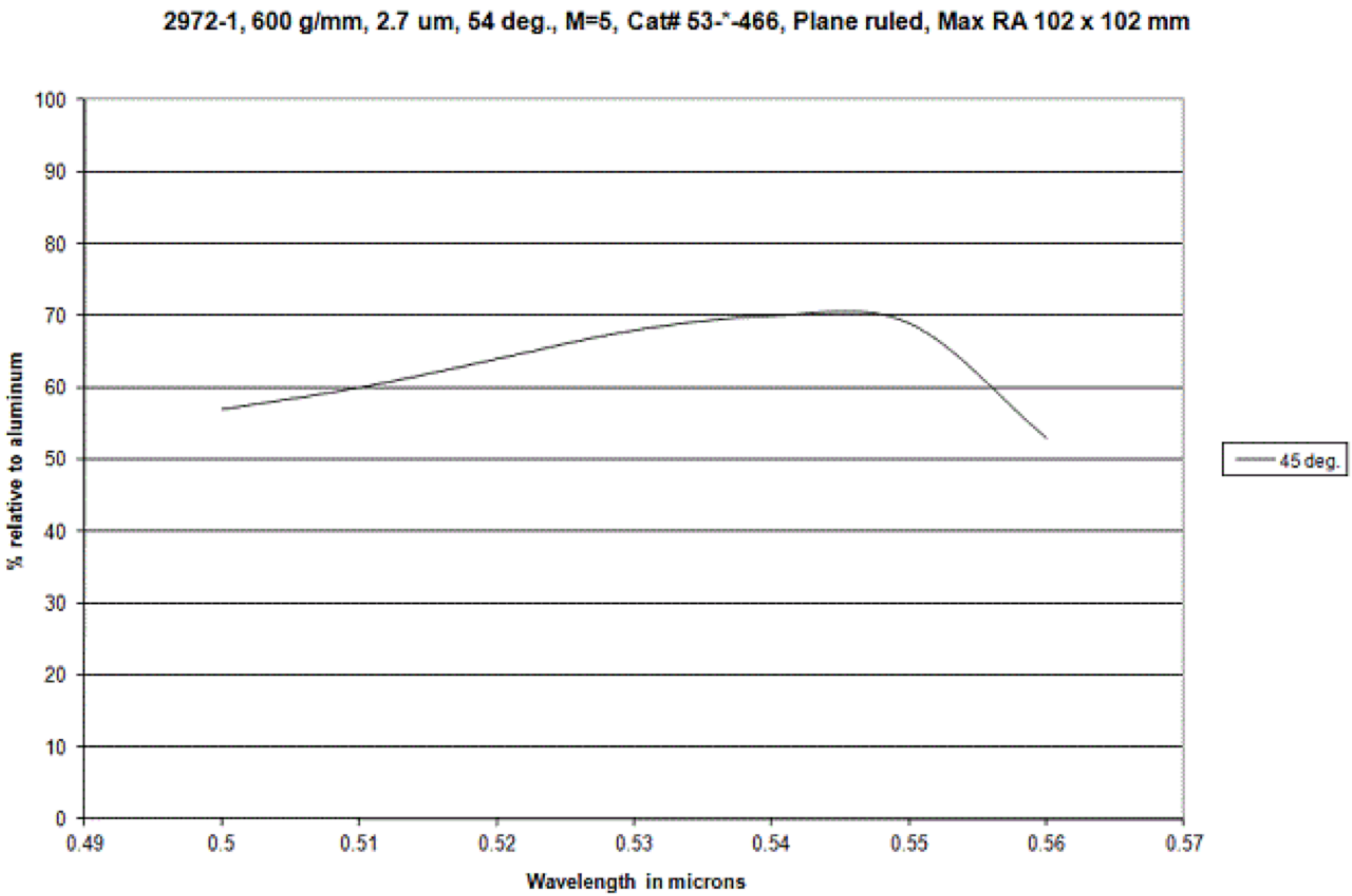

532 nm

Diffraction grating efficiency (Richardson Gratings Lab)

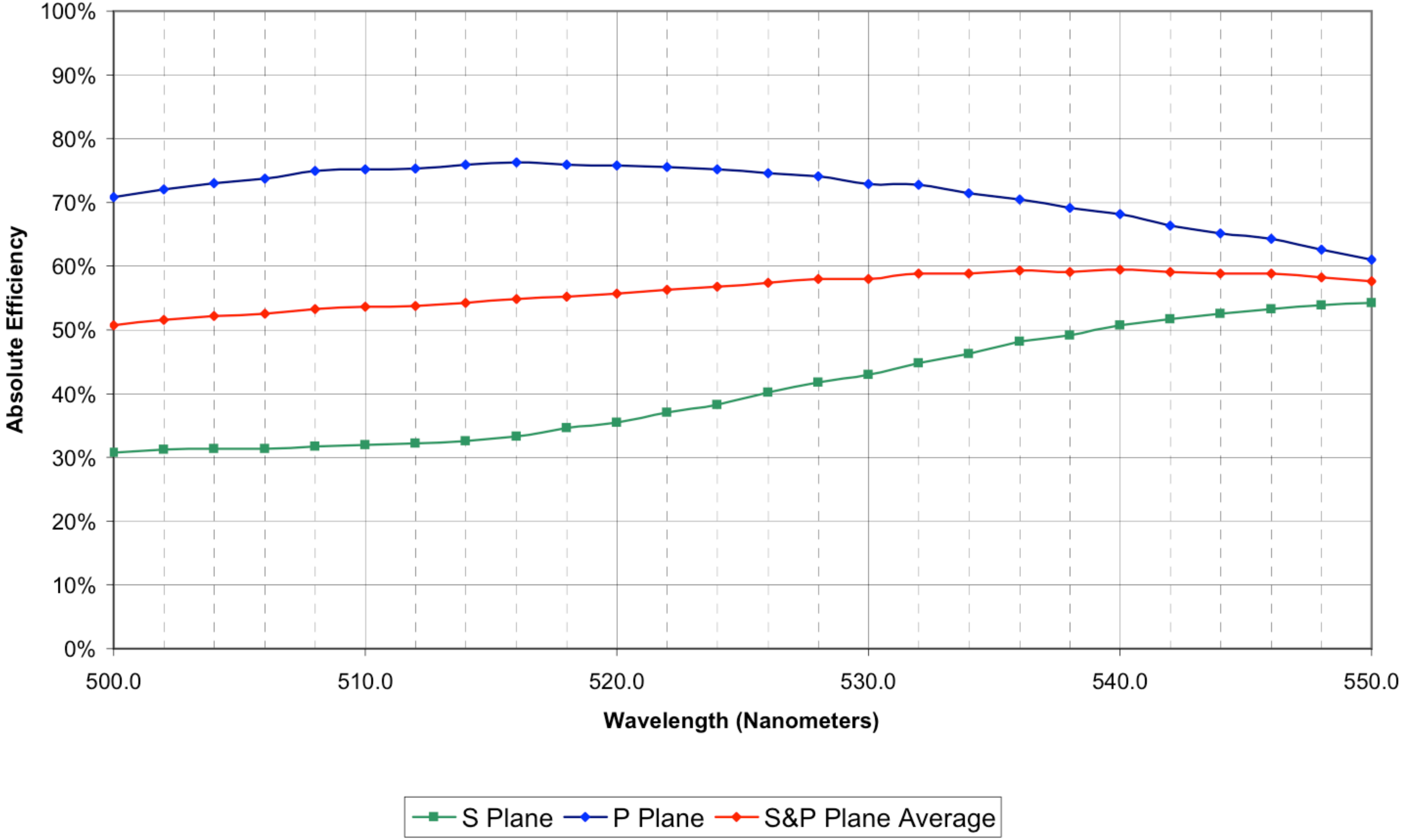

532 nm

Elastic light suppression

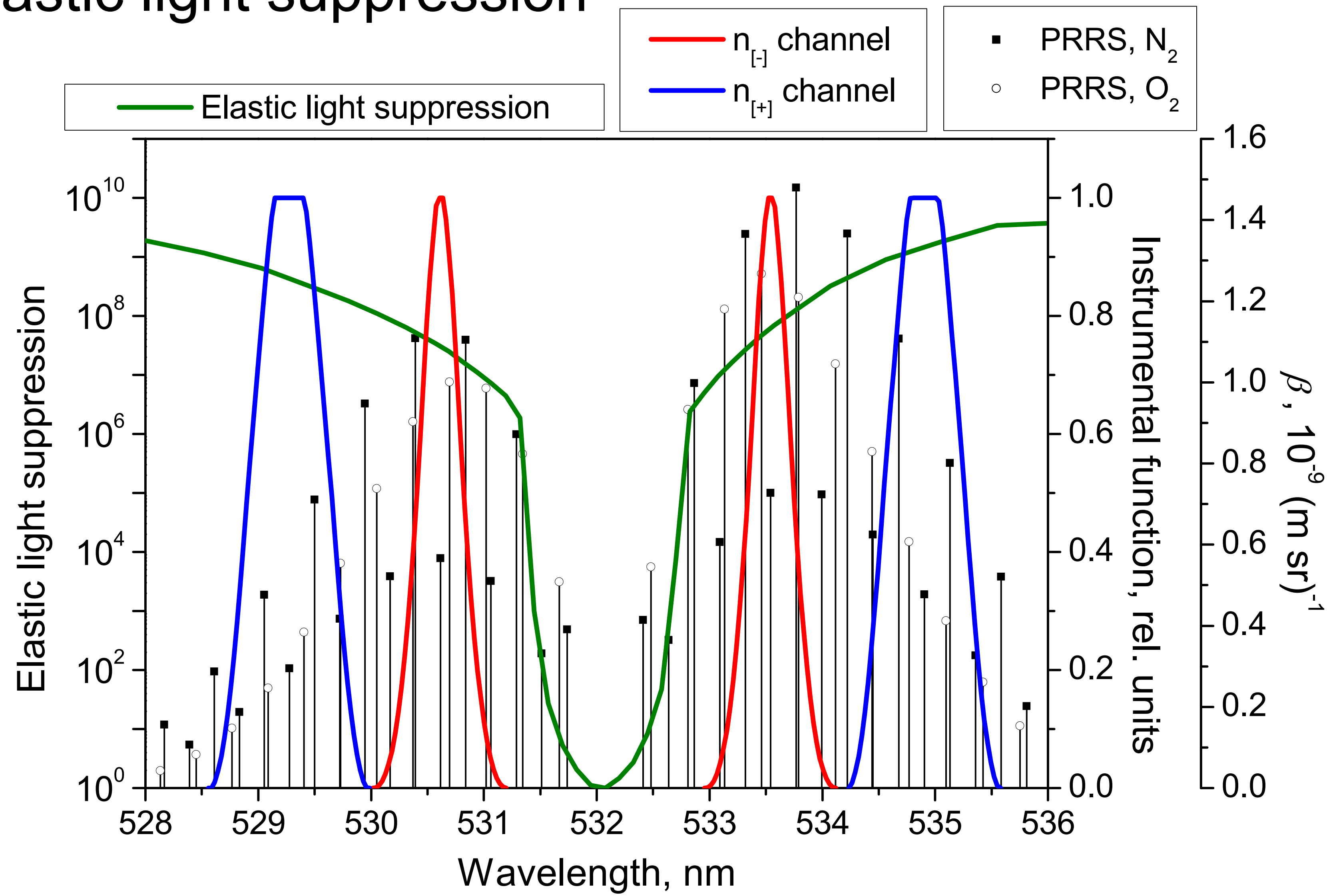

Grating polychromator: efficiency and stray light suppression

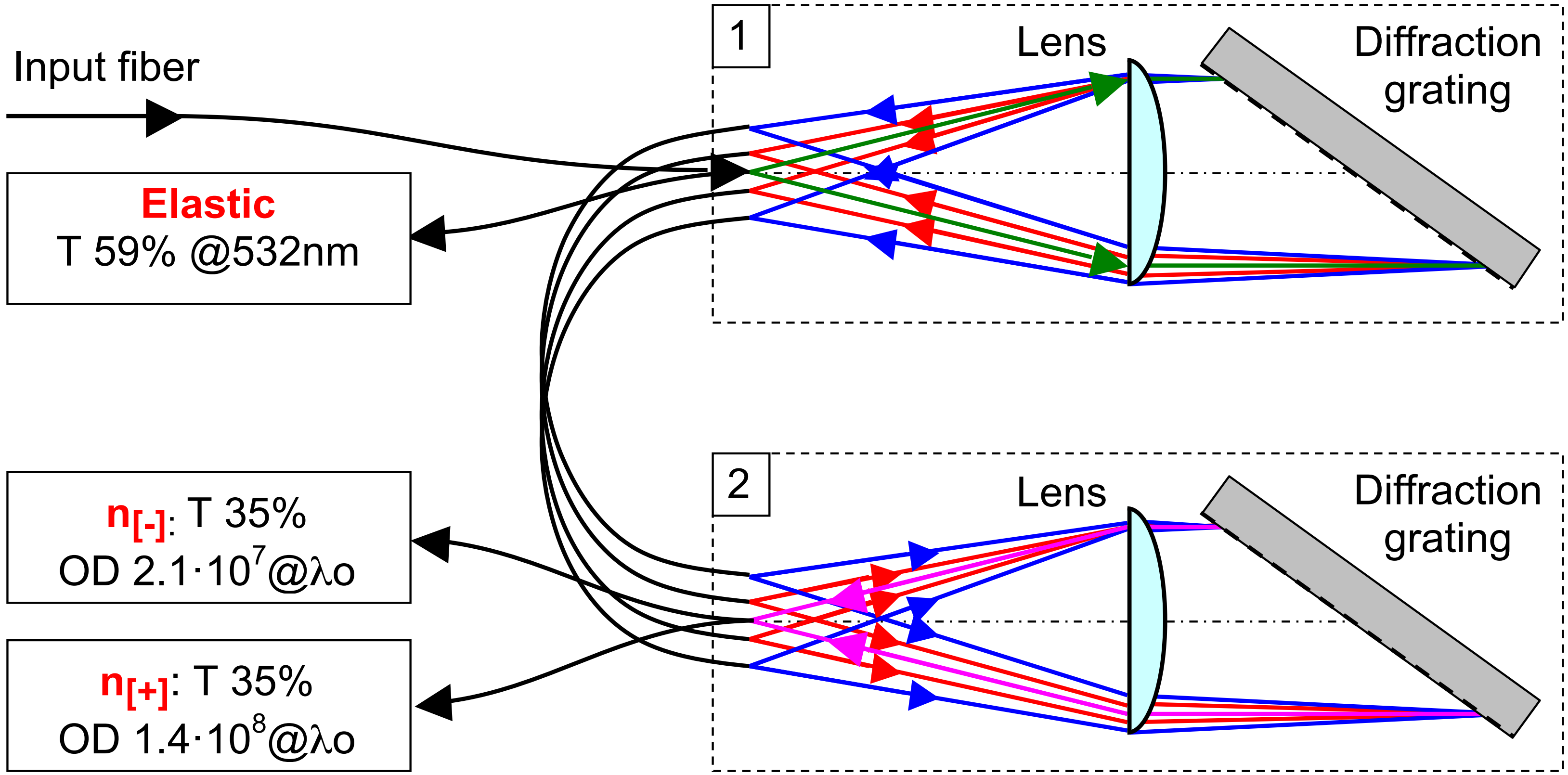

"Effective" polychromator transmission: $n_{[-]}$ T =78%, $n_{[+]}$ T =100%

$$\left.\frac{n_{[-]}^{total}}{n_{[-]}^{anti-stokes}}\right|_{220K} = 2.24$$

$$\left.\frac{n_{[+]}^{total}}{n_{[+]}^{anti-stokes}}\right|_{220K} = 2.86$$

$$N_{lines}^{eff} = 5.3 \div 7 \ \ @273K$$

Isolating "temperature-sensitive" lines with interference filters

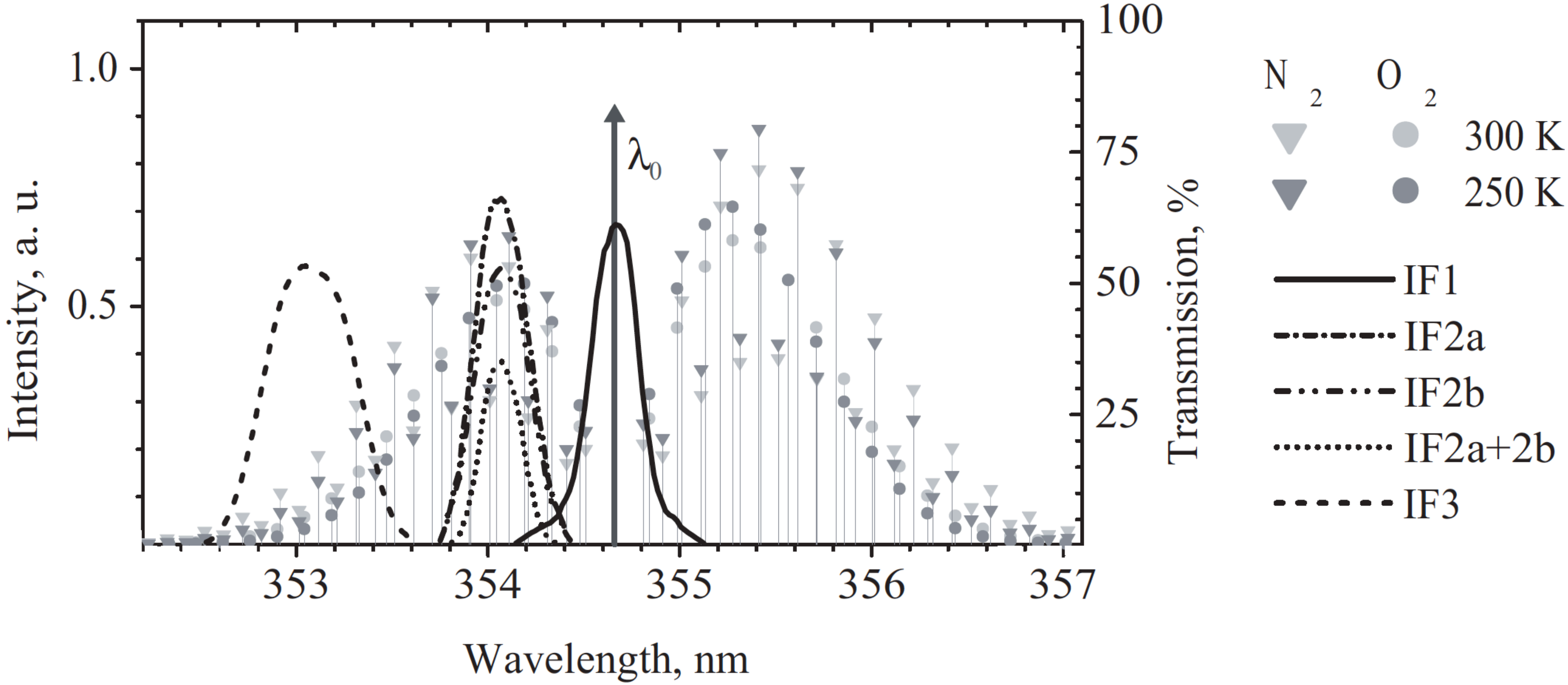

"Transmission of interference filters and PRRS of N_2 and O_2 at 300K and 250K"

after Radlach et al. "Scanning rotational Raman lidar at 355nm for the measurement of tropospheric temperature fields", Atmos. Chem. Phys., 8, 159–169, 2008

Isolating “temperature-sensitive” lines with interference filters

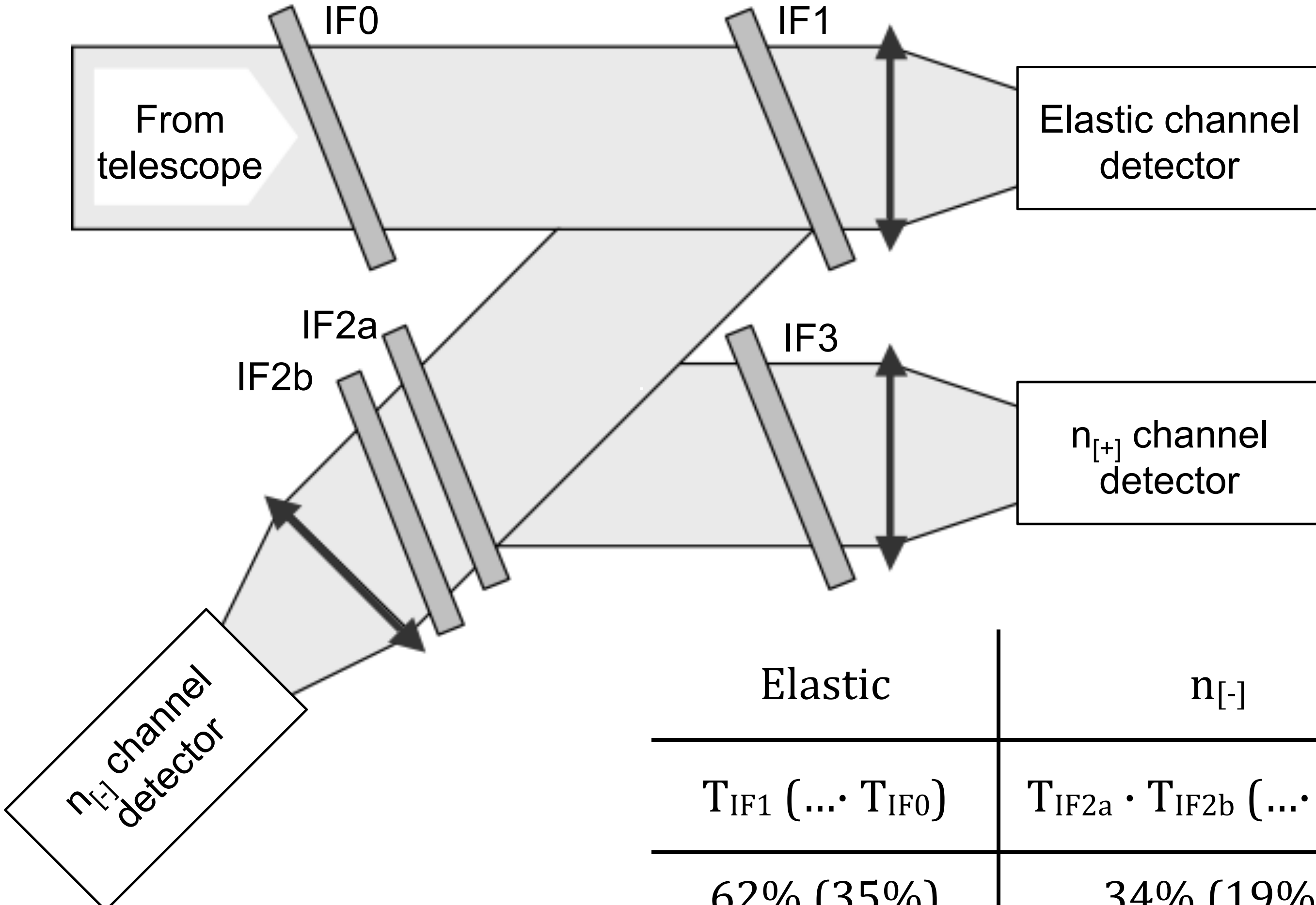

Elastic	$n_{[-]}$	$n_{[+]}$
T_{IF1} (…· T_{IF0})	$T_{IF2a} \cdot T_{IF2b}$ (…· T_{IF0})	T_{IF3} (…· T_{IF0})
62% (35%)	34% (19%)	52% (29%)
	OD7@355nm	OD7@355nm

after Radlach et al. “Scanning rotational Raman lidar at 355nm for the measurement of tropospheric temperature fields”, Atmos. Chem. Phys., 8, 159–169, 2008

Elastic light suppression

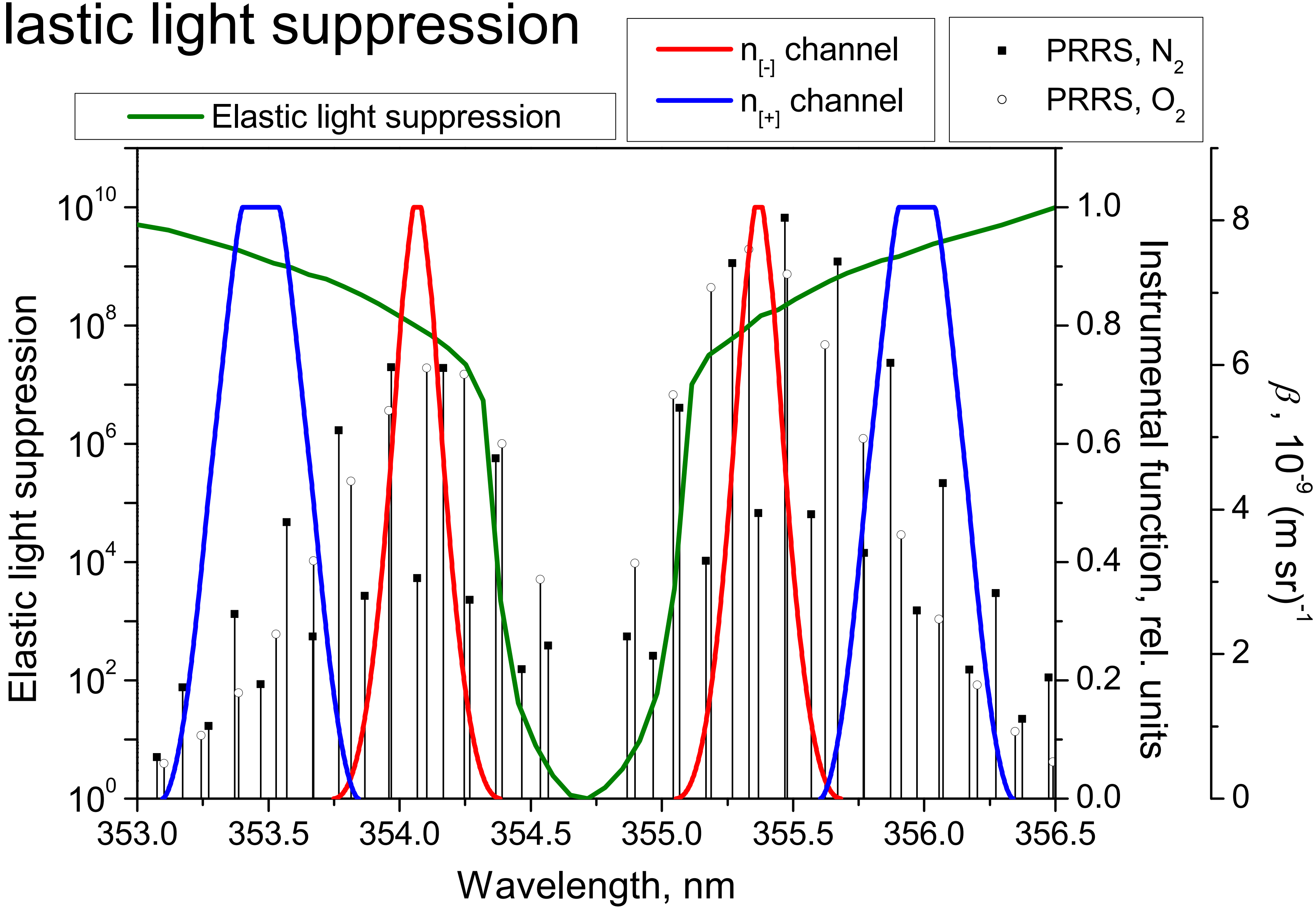

355 nm

Grating polychromator: efficiency and stray light suppression

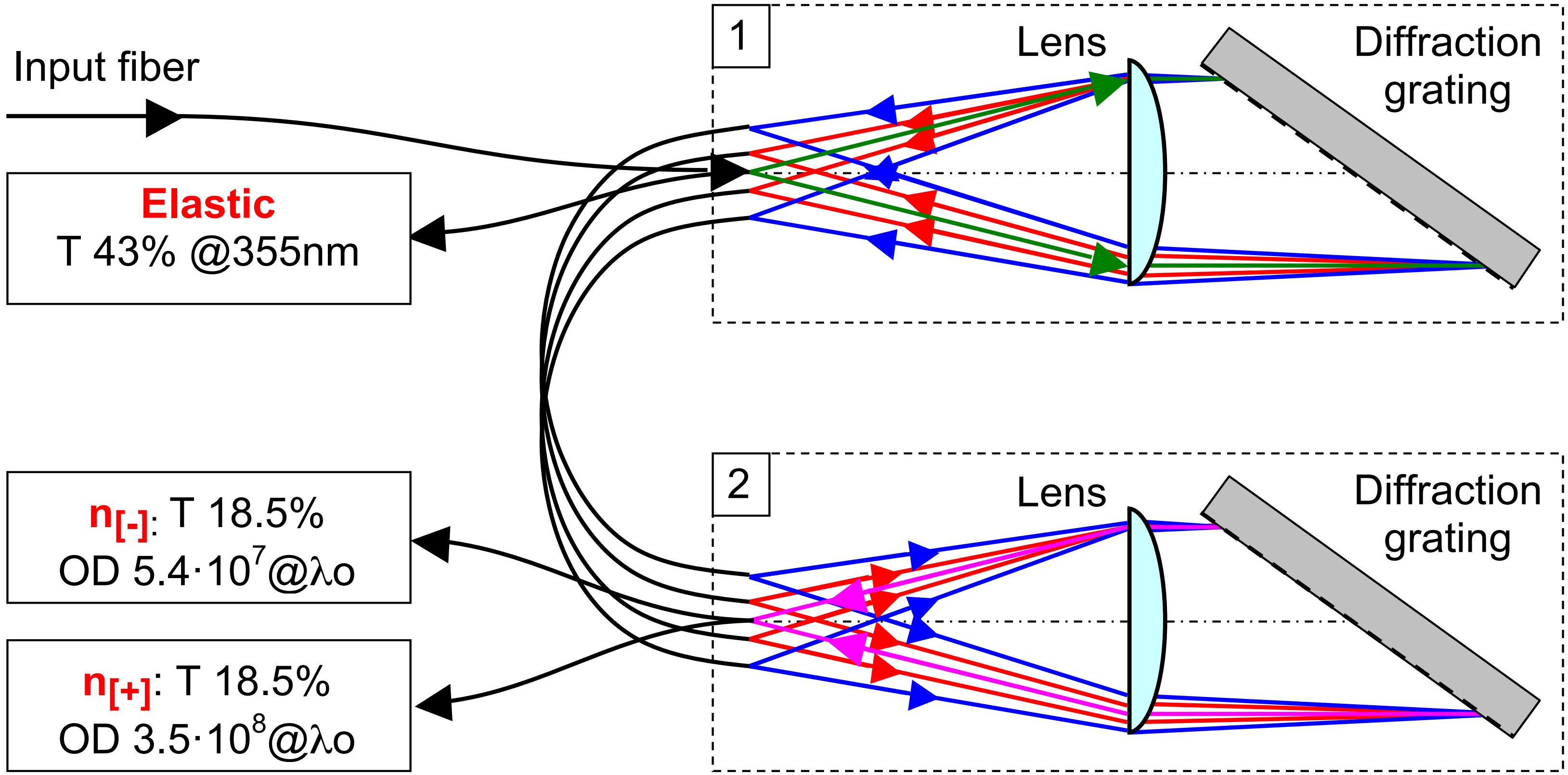

"Effective" polychromator transmission: $n_{[-]}$ T =41%, $n_{[+]}$ T =53%

$$\left.\frac{n_{[-]}^{total}}{n_{[-]}^{anti-stokes}}\right|_{220K} = 2.24$$

$$\left.\frac{n_{[+]}^{total}}{n_{[+]}^{anti-stokes}}\right|_{220K} = 2.86$$

Temperature dependence of combined PRRS signal

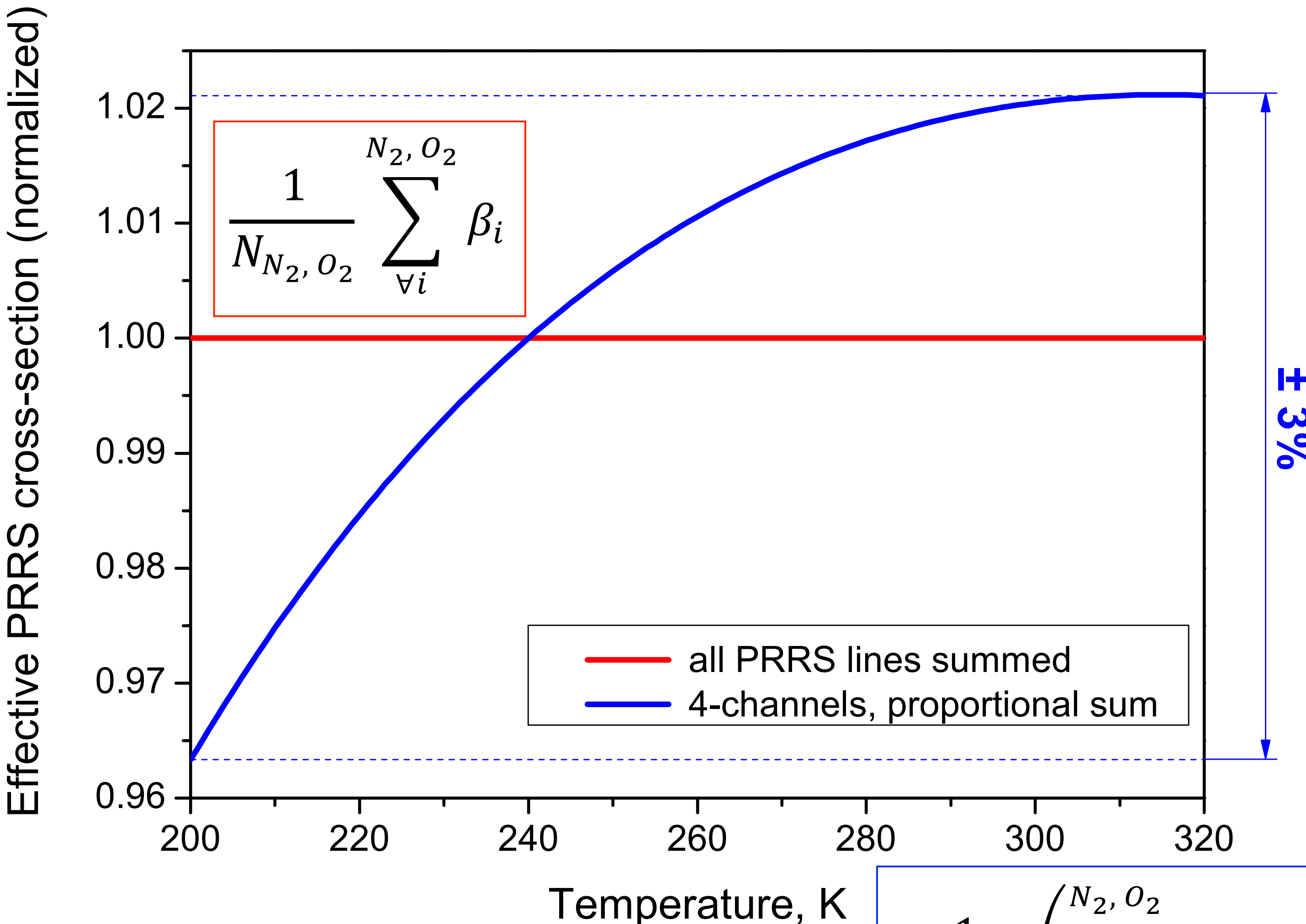

$$\frac{1}{N_{N_2,O_2}} \left(\sum_{\forall i}^{N_2,O_2} G_i^{[-]} \beta_i + \sum_{\forall i}^{N_2,O_2} G_i^{[+]} \beta_i \right)$$

355 nm

Temperature dependence of combined PRRS signal

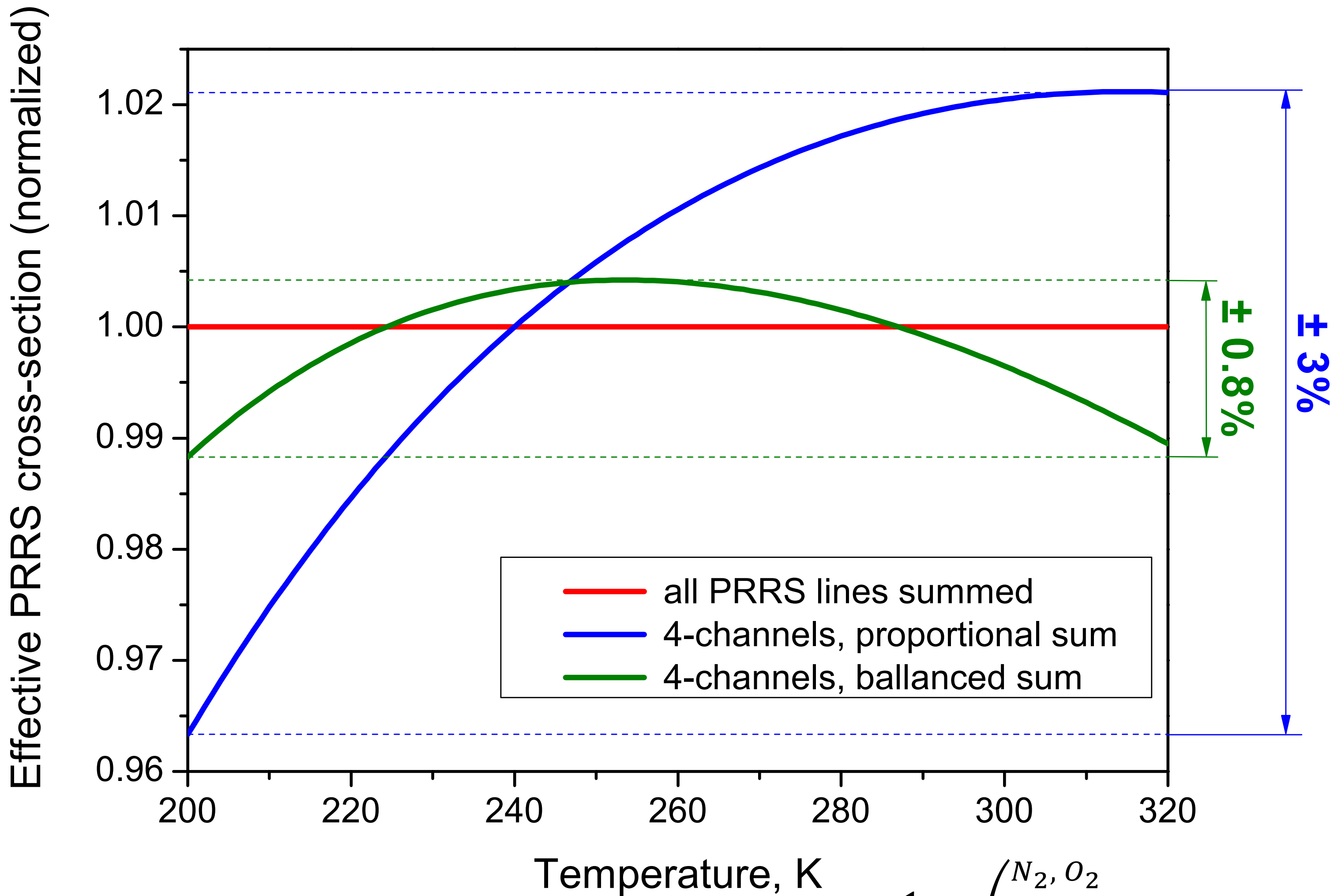

$$\frac{1}{N_{N_2,\,O_2}}\left(\sum_{\forall i}^{N_2,\,O_2} G_i^{[-]}\beta_i + \boxed{coef}\cdot\sum_{\forall i}^{N_2,\,O_2} G_i^{[+]}\beta_i\right)$$

Temperature dependence of combined PRRS signal

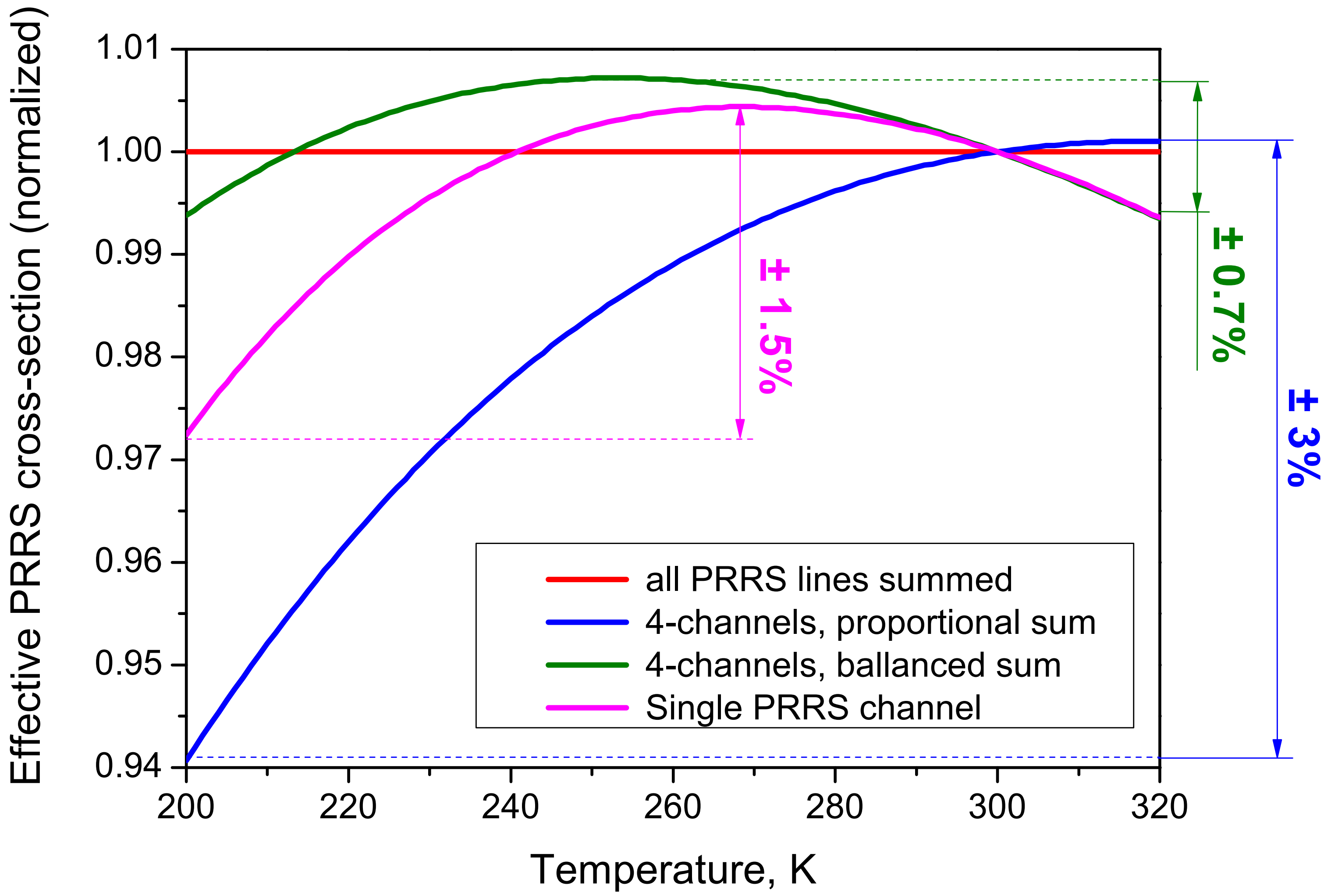

532 nm

“Four telescopes” configuration

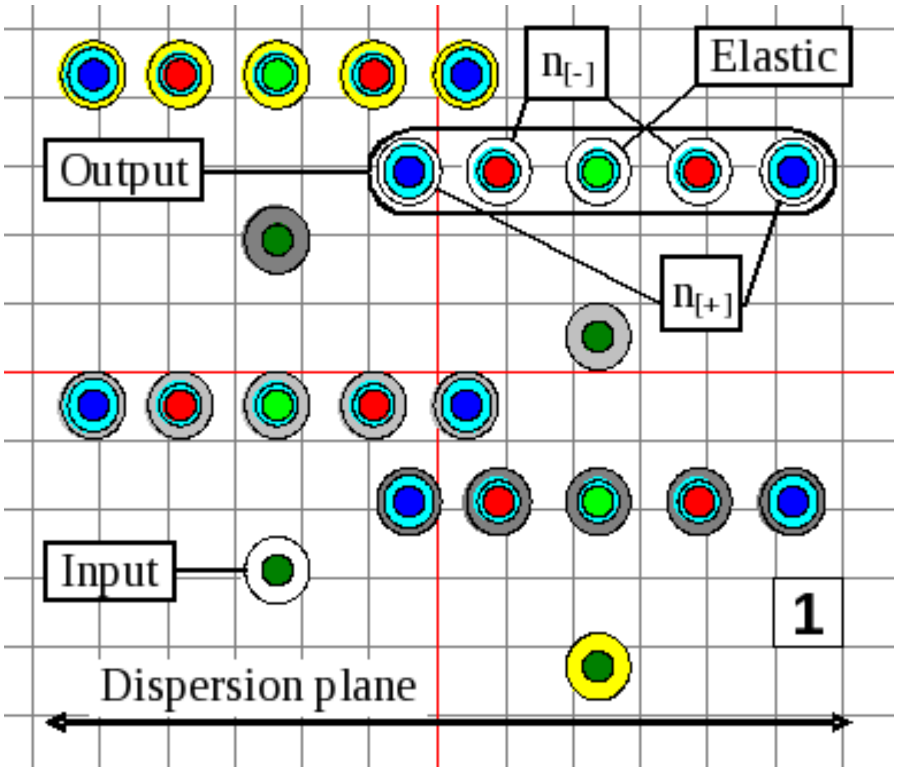

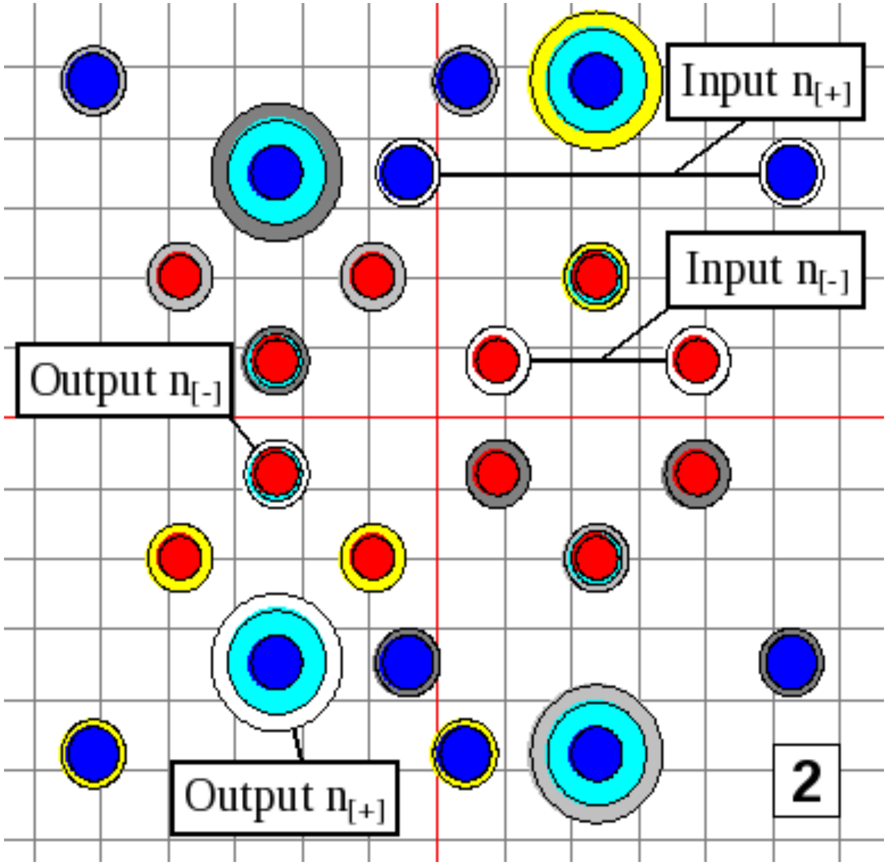

first unit

second unit

animation?

Lidar signal and skylight background

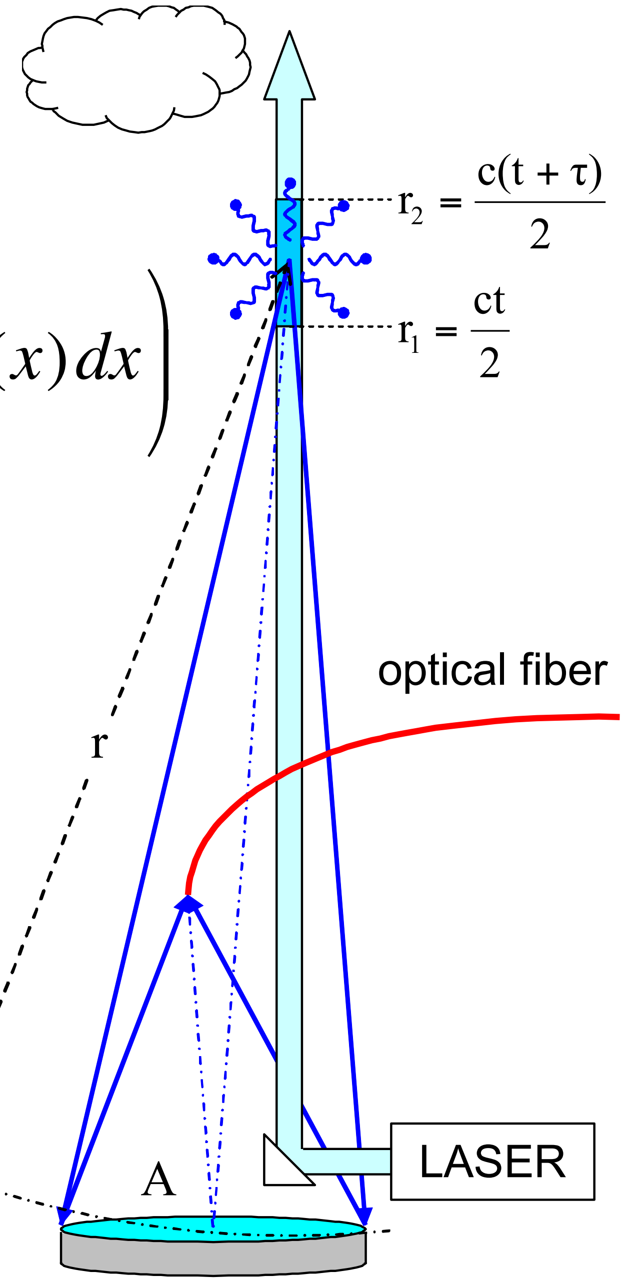

Atmospheric response:

$$P(r) = E_0 \, f_L \, Q(r) \, K \frac{A}{r^2} \frac{c\tau}{2} \beta_\pi(r) \exp\left(-2\int_0^r \alpha(x)\,dx\right)$$

Sky background: $P_{BGR} = E_\nu K A \, \Delta\Omega \, \Delta\nu \, f_L \tau$

Signal to background: $\dfrac{P}{P_{BGR}} \sim \dfrac{E_0 \, \beta_\pi}{\Delta\Omega \, \Delta\nu}$

E_0 laser pulse energy

f_L pulse repetition rate

K total throughput

A receiving telescope area

τ time bin length

$Q(r)$ overlap function

E_ν sky brightness density

$\beta_\pi(r)$ backscatter coefficient

$\alpha(r)$ extinction coefficient

$\Delta\nu$ spectral passband

$\Delta\Omega$ solid angle of "field-of-view"

Temperature channel for night-time operation

$$R = \frac{N_{[-]}}{N_{[+]}}$$

$$\frac{\Delta R}{\overline{R}} = \sqrt{\frac{\mu_2\left(N_{[-]}\right)}{\overline{N_{[-]}}^2} + \frac{\mu_2\left(N_{[+]}\right)}{\overline{N_{[+]}}^2}}$$

$$\frac{\Delta R}{\overline{R}} = \sqrt{\frac{1}{\overline{\overline{N_{[-]}}}} + \frac{1}{\overline{\overline{N_{[+]}}}}}$$

$$\Delta R = \pm 2.24\overline{R}\sqrt{\frac{1}{\overline{\overline{N_{[-]}}}} + \frac{1}{\overline{\overline{N_{[+]}}}}}$$

$$\Delta R = \frac{dR}{dT}\Delta T$$

$$\Delta T = \frac{4.48}{\sqrt{\Delta t}}\sqrt{\frac{1}{\overline{\overline{n_{[-]}}}} + \frac{1}{\overline{\overline{n_{[+]}}}}}\,\frac{1}{\frac{1}{\overline{\overline{R}}}\frac{dR}{dT}}$$

$$\Delta t = \left(\frac{1}{\overline{\overline{n_{[-]}}}} + \frac{1}{\overline{\overline{n_{[+]}}}}\right)\left(\frac{4.48}{\Delta T}\,\frac{1}{\frac{1}{\overline{\overline{R}}}\frac{dR}{dT}}\right)^2$$

$$\delta t = \frac{\Delta t}{\left[\Delta t\right]_{norm}}$$

Optimum spectral intervals (night-time)

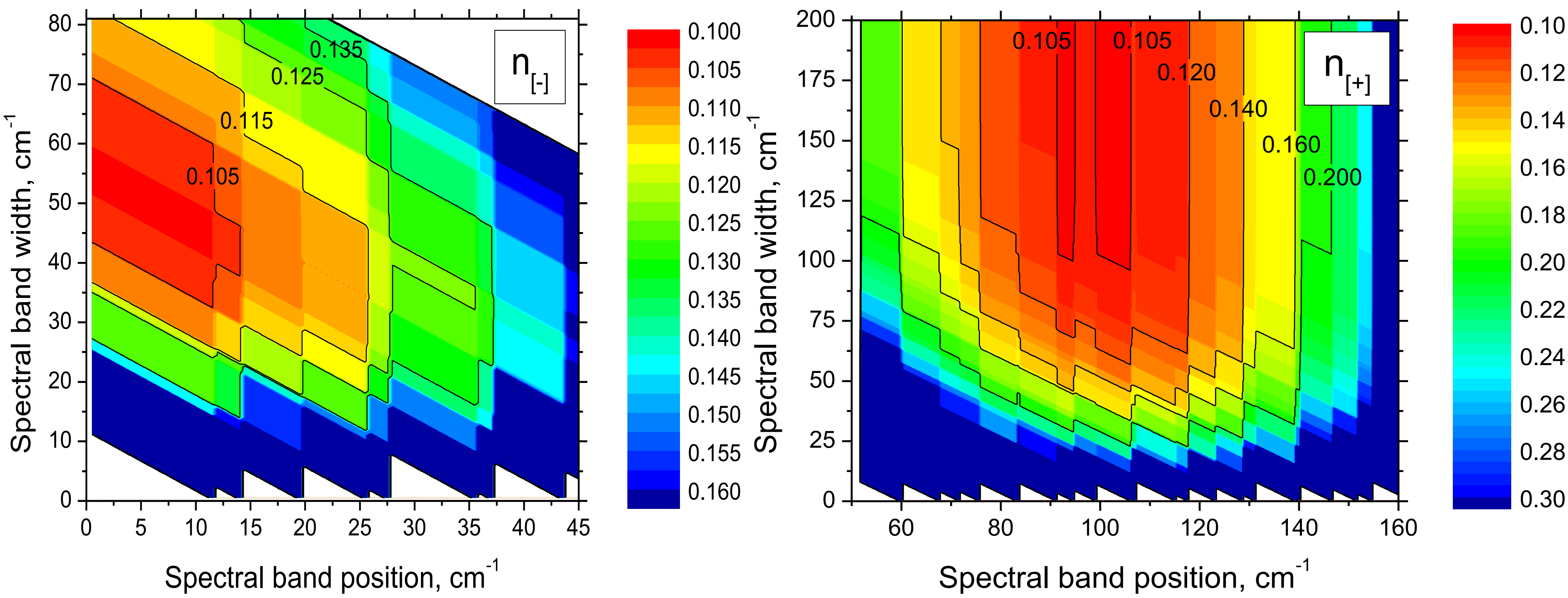

Temperature channel for daytime operation

$$\tilde{N}_{[-]} = \left(n_{[-]} + n_{\nu}^{sky} \cdot \Delta\nu_{[-]}\right)\Delta t \qquad \tilde{N}_{[+]} = \left(n_{[+]} + n_{\nu}^{sky} \cdot \Delta\nu_{[+]}\right)\Delta t$$

$$R = \frac{\tilde{N}_{[-]} - \overline{n_{\nu}^{sky}}\Delta\nu_{[-]}\Delta t}{\tilde{N}_{[+]} - \overline{n_{\nu}^{sky}}\Delta\nu_{[+]}\Delta t}$$

$$\Delta t = \left(\frac{\overline{n_{[-]}} + \overline{n_{\nu}^{sky}}\Delta\nu_{[-]}}{\overline{n_{[-]}}^{2}} + \frac{\overline{n_{[+]}} + \overline{n_{\nu}^{sky}}\Delta\nu_{[+]}}{\overline{n_{[+]}}^{2}}\right)\left(\frac{4.48}{\Delta T}\frac{1}{\frac{1}{\overline{R}}\frac{dR}{dT}}\right)^{2}$$

Optimum spectral intervals (daytime)

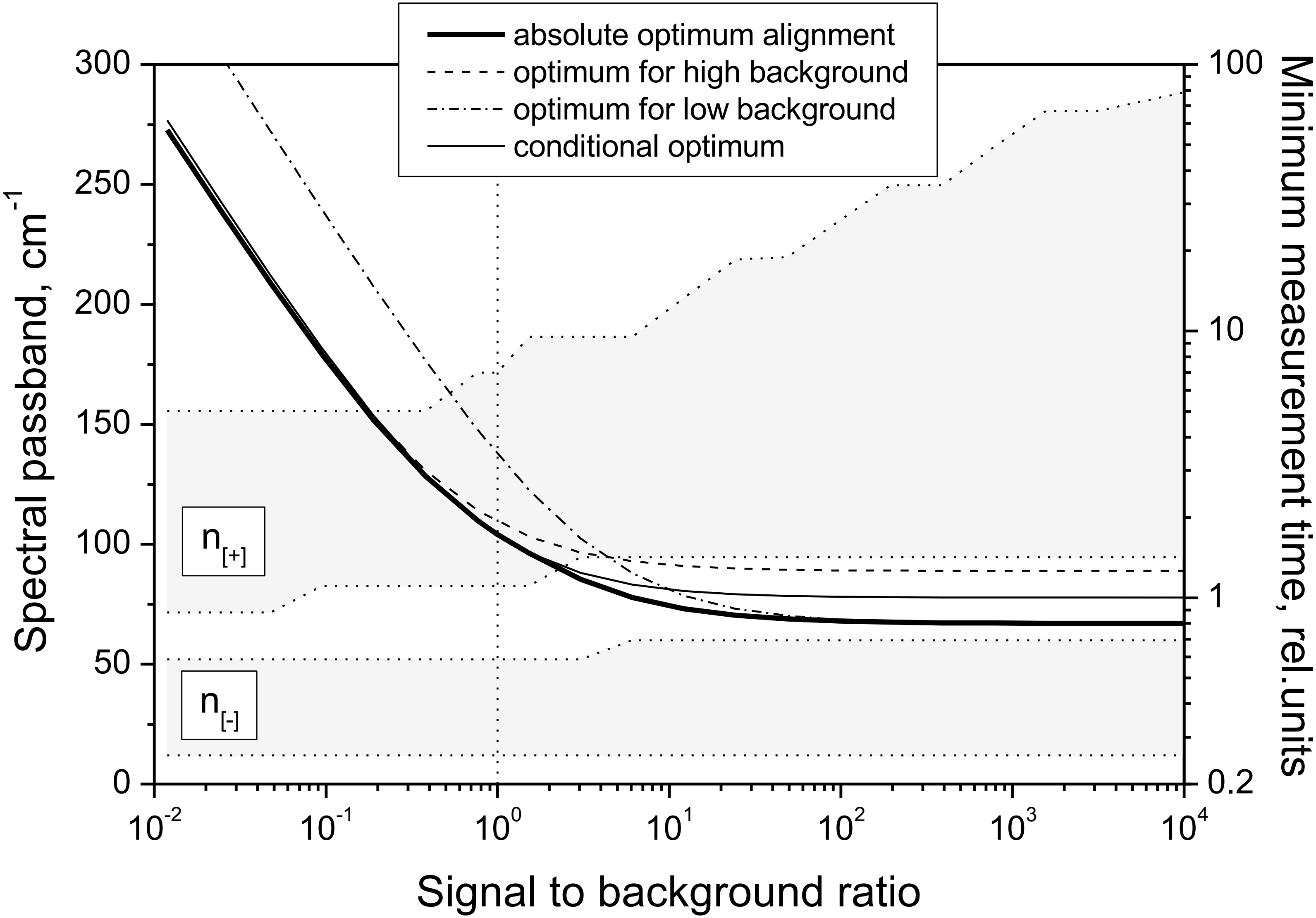

Optimum spectral intervals (daytime)

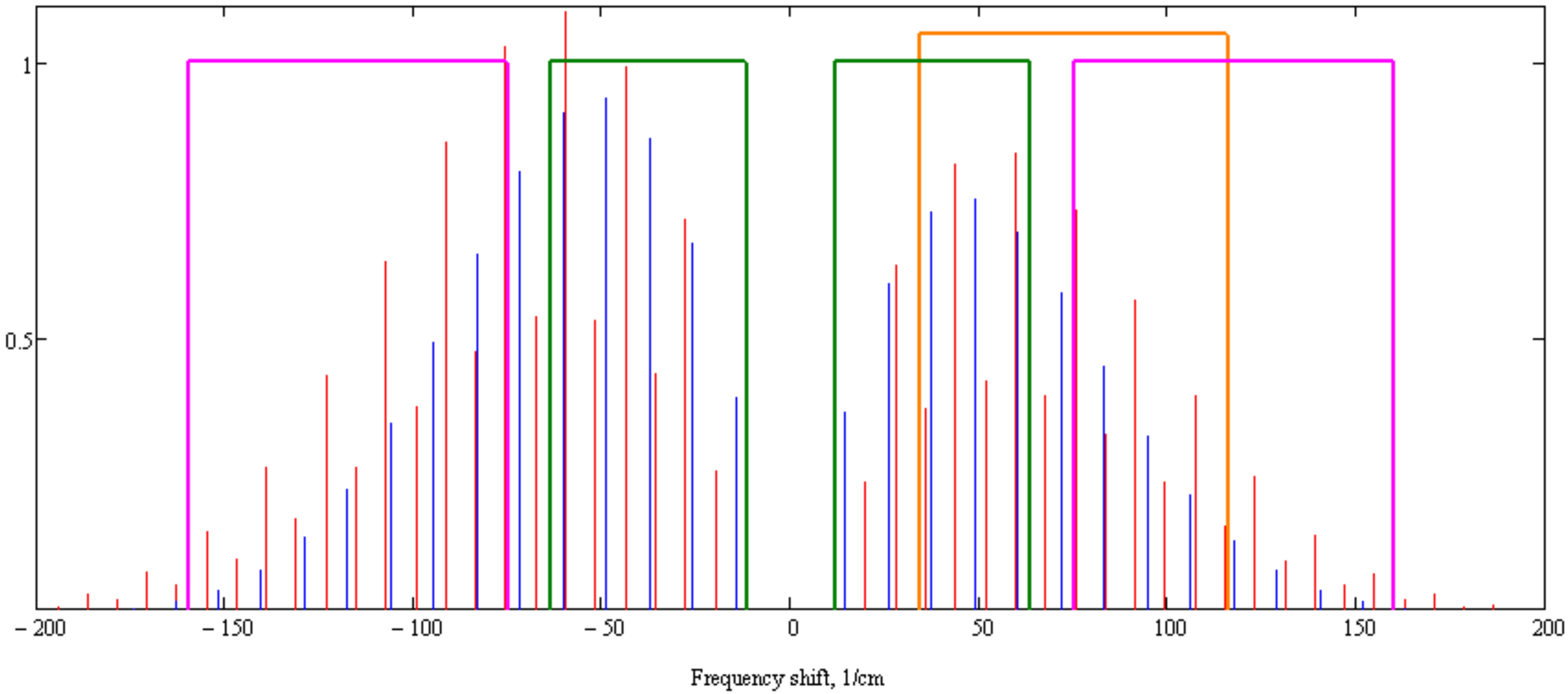

Optimum spectral intervals (daytime)

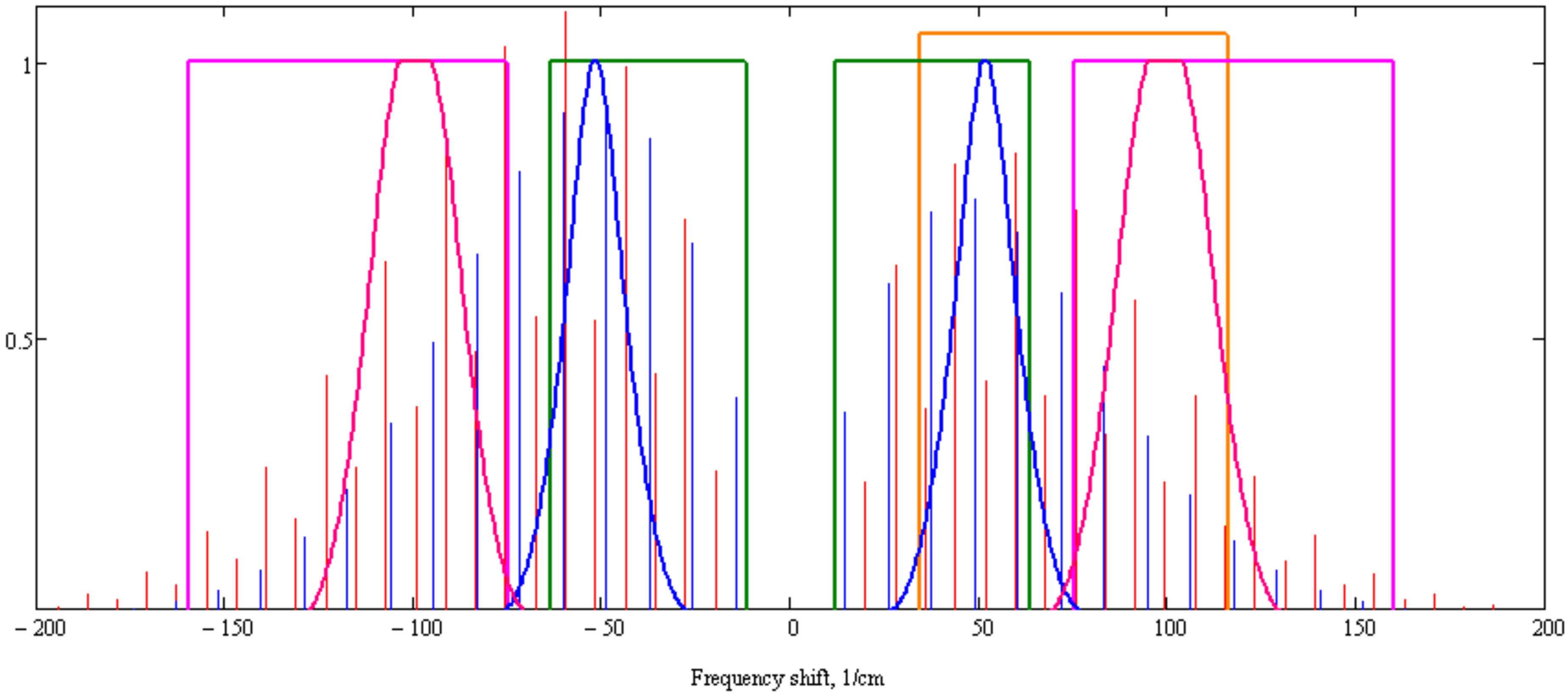

Optimum spectral intervals (daytime)

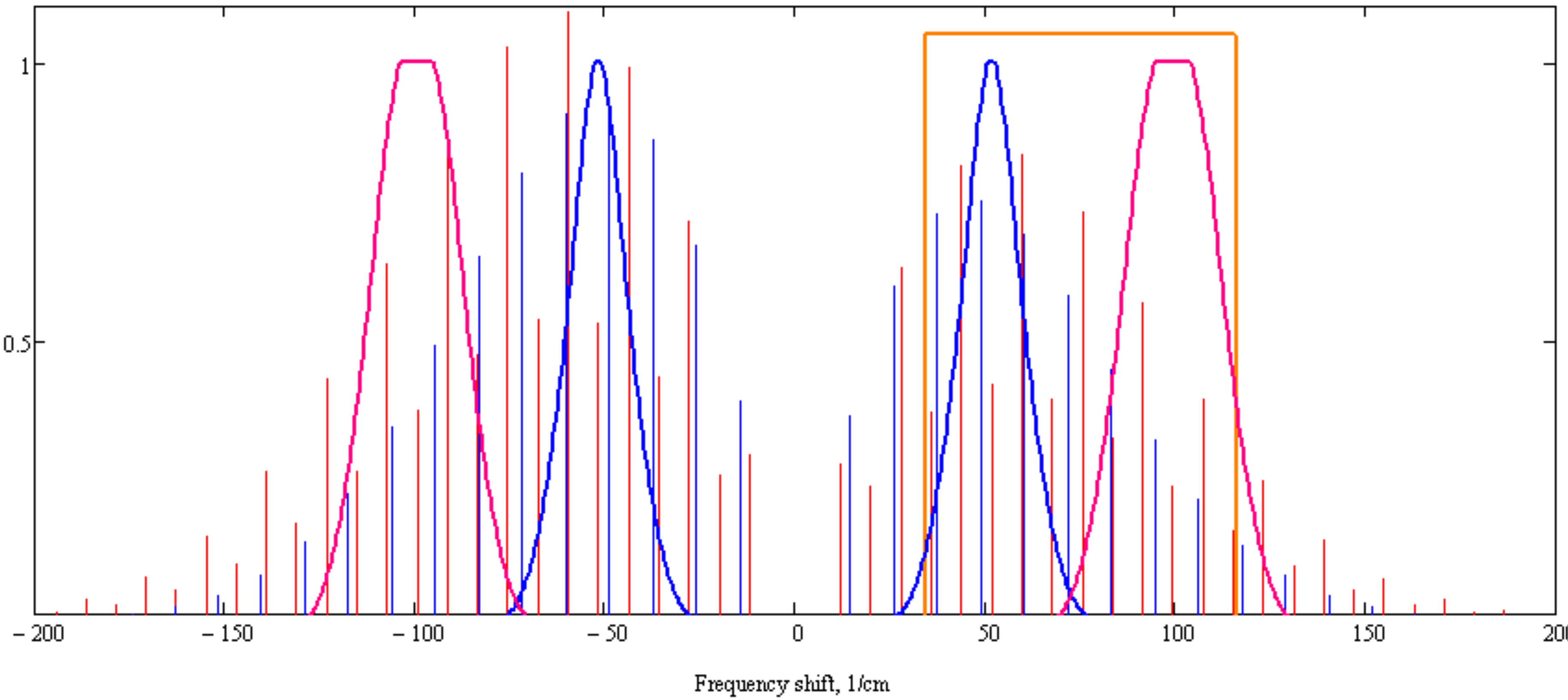

Lidar signal and skylight background

Atmospheric response:

$$P(r) = E_0 f_L Q(r) K \frac{A}{r^2} \frac{c\tau}{2} \beta_\pi(r) \exp\left(-2\int_0^r \alpha(x)\,dx\right)$$

Sky background:

$$P_{BGR} = E_\nu K A \Delta\Omega \Delta\nu f_L \tau$$

Signal to background:

$$\frac{P}{P_{BGR}} \sim \frac{E_0 \beta_\pi}{\Delta\Omega \Delta\nu}$$

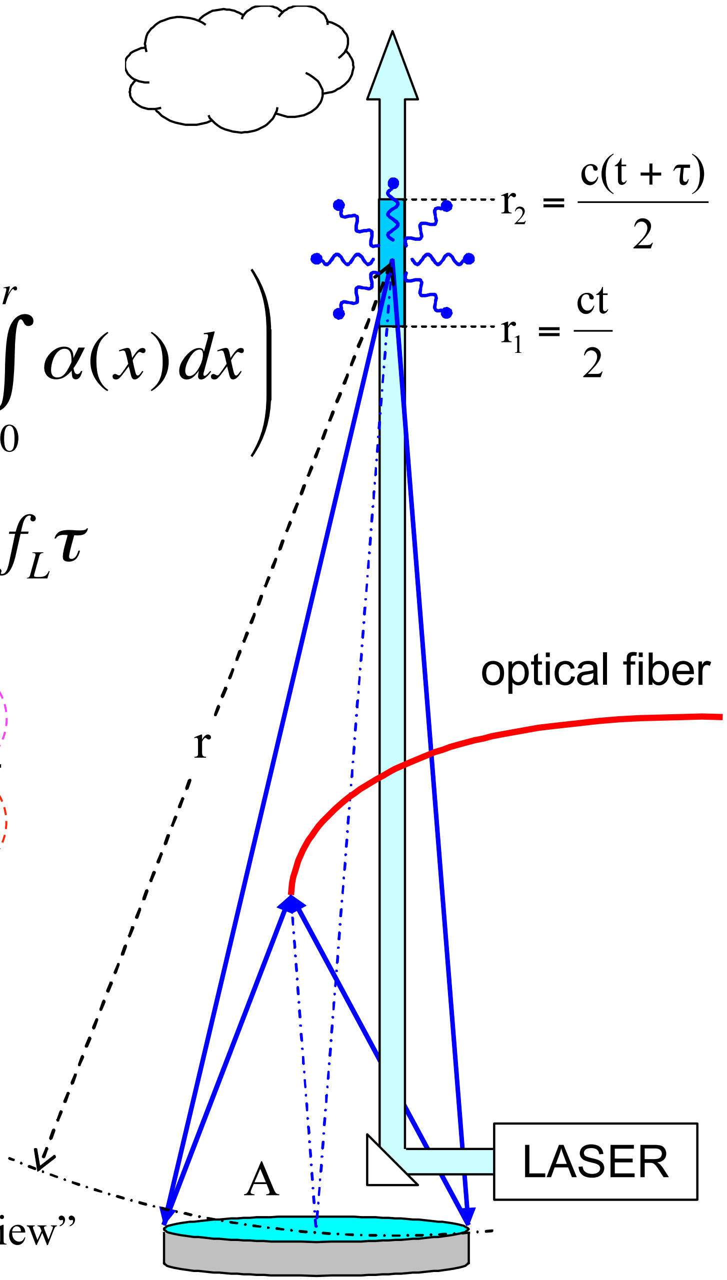

E_0 laser pulse energy

f_L pulse repetition rate

K total throughput

A receiving telescope area

τ time bin length

$Q(r)$ overlap function

E_ν sky brightness density

$\beta_\pi(r)$ backscatter coefficient

$\alpha(r)$ extinction coefficient

$\Delta\nu$ spectral passband

$\Delta\Omega$ solid angle of “field-of-view”

Lidar signal and skylight background

Atmospheric response:

$$P(r) = E_0 f_L Q(r) K \frac{A}{r^2} \frac{c\tau}{2} \beta_\pi(r) \exp\left(-2\int_0^r \alpha(x)\,dx\right)$$

Sky background:

$$P_{BGR} = E_\nu K A \Delta\Omega \Delta\nu f_L \tau$$

Signal to background:

$$\frac{P}{P_{BGR}} \sim \frac{E_0 \beta_\pi}{\Delta\Omega \Delta\nu}$$

$$\frac{\Delta\Omega(1\,mrad)}{\Delta\Omega(0.2\,mrad)} = 25$$

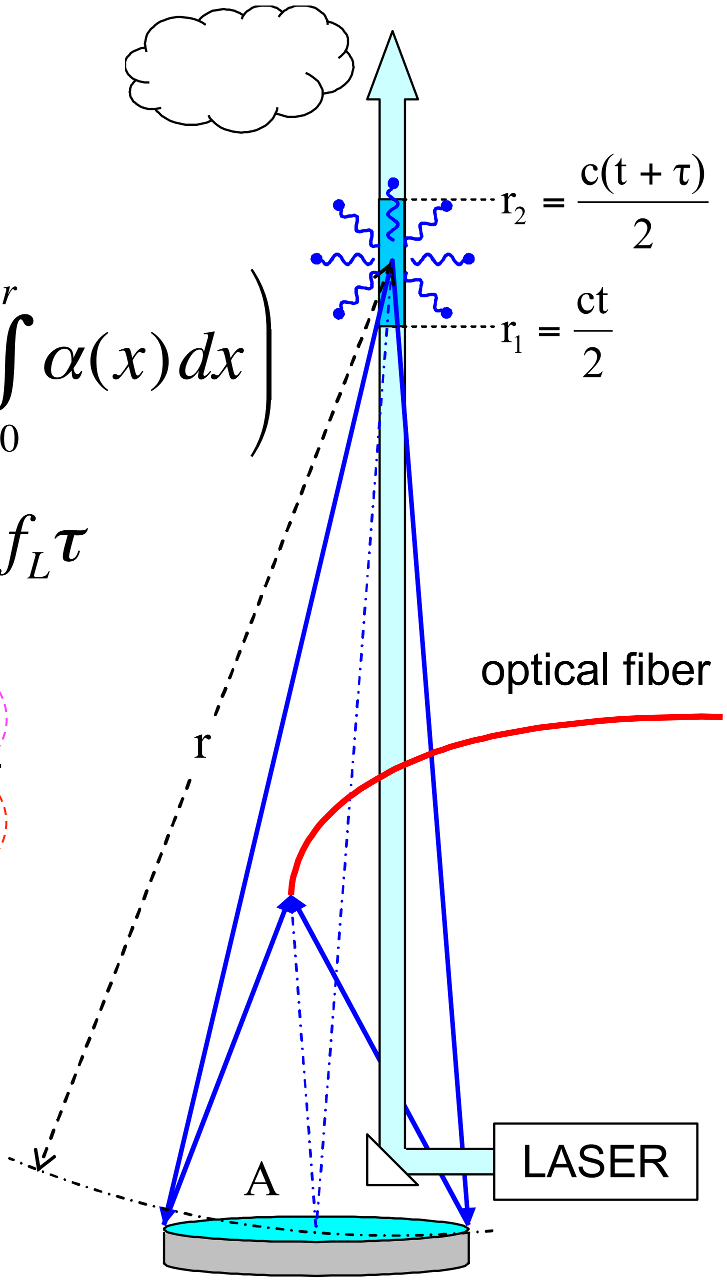

Overlap function: efficiency of light collection

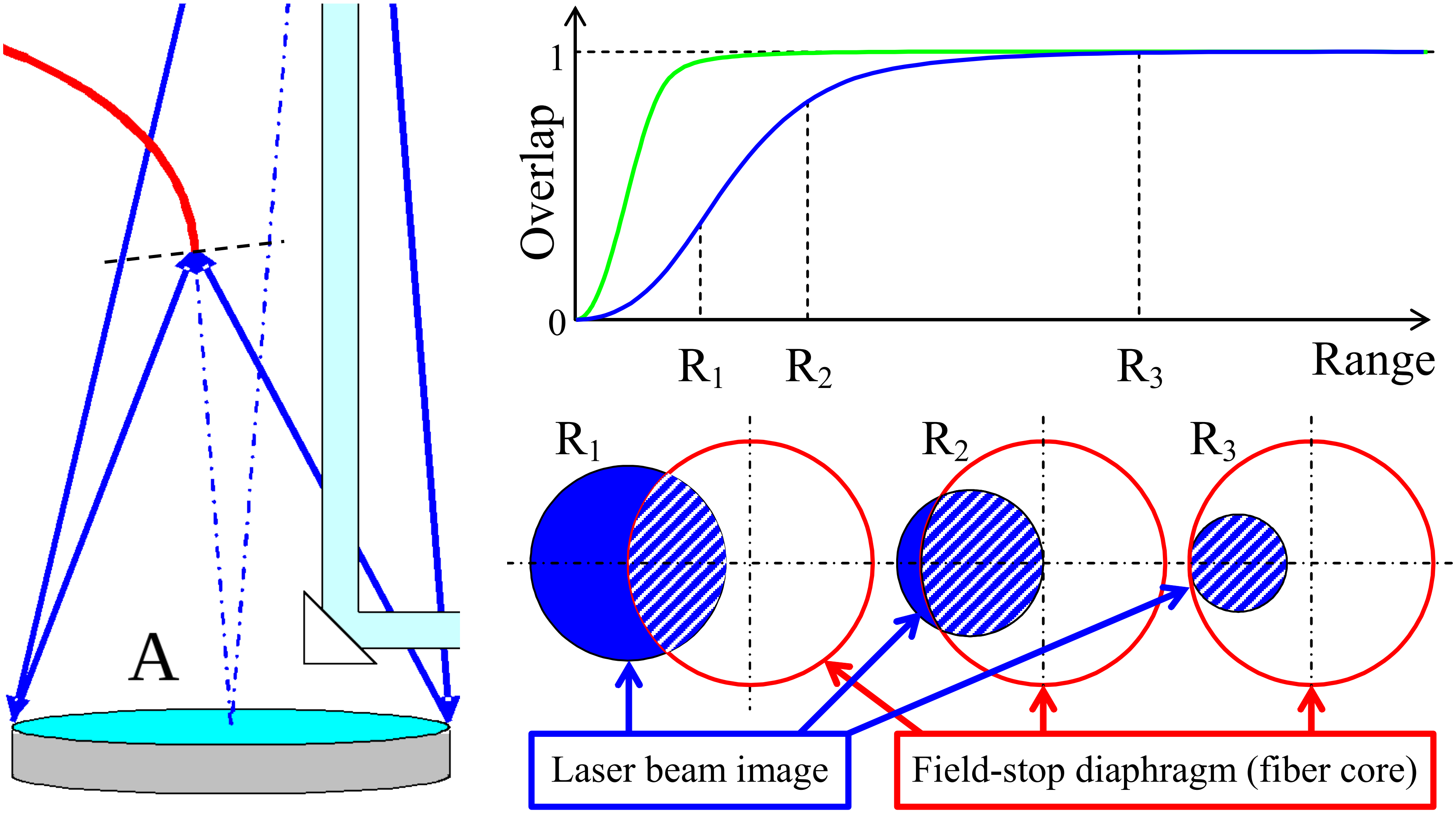

Telescope assignment

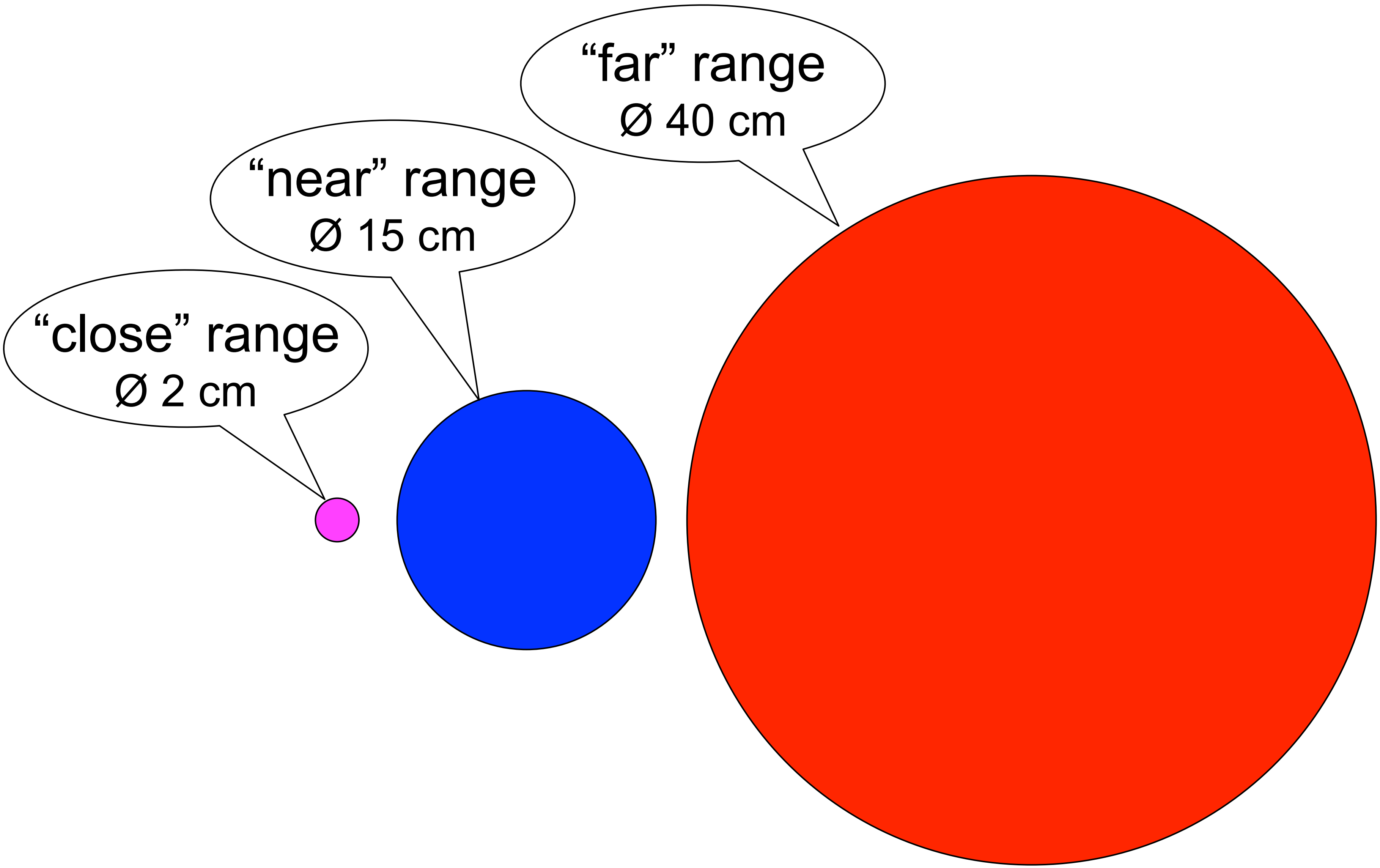

Overlap function & lidar returns

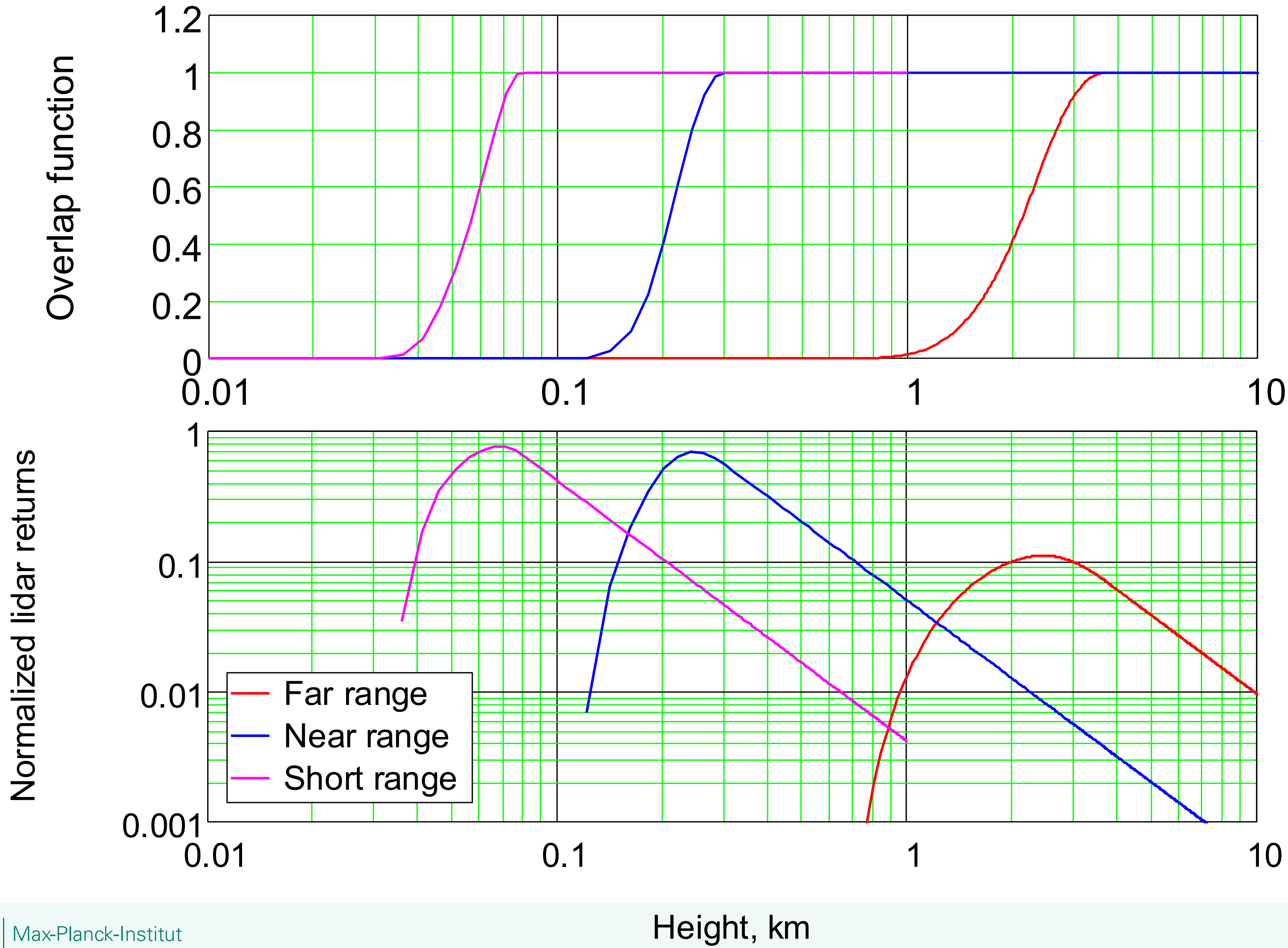

Principle lidar layout

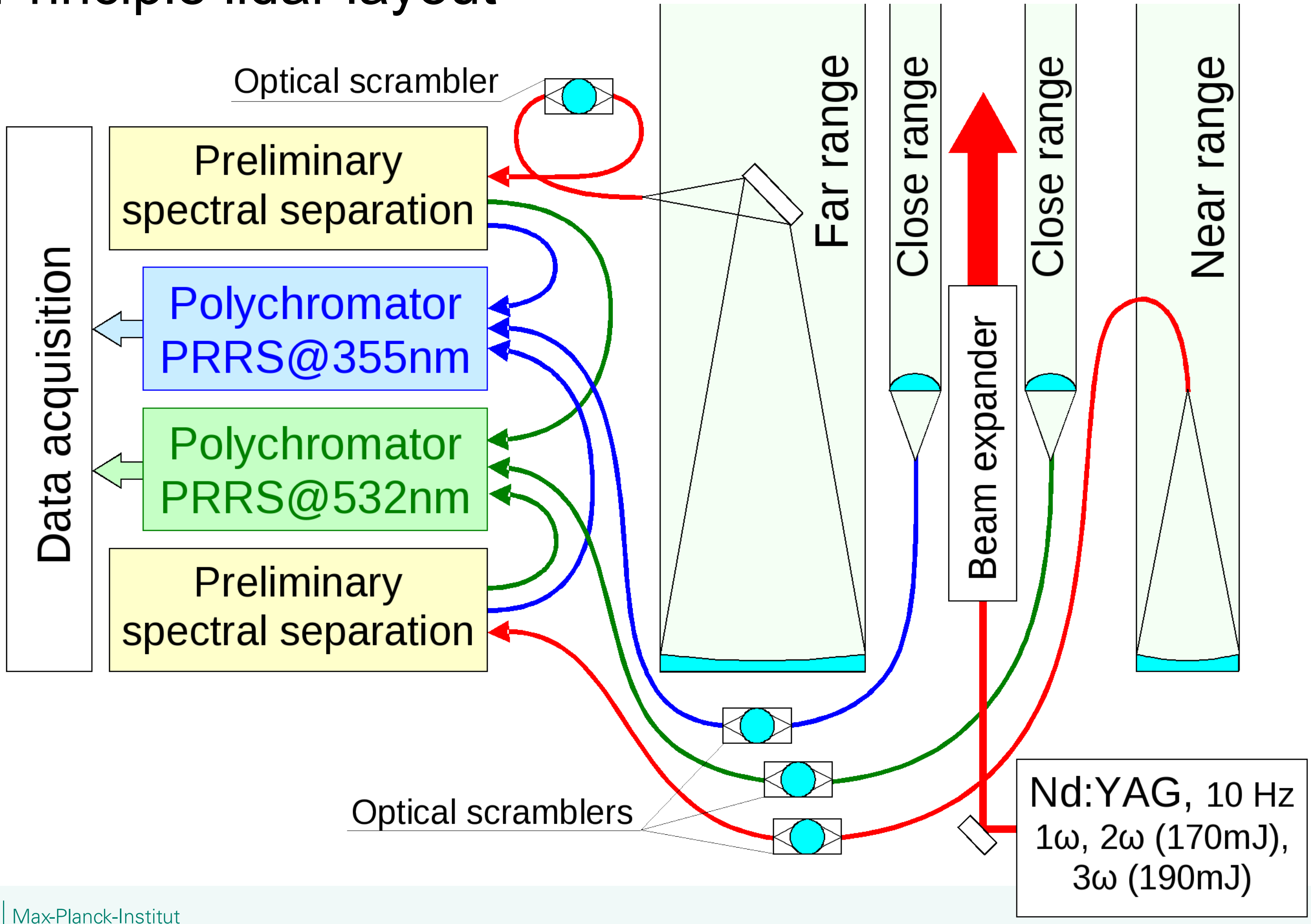

Preliminary spectral separation

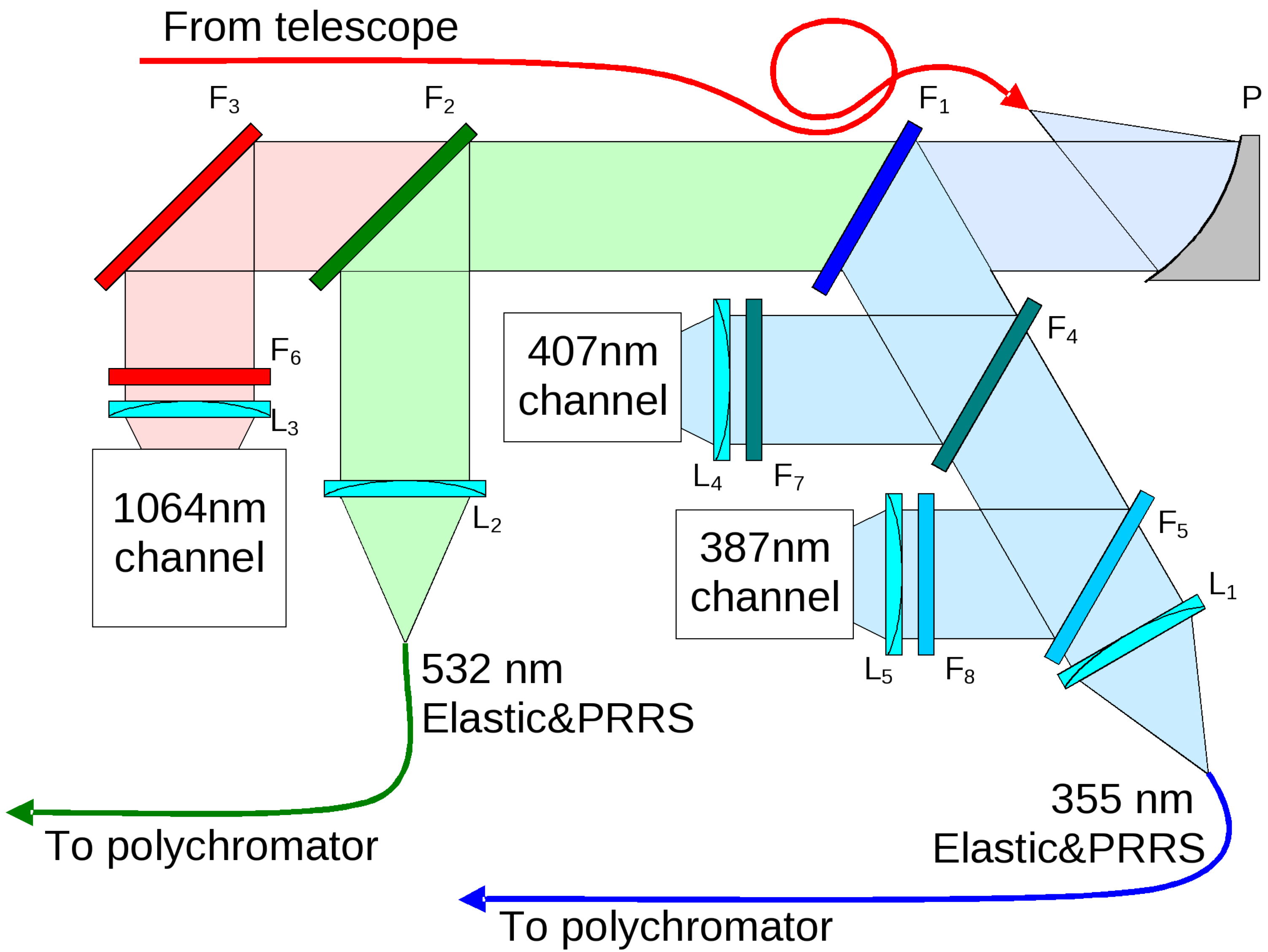

“Four telescopes” configuration

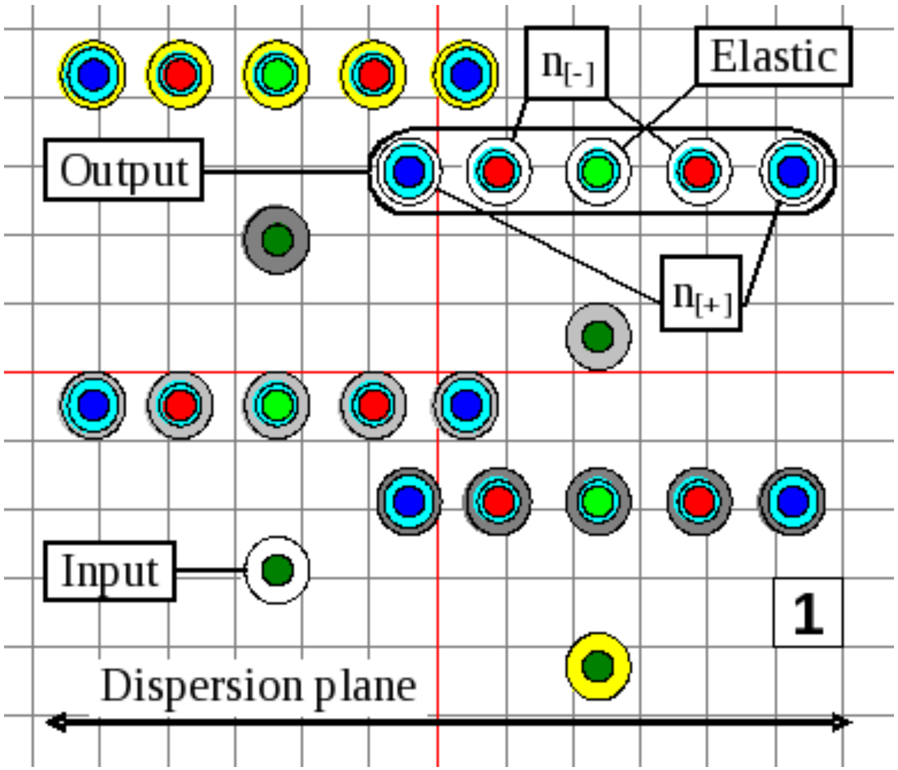

first unit

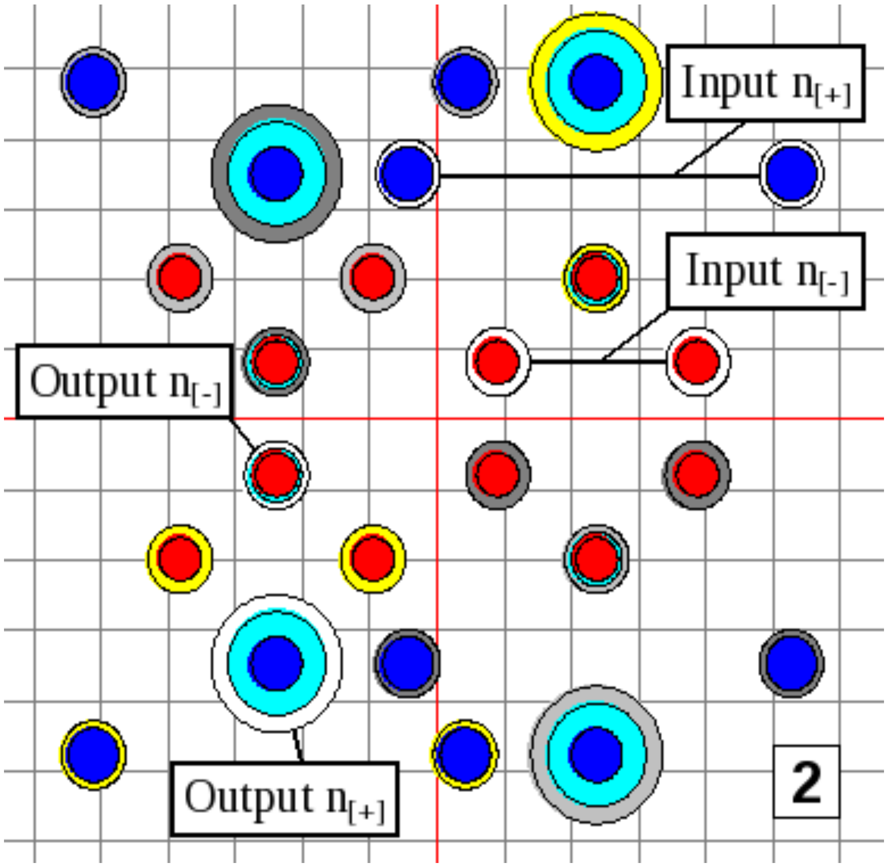

second unit

Overlap function, far range telescope

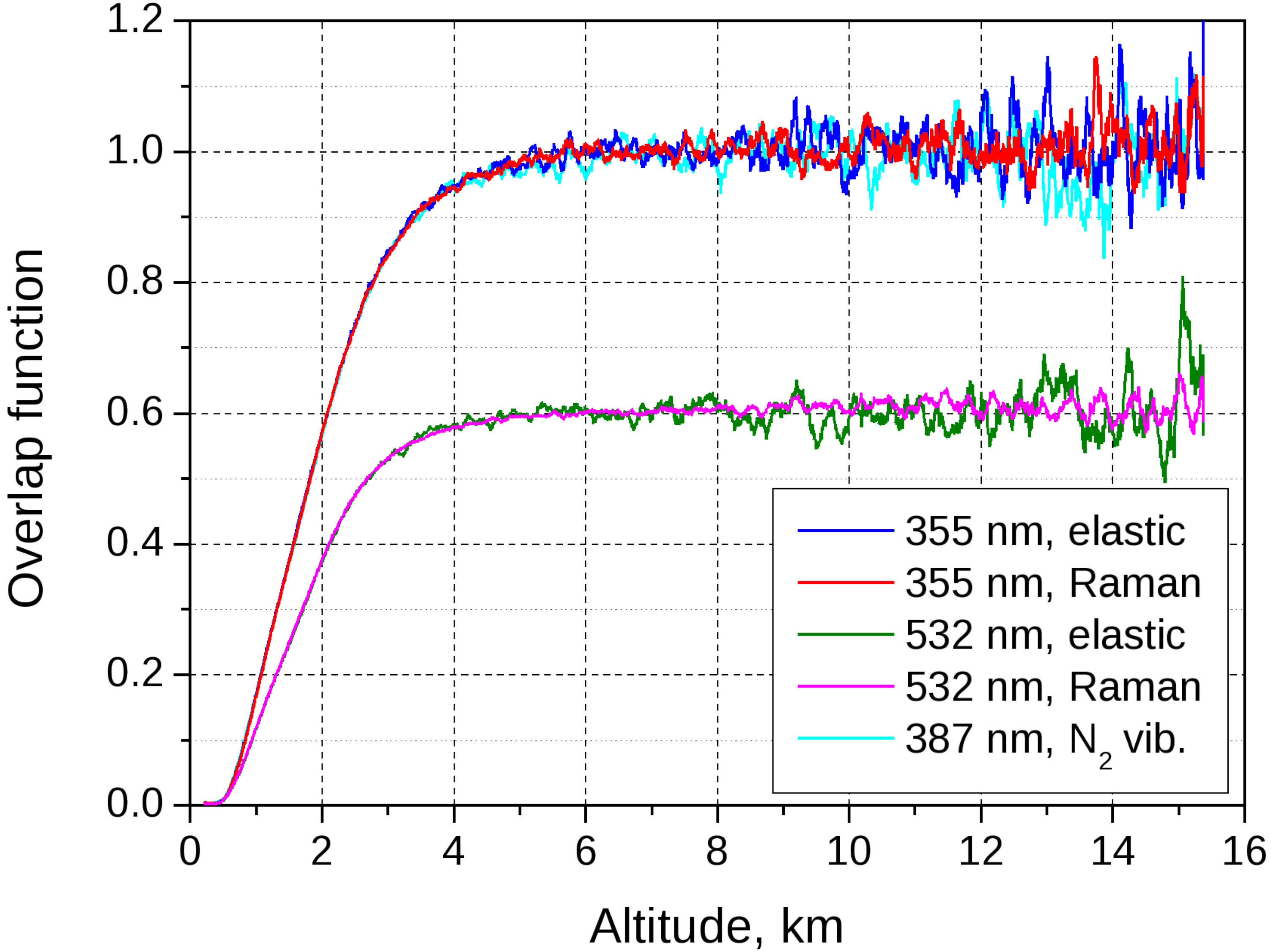

Overlap function, near range telescope

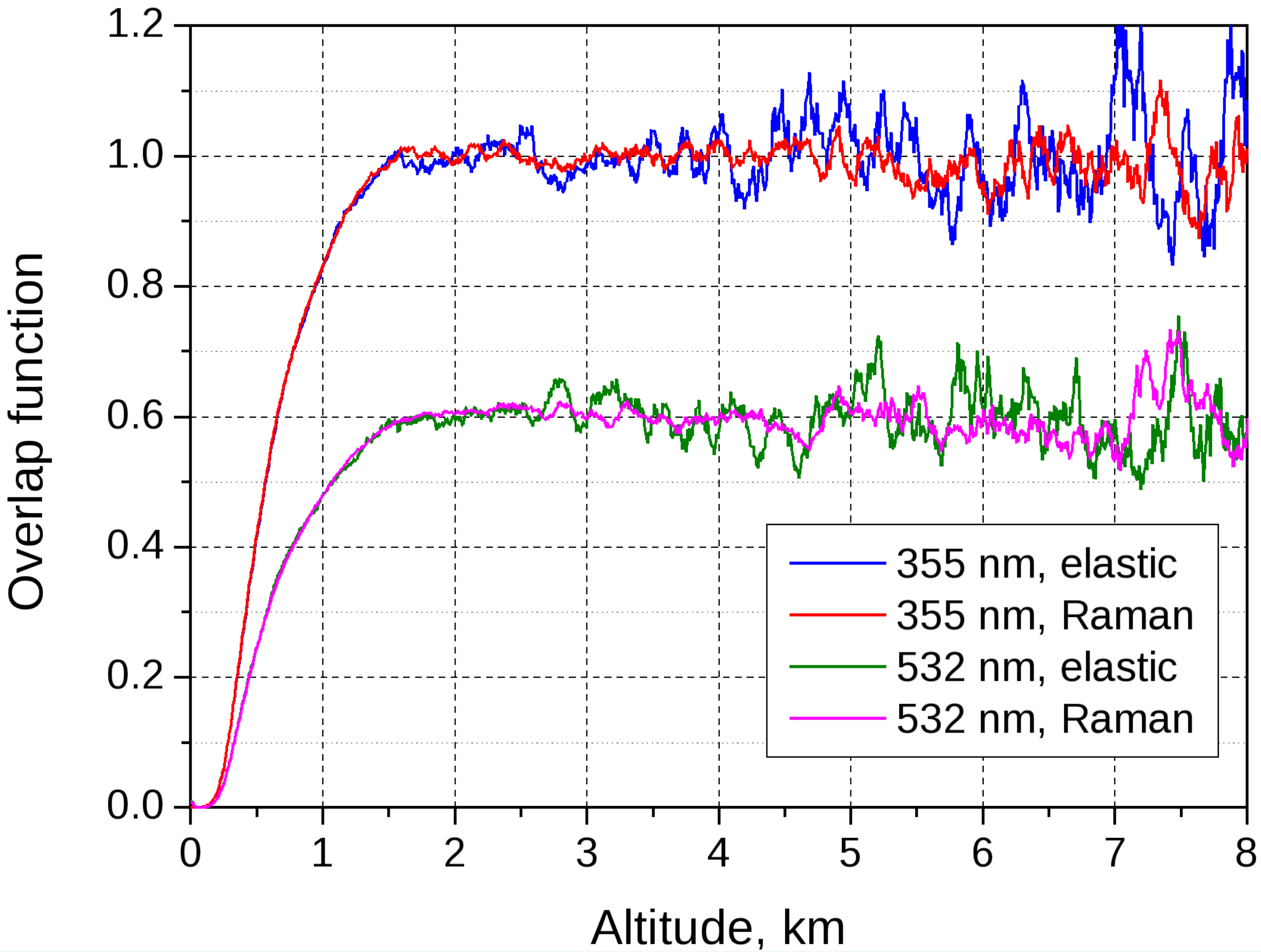

Particle backscatter 355 & 532, far- and near-range

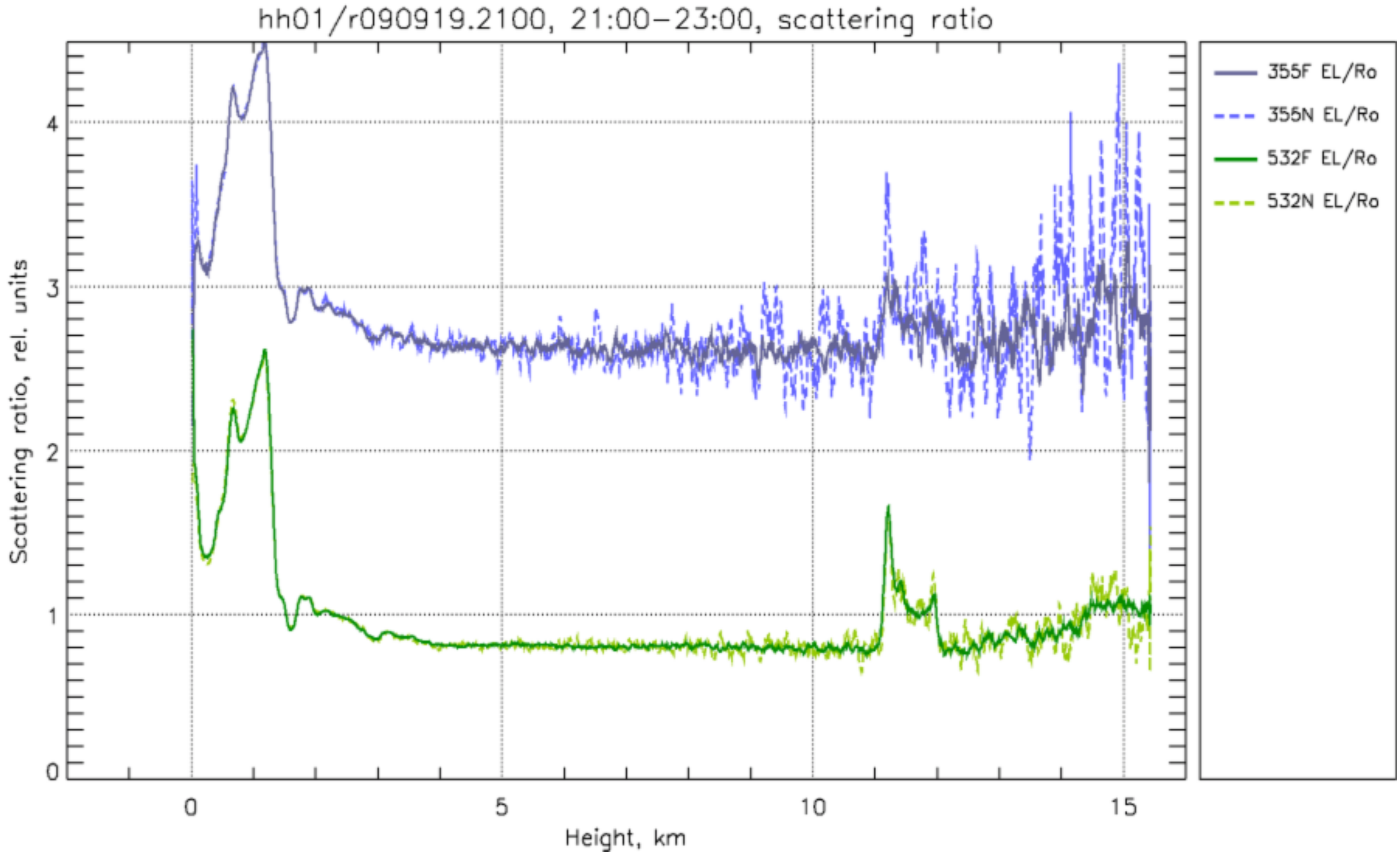

resolution: 30 minutes, 60÷180 meters; midnight

Particle backscatter 355 & 532, far- and near-range

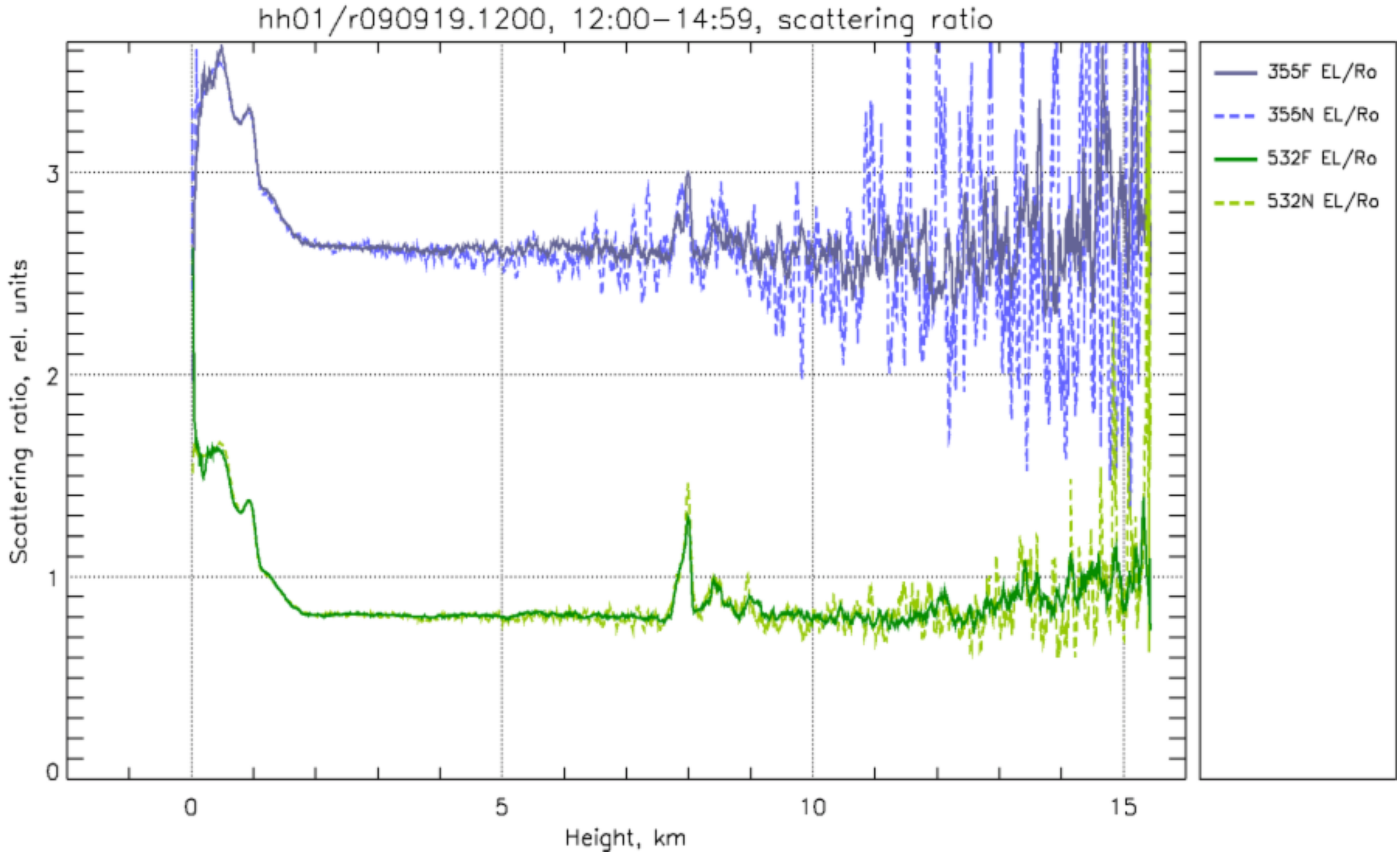

Max-Planck-Institut
für Meteorologie

resolution: 30 minutes, 60÷180 meters; midday

Particle backscatter 532nm, far & close range

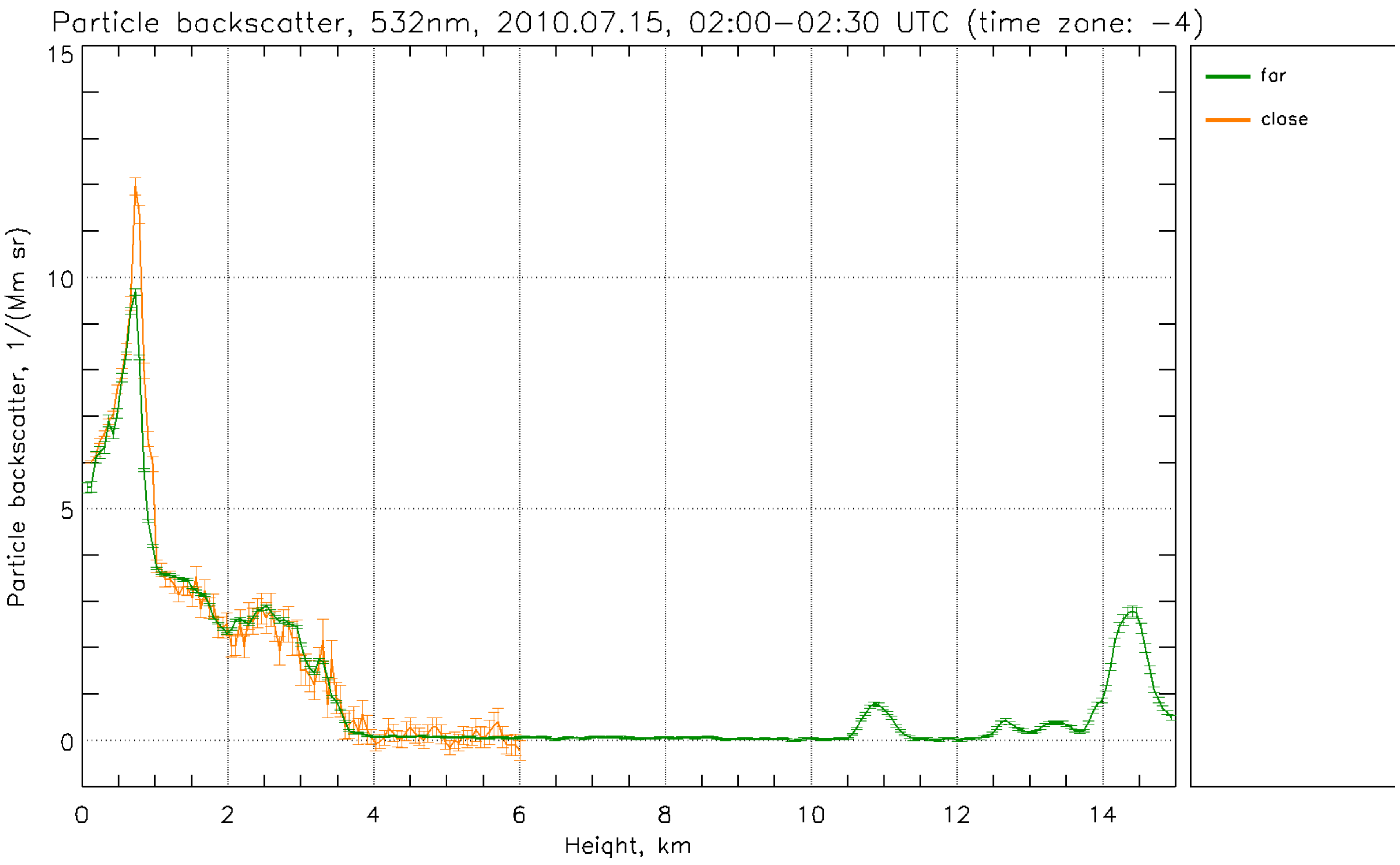

Max-Planck-Institut für Meteorologie

resolution: 30 minutes, 60÷180 meters; 22:00 Barbados time

Particle backscatter 532nm, far & close range

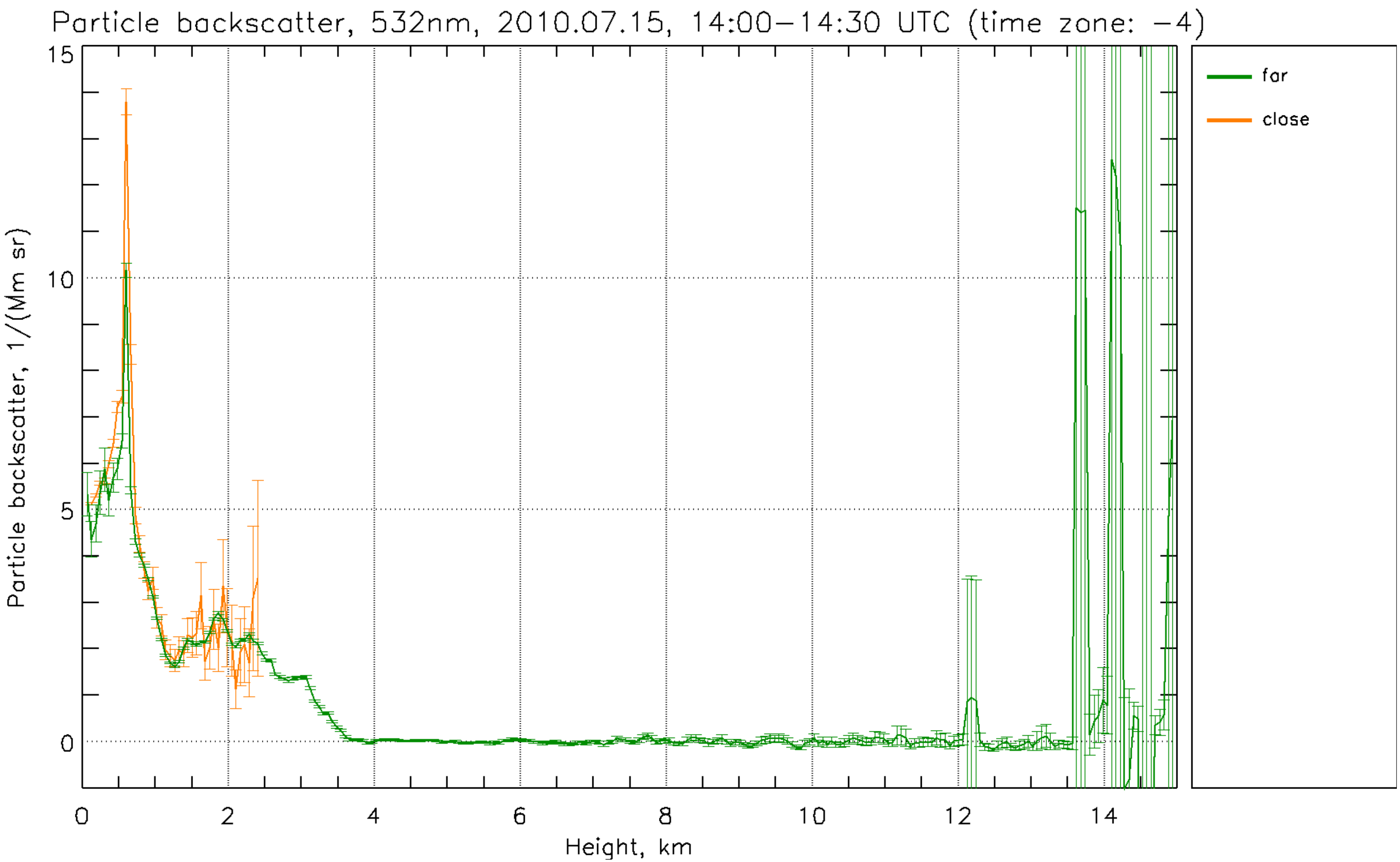

Max-Planck-Institut für Meteorologie

resolution: 30 minutes, 60÷180 meters; 10:00 Barbados time

Particle backscatter 532nm, far & close range

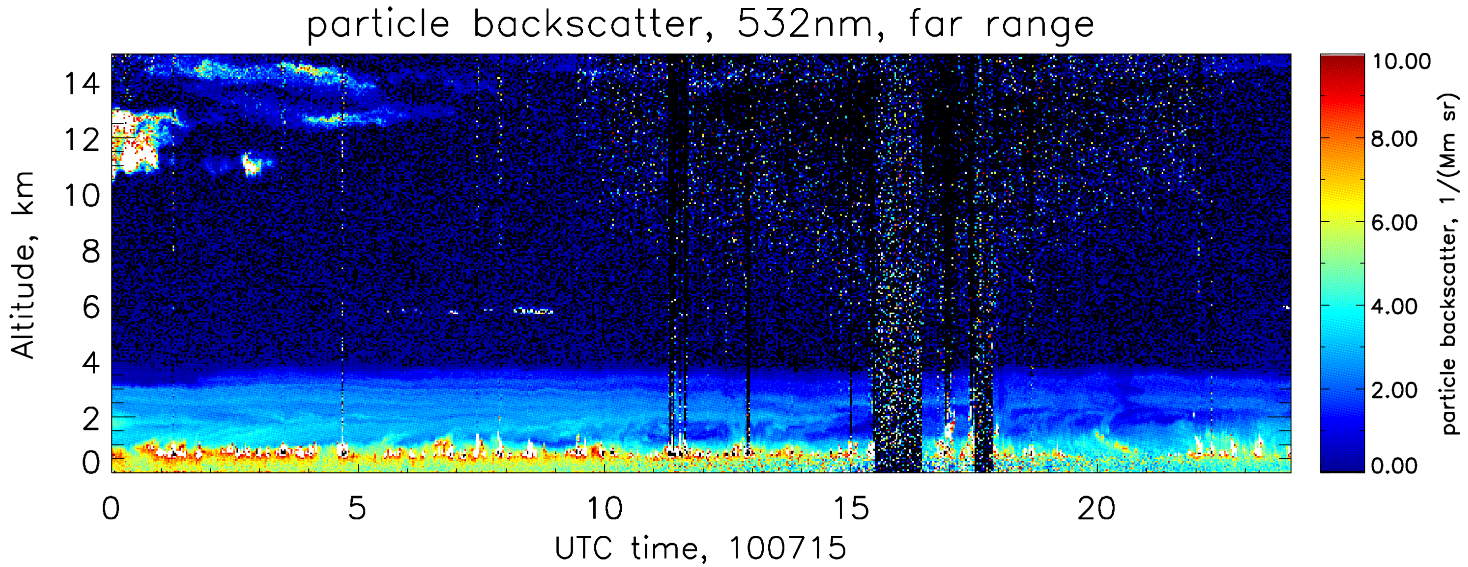

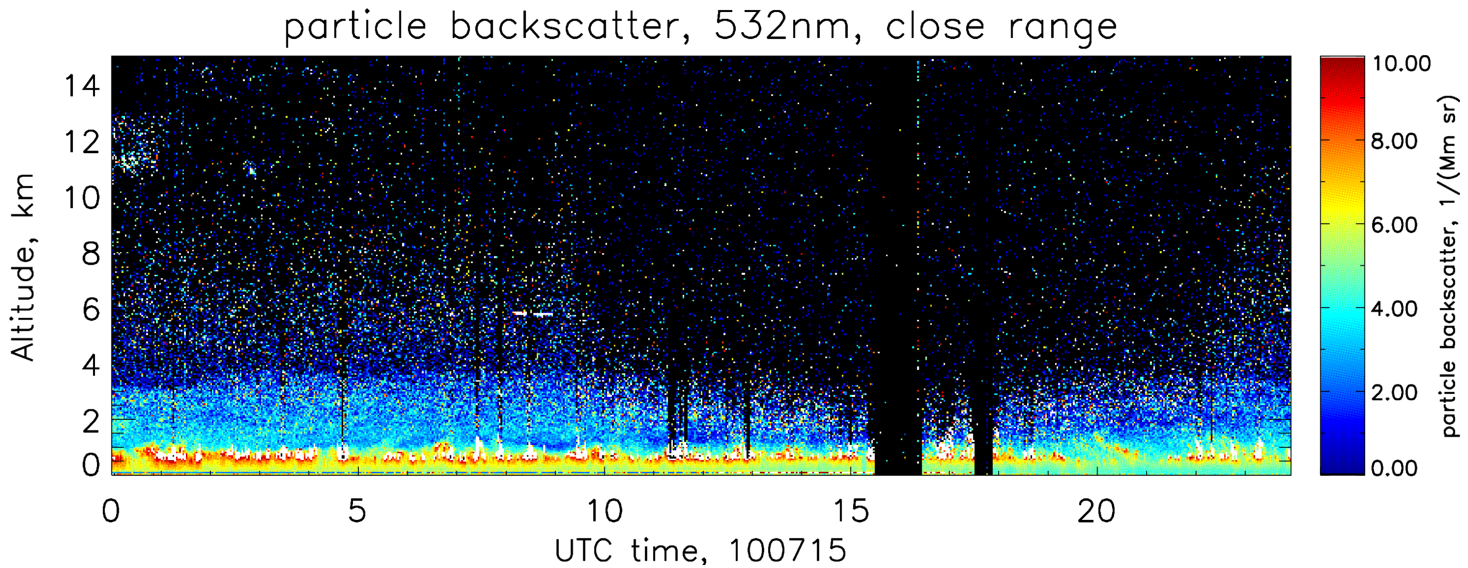

resolution: 2 minutes, 60 meters

Particle backscatter 532nm, far & close range

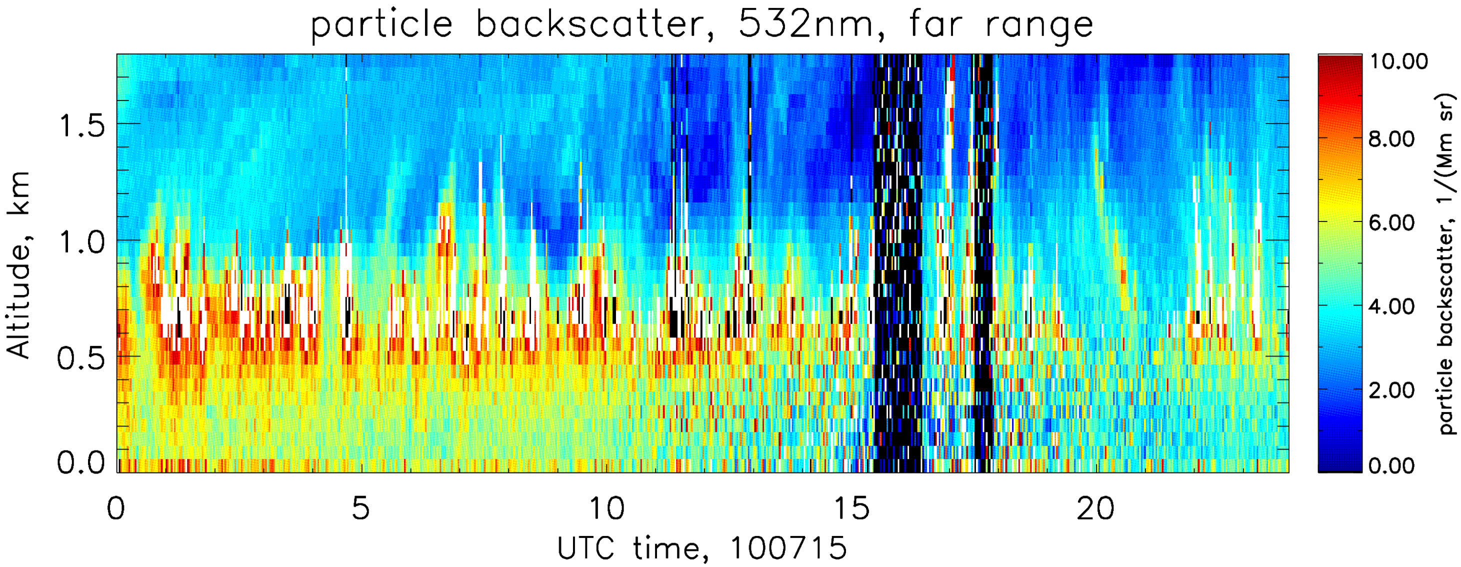

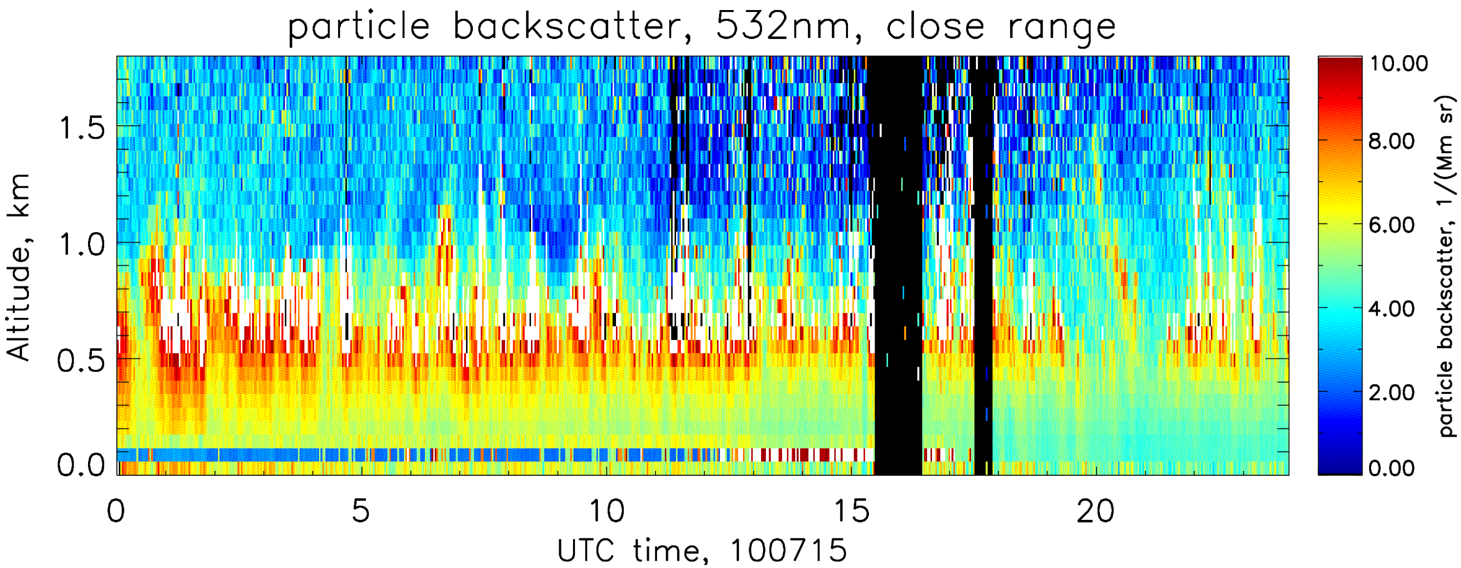

resolution: 2 minutes, 60 meters

Particle backscatter 355nm, far & near range

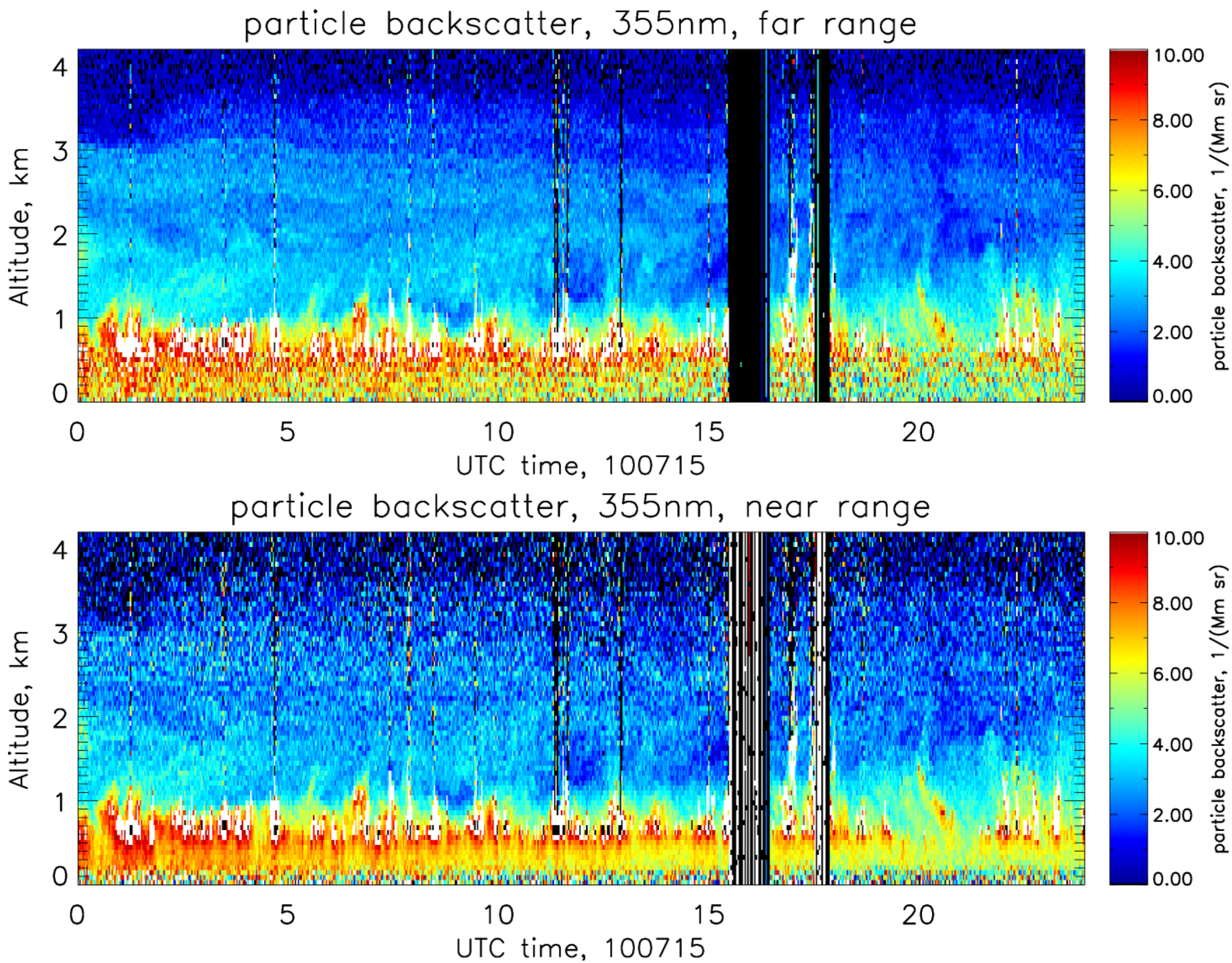

resolution: 2 minutes, 60 meters

Raman lidar returns, 532nm, near & far range

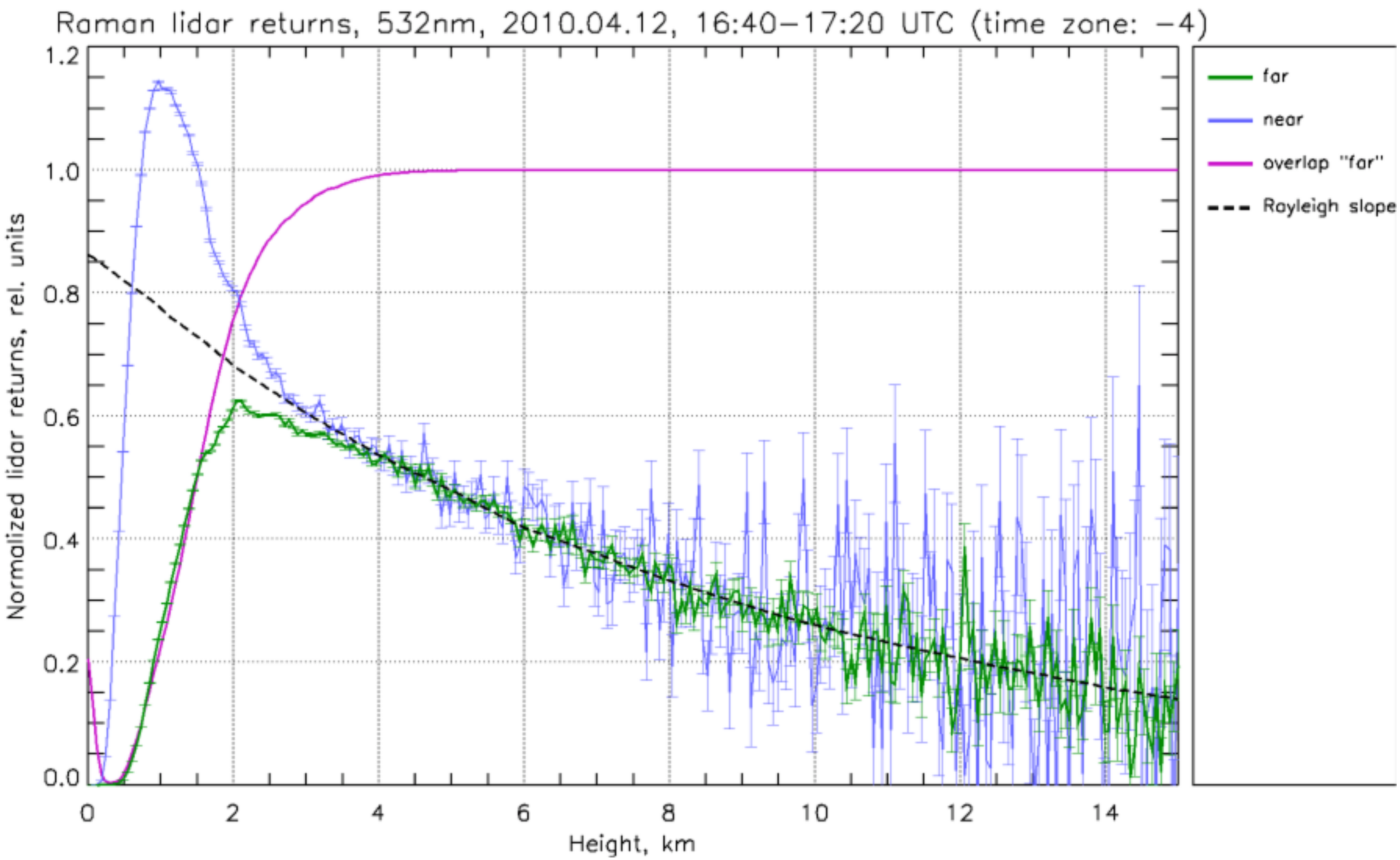

resolution: signals: 40 minutes, 60m
overlap: 3 hours, 60m÷5km

Statistical uncertainty of lidar returns, near & far range

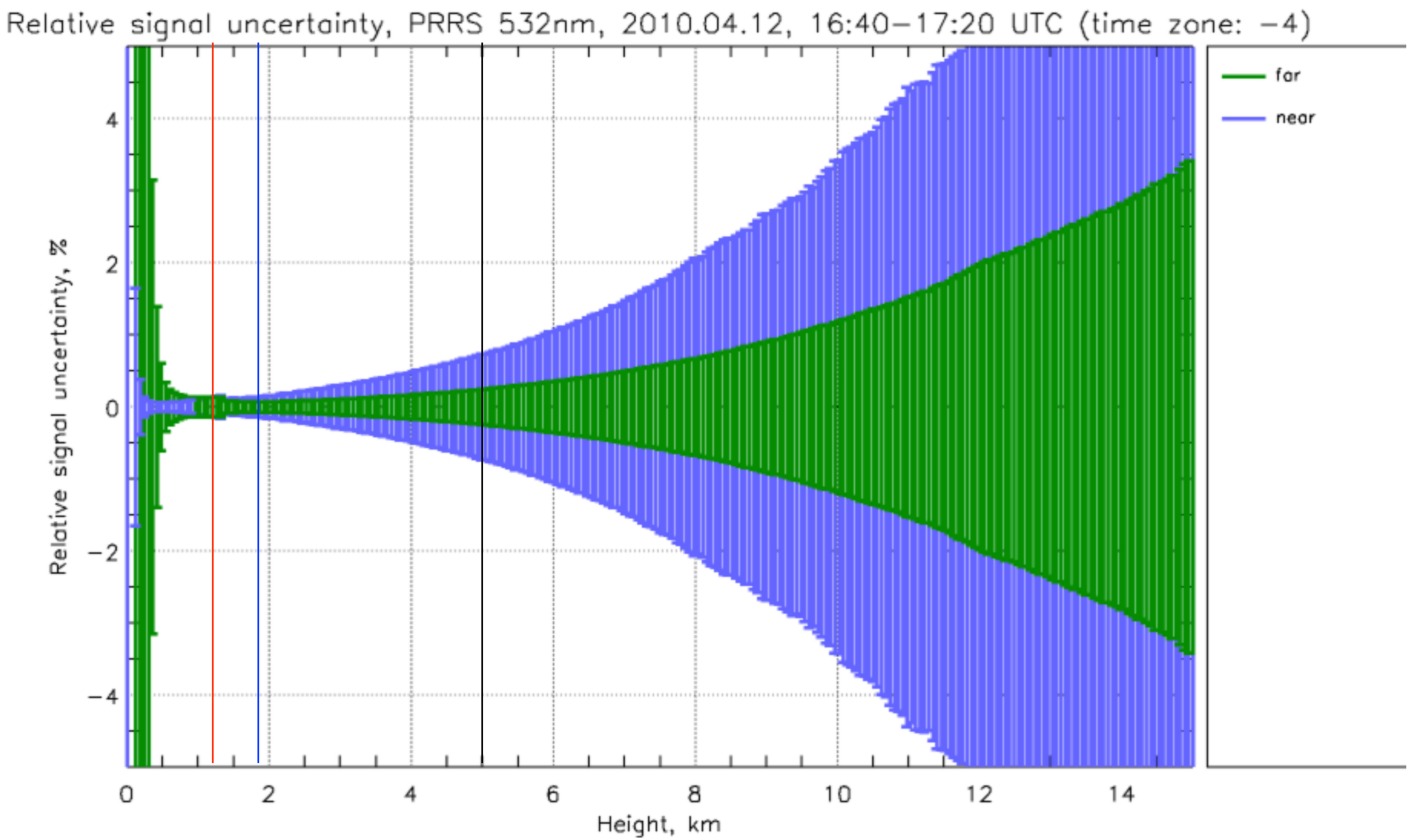

Raman lidar returns, 532nm, near & far range

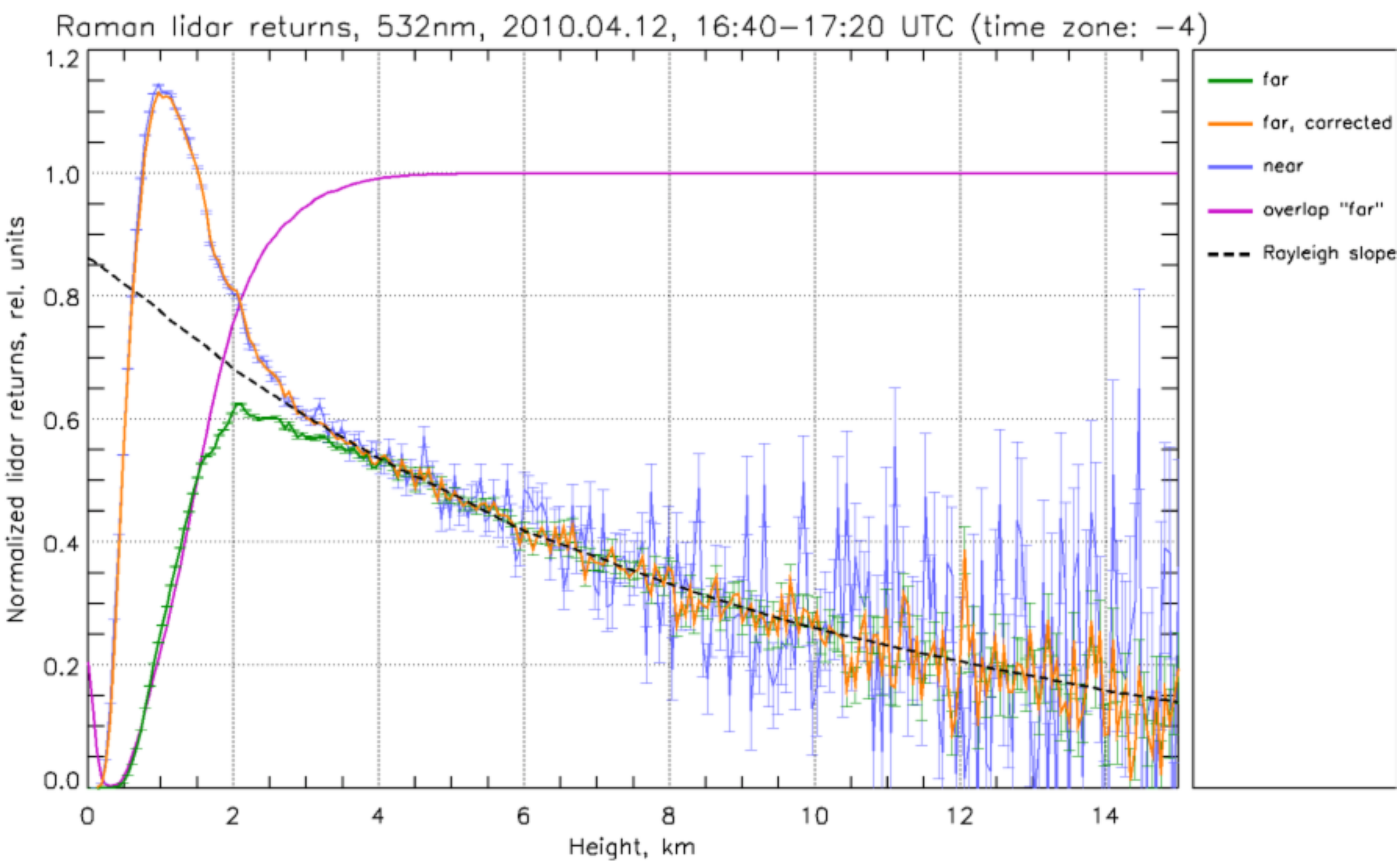

resolution: signals: 40 minutes, 60m
overlap: 3 hours, 60m÷5km

Particle extinction, 532nm, near & far range

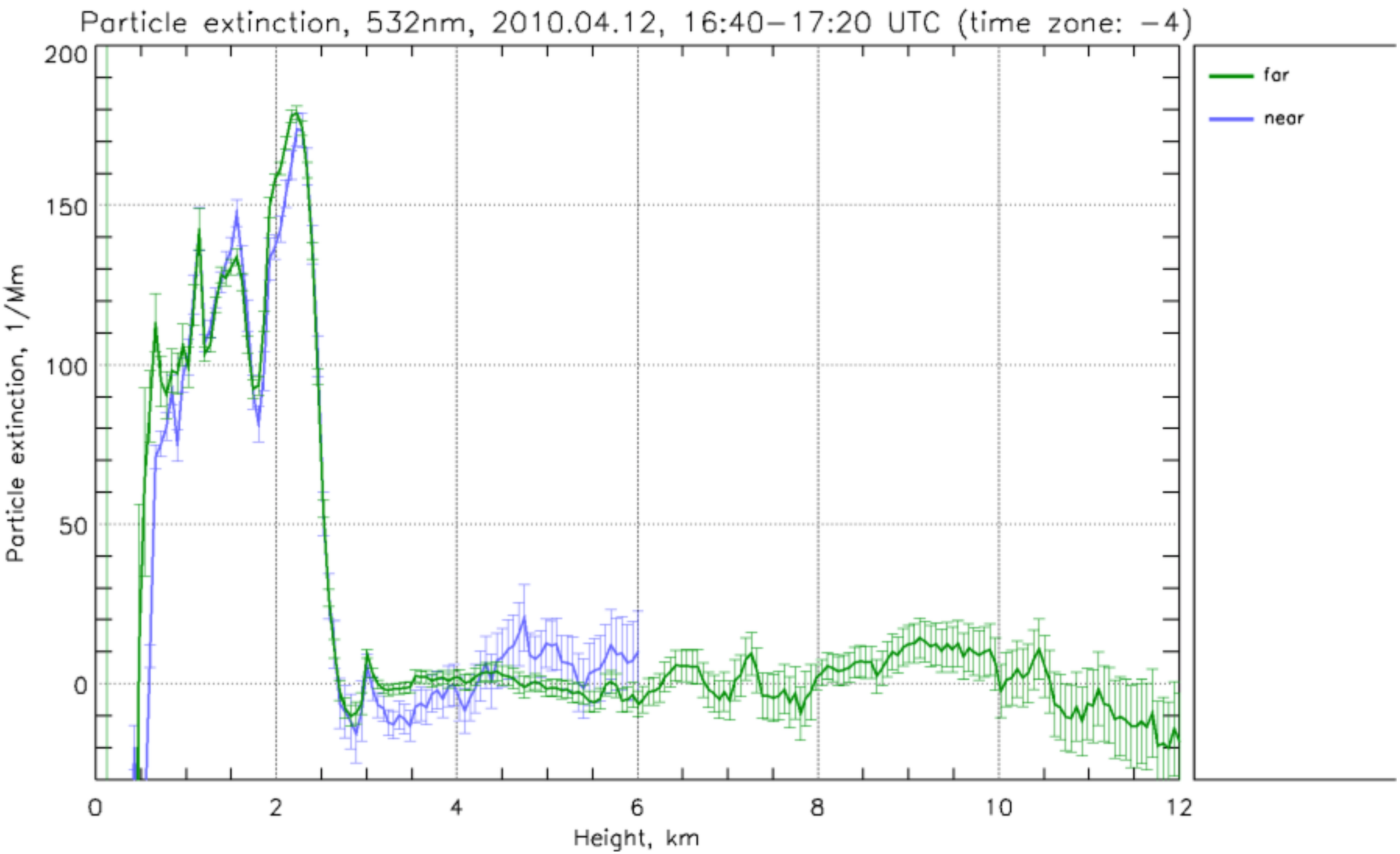

resolution: 40 minutes, 0.18÷3km

Overlap long term stability

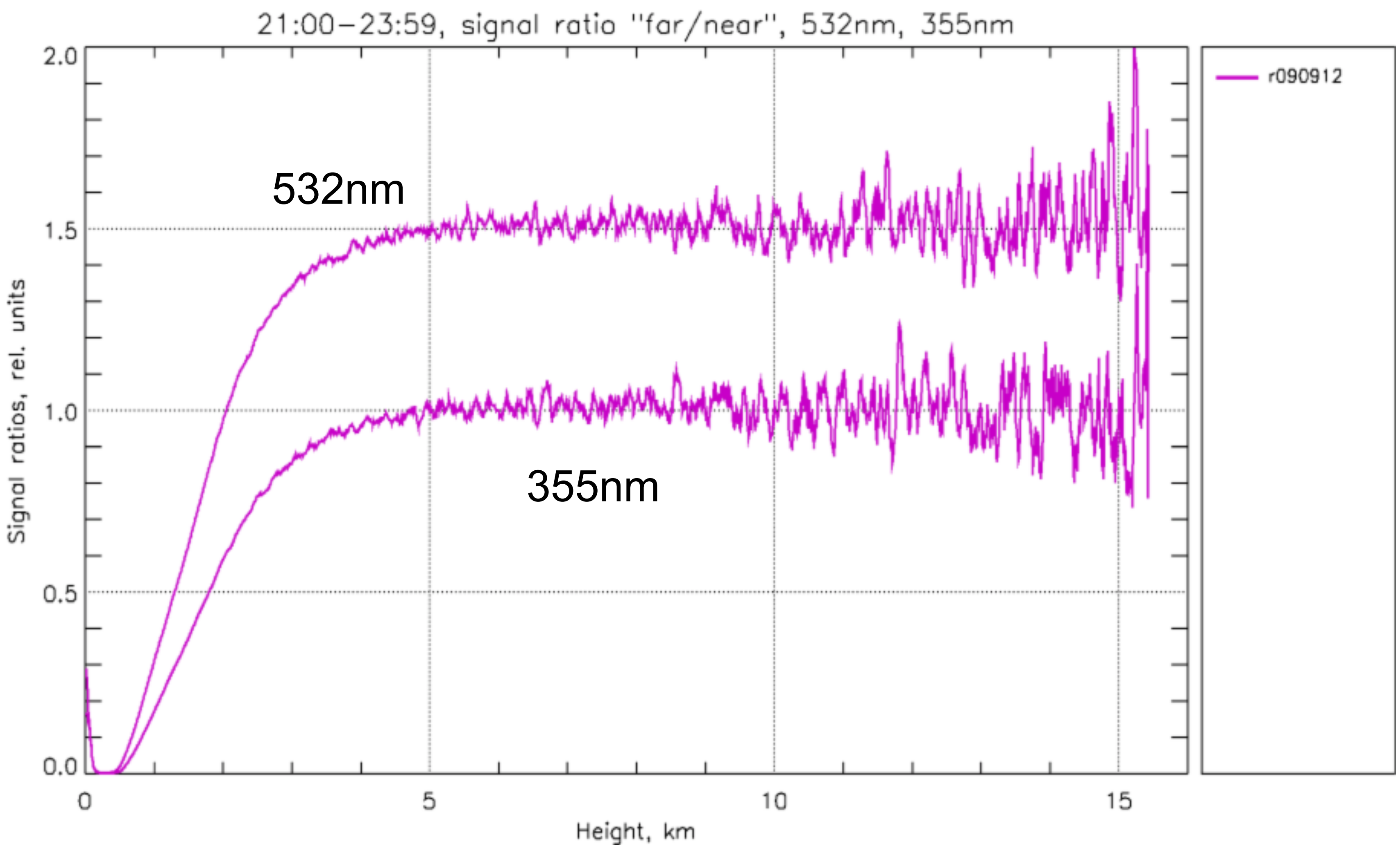

Overlap long term stability

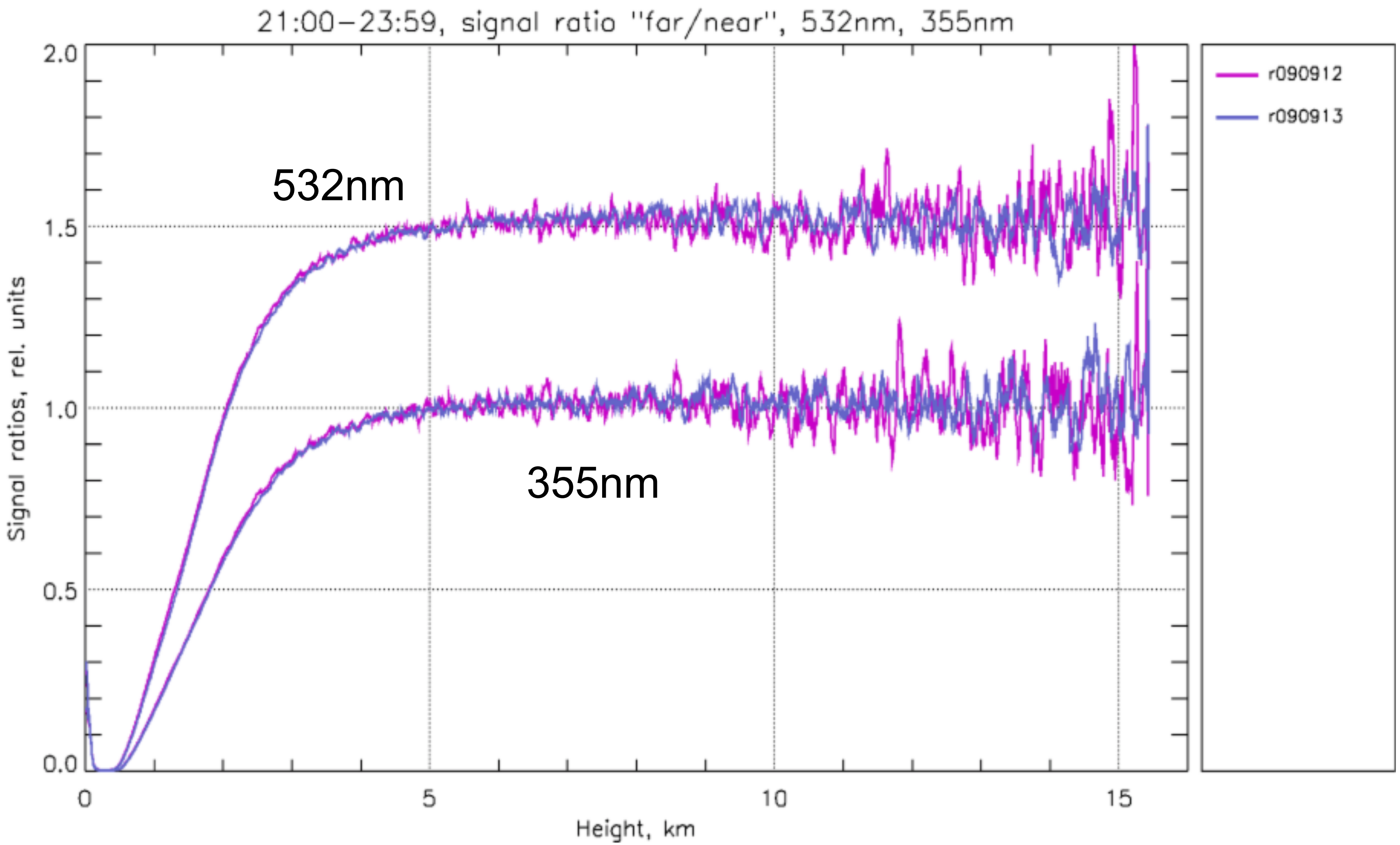

Overlap long term stability

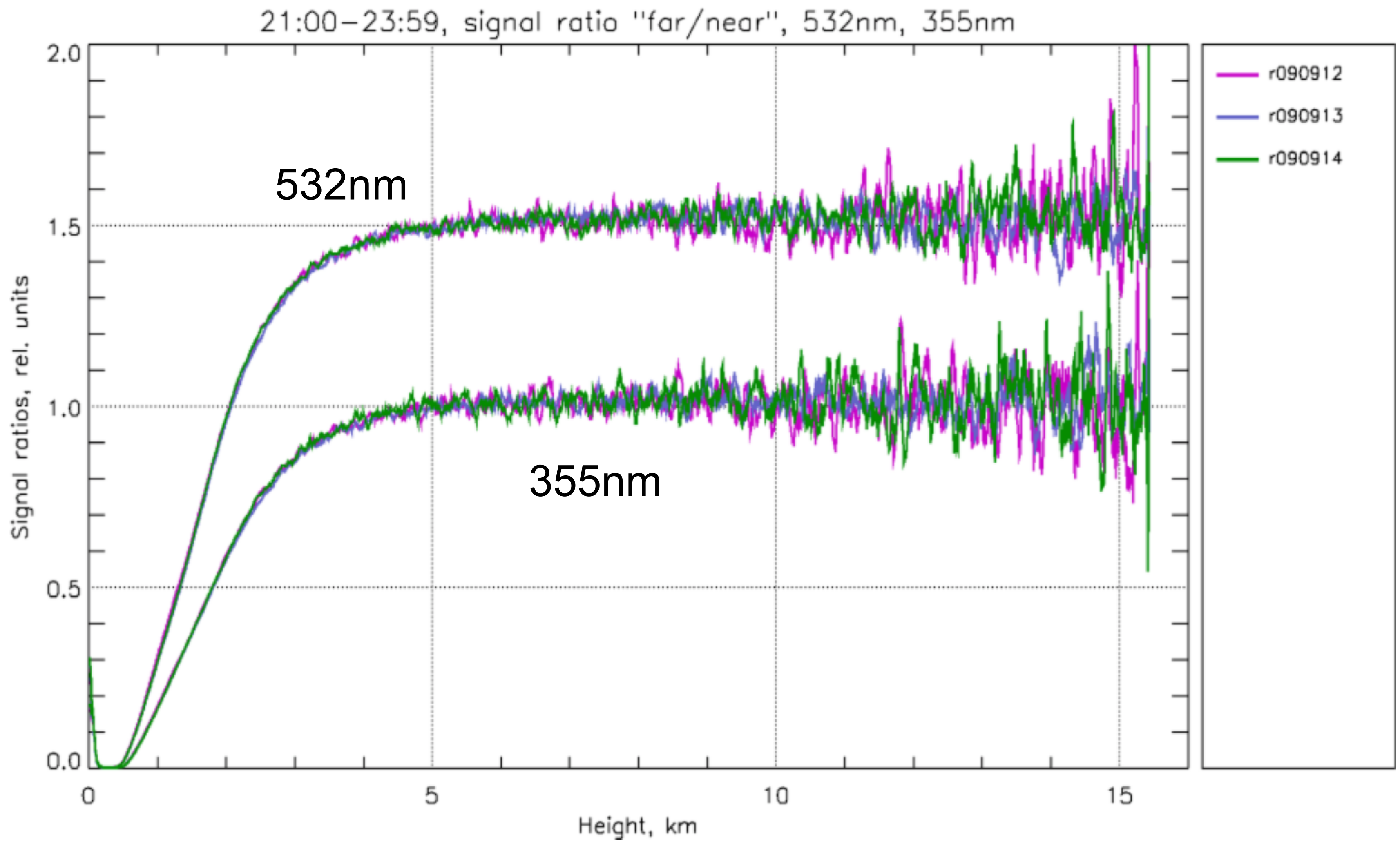

Overlap long term stability

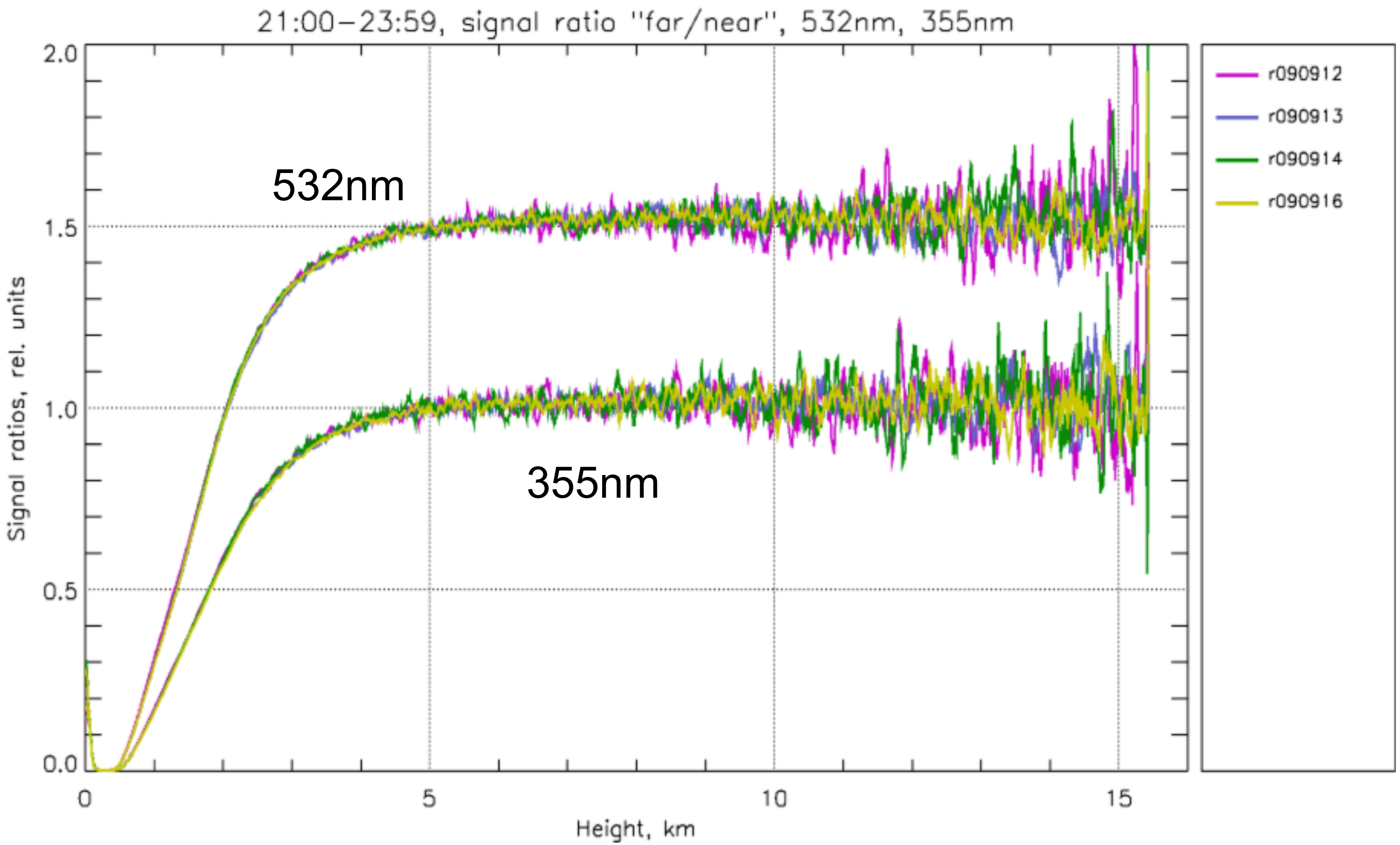

Overlap long term stability

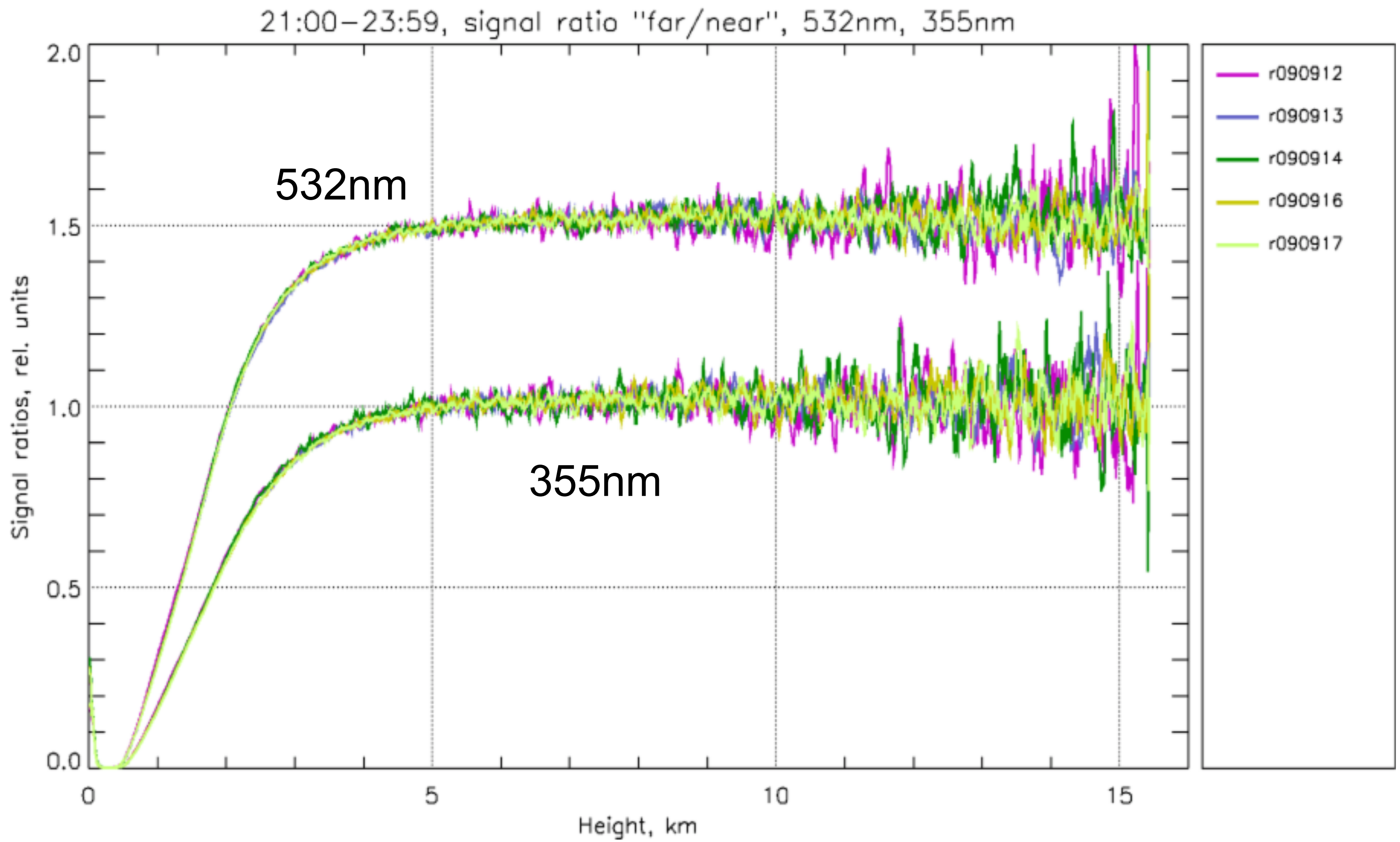

Overlap long term stability

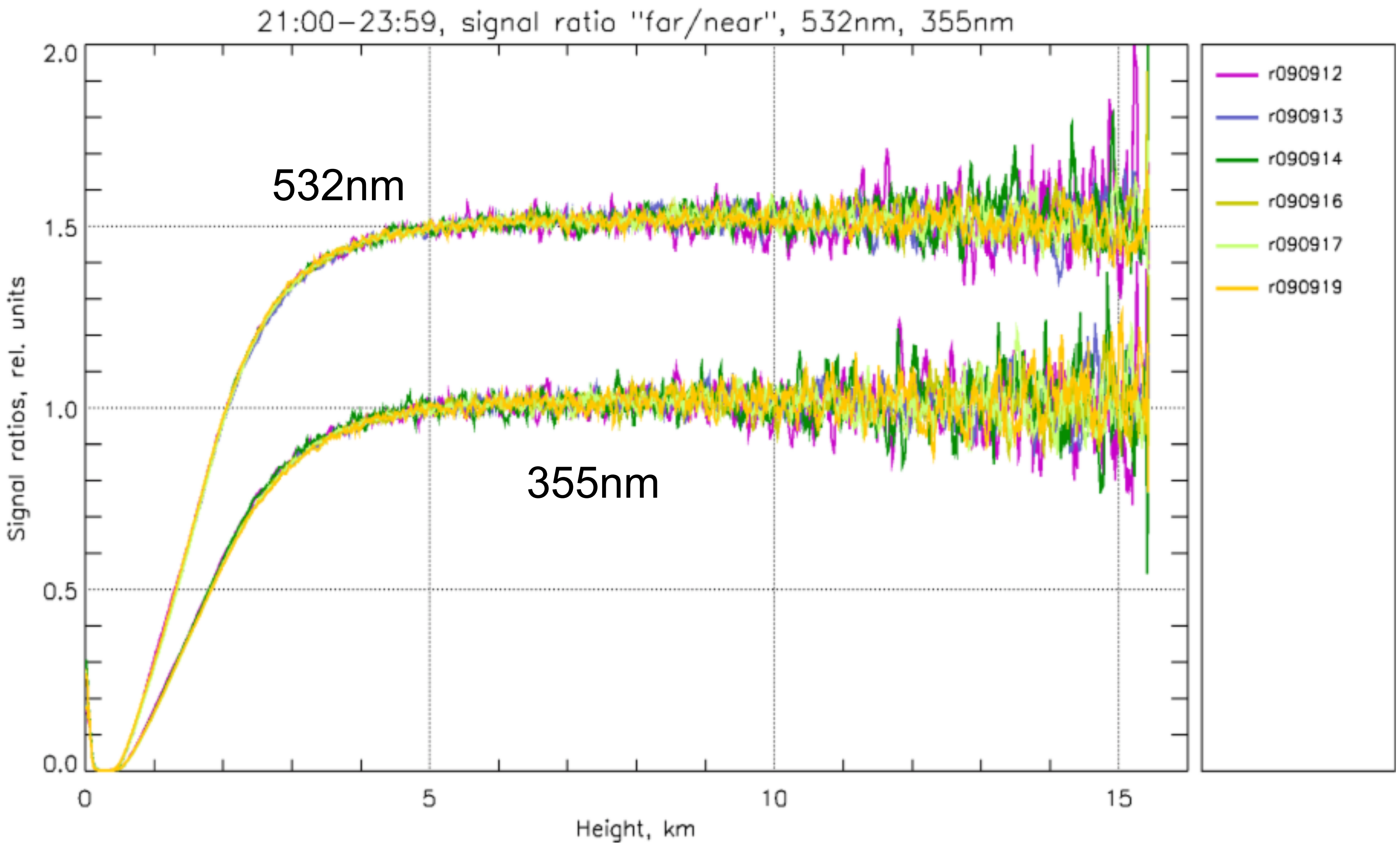

Overlap long term stability

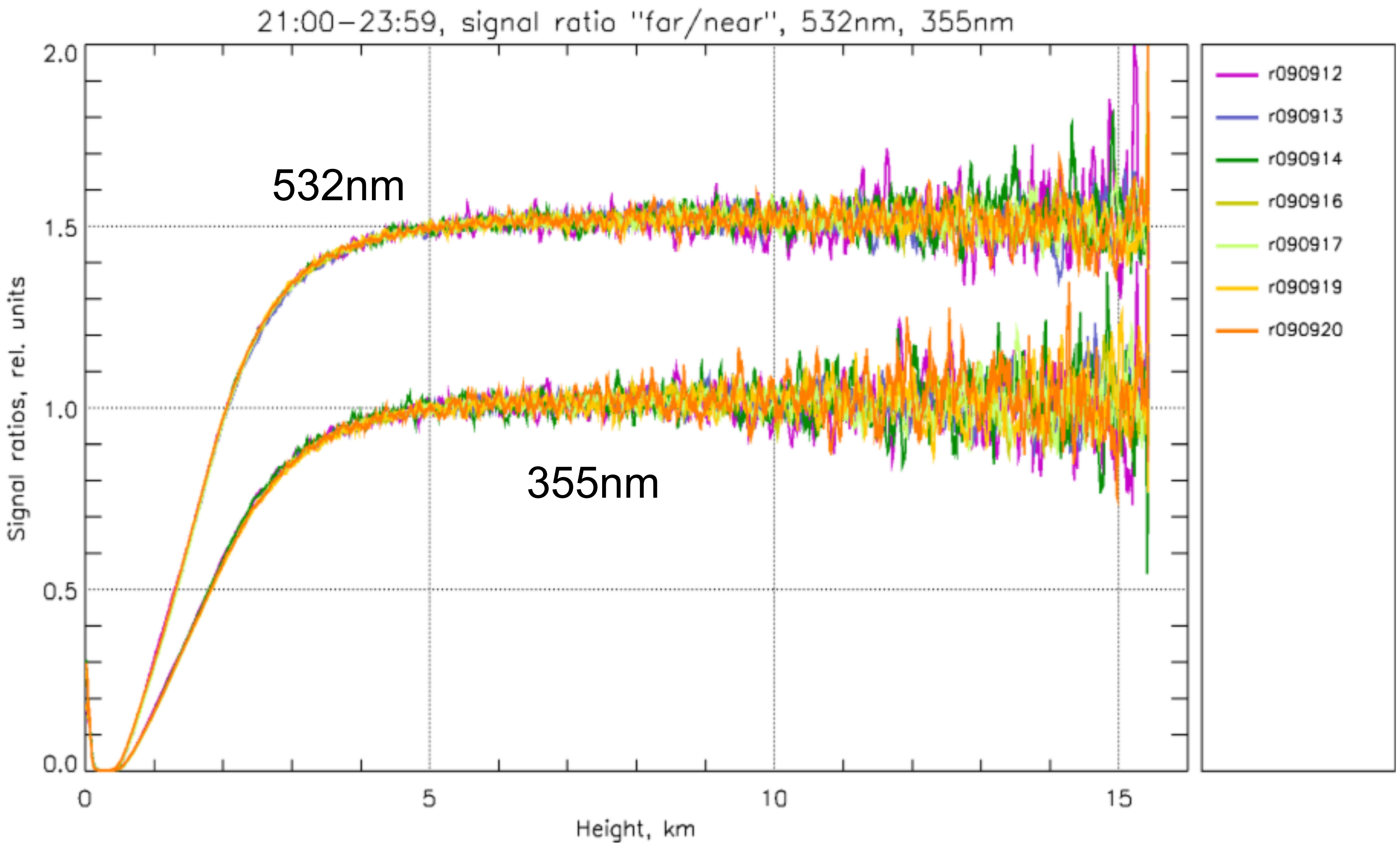

Overlap, 24h stability

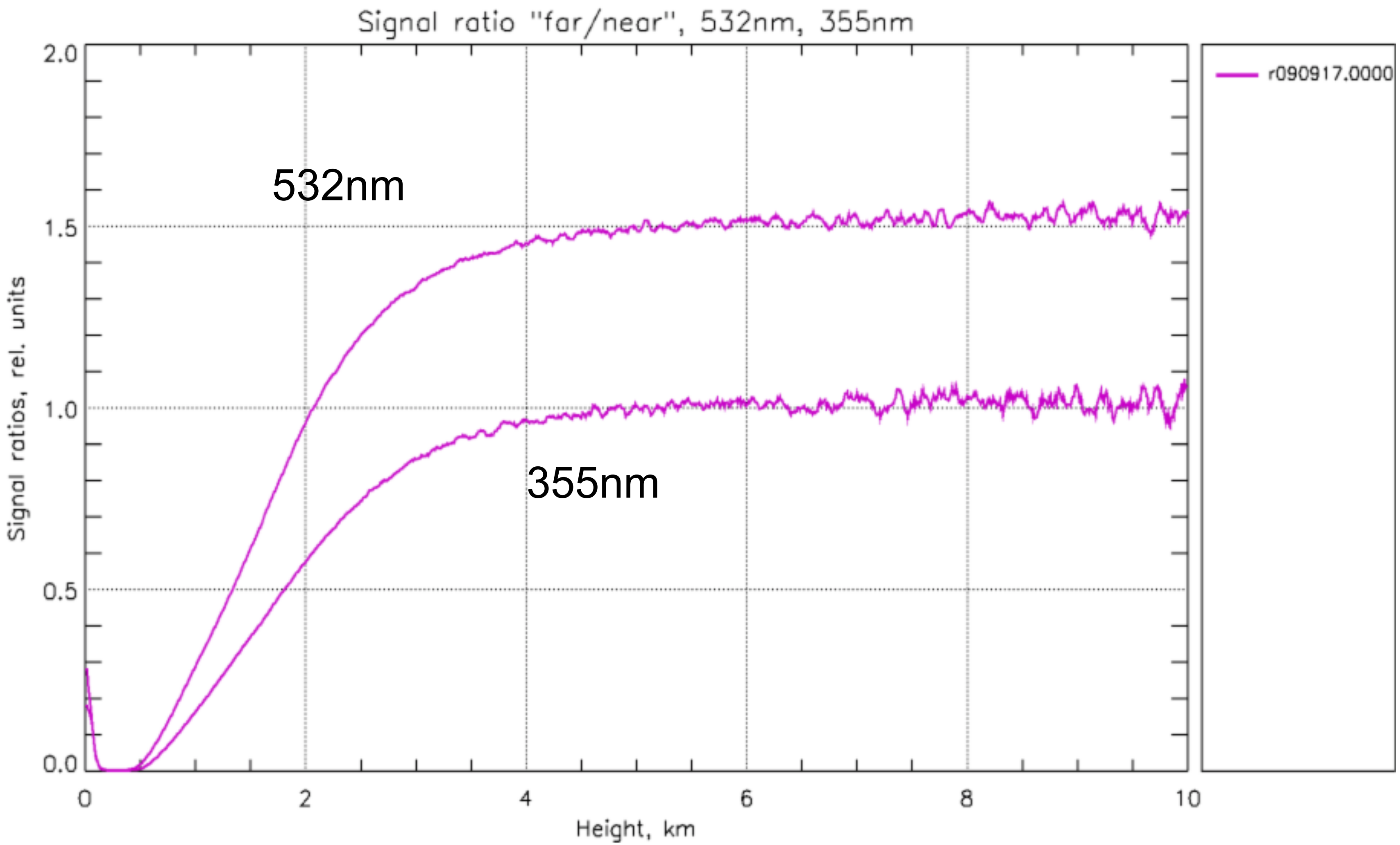

Overlap, 24h stability

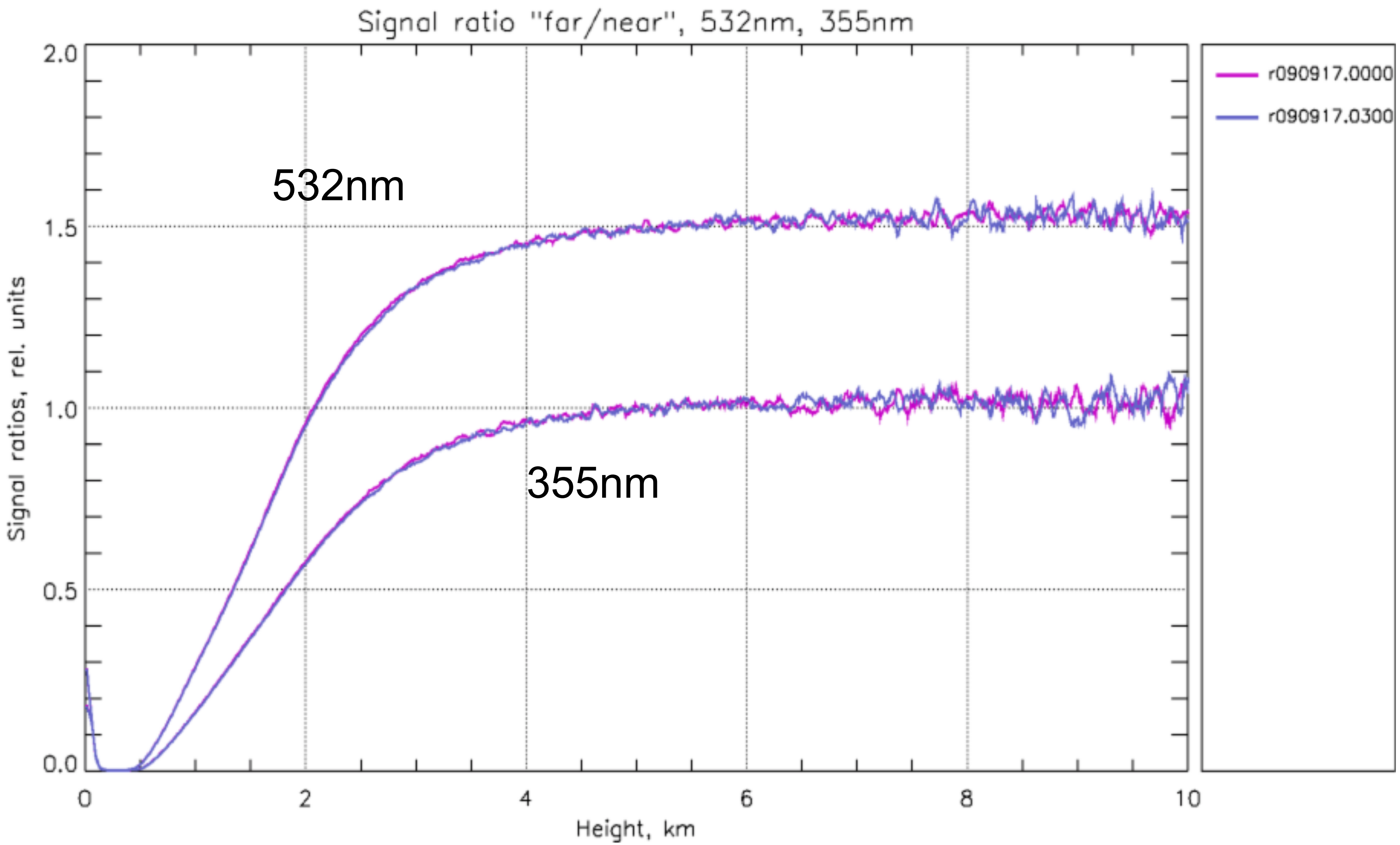

Overlap, 24h stability

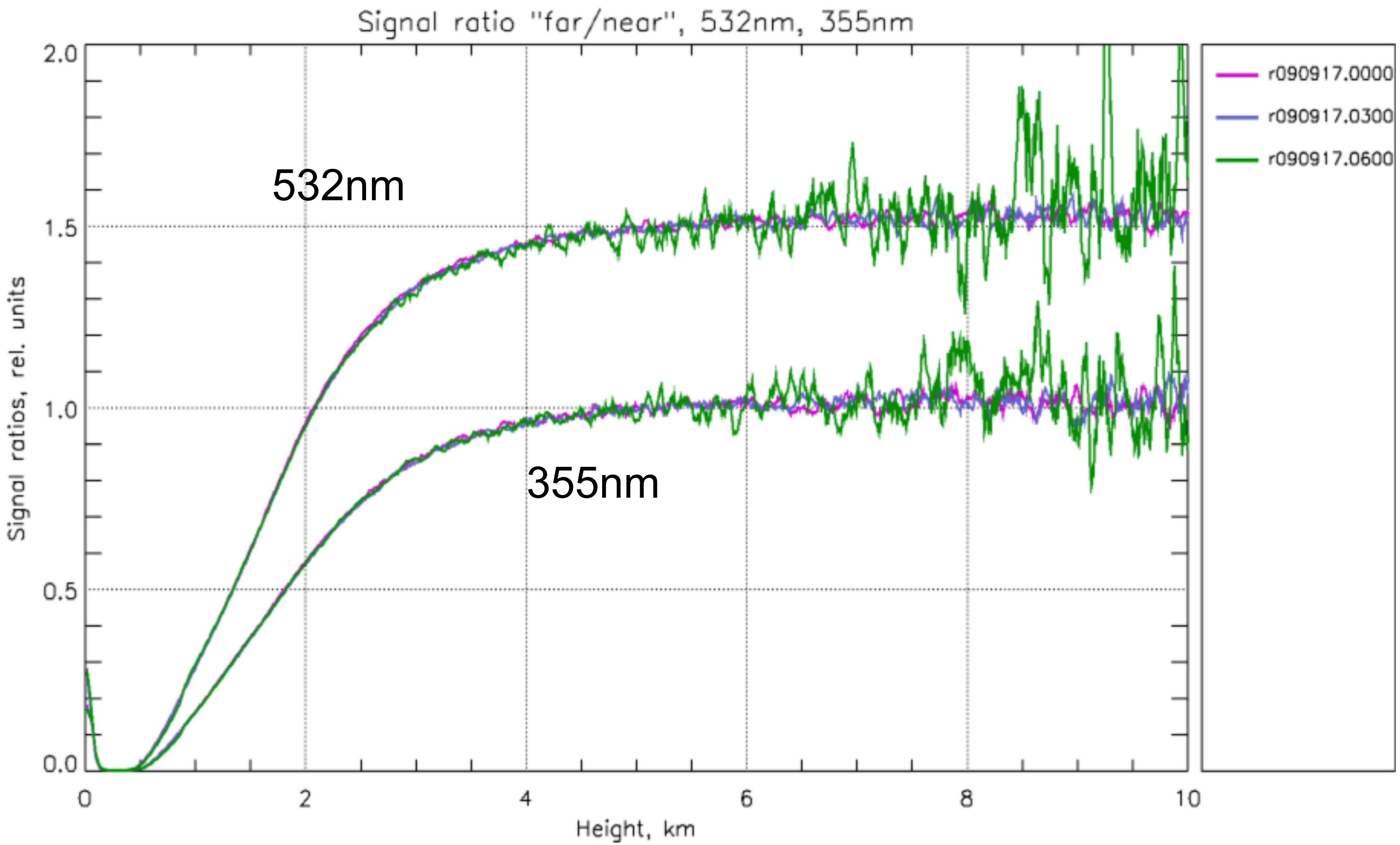

Overlap, 24h stability

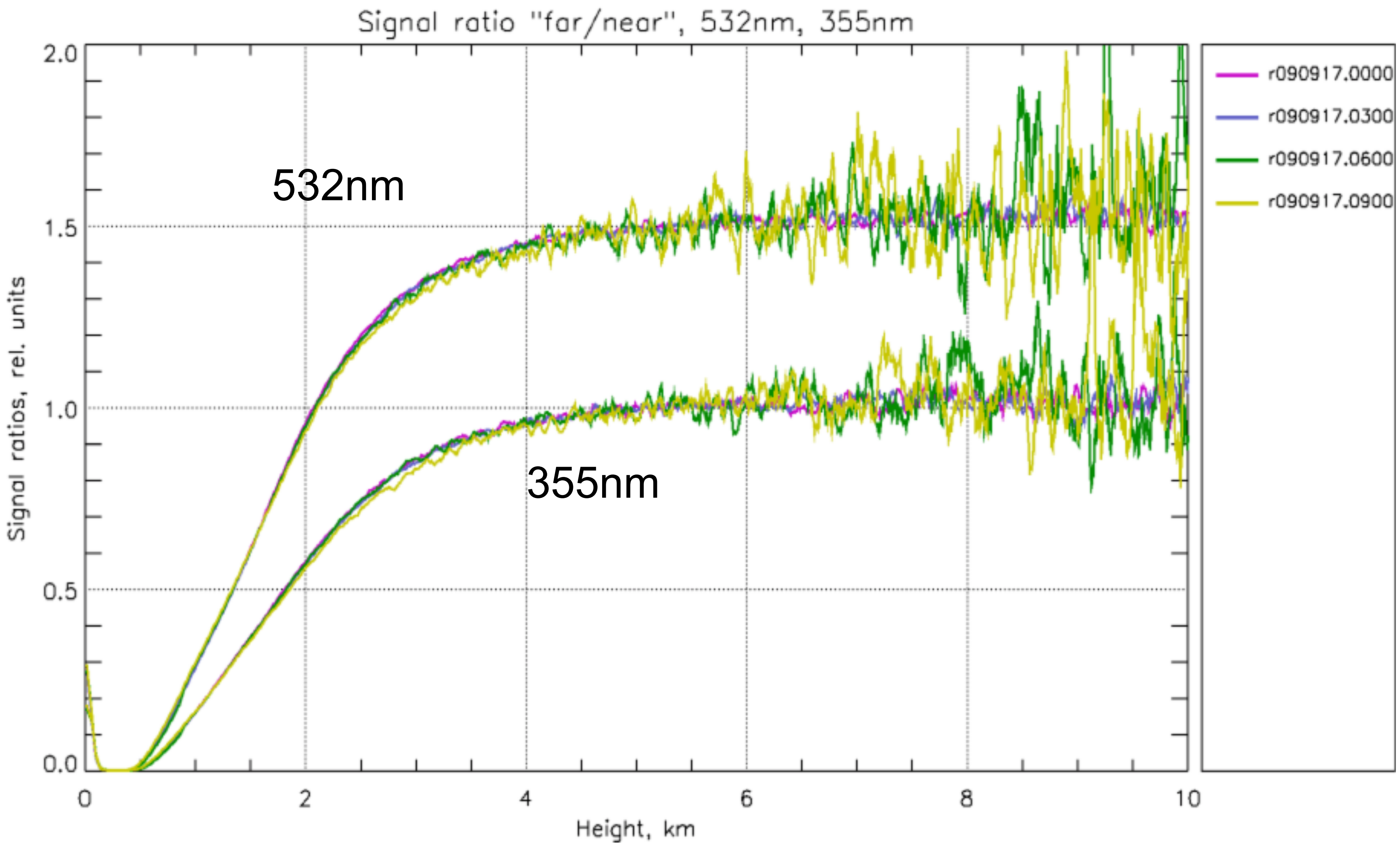

Max-Planck-Institut
für Meteorologie

Overlap, 24h stability

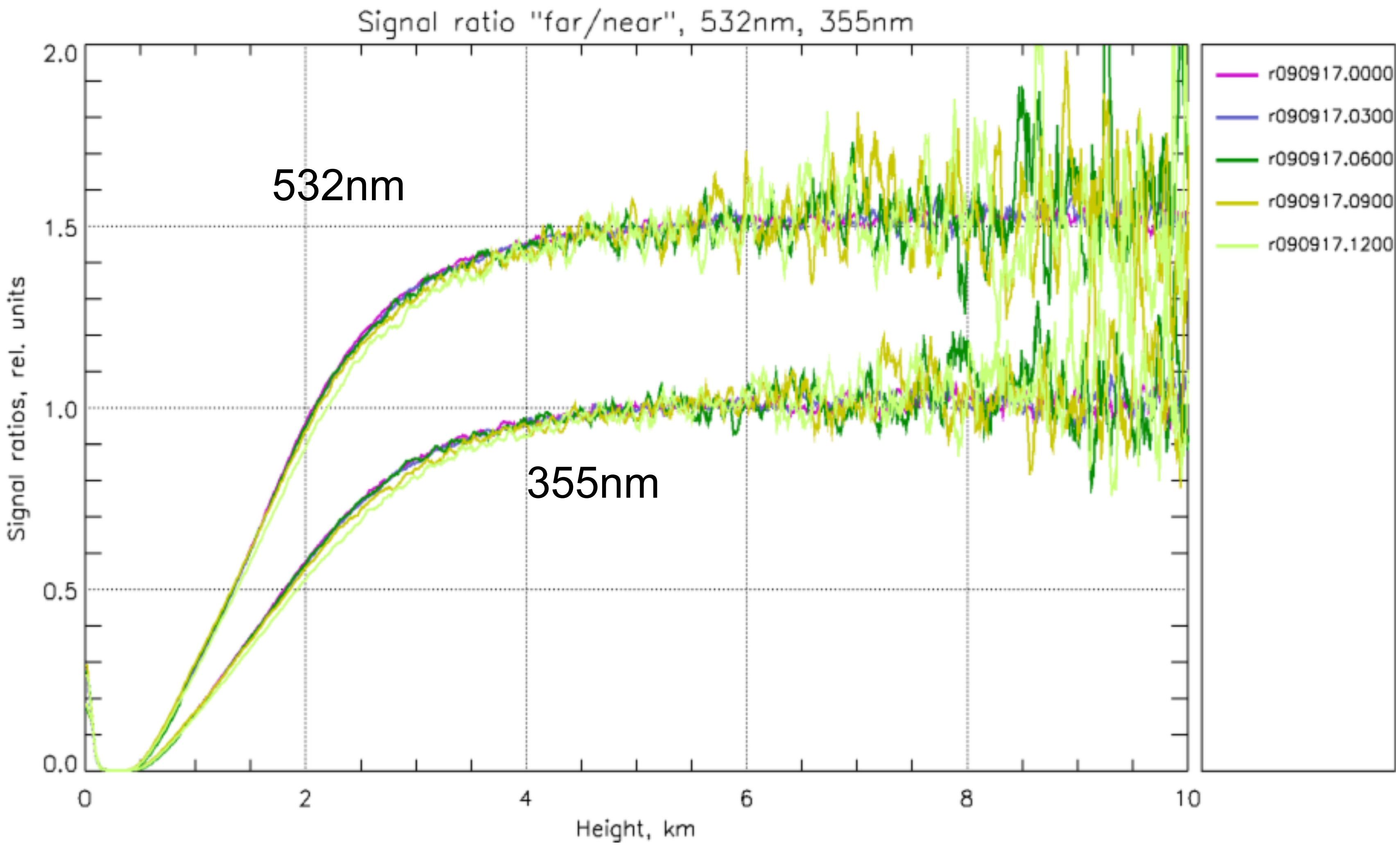

Overlap, 24h stability

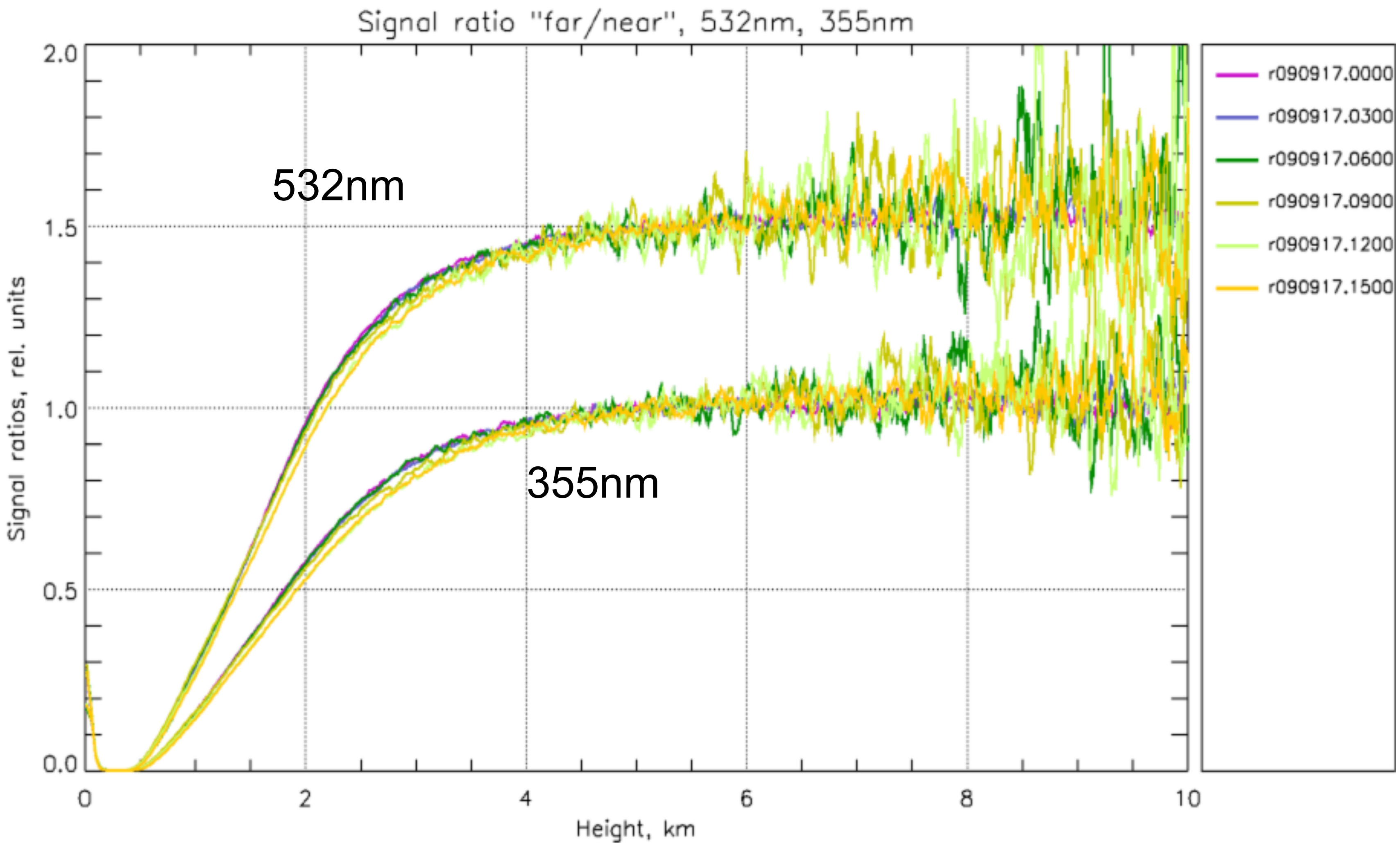

Overlap, 24h stability

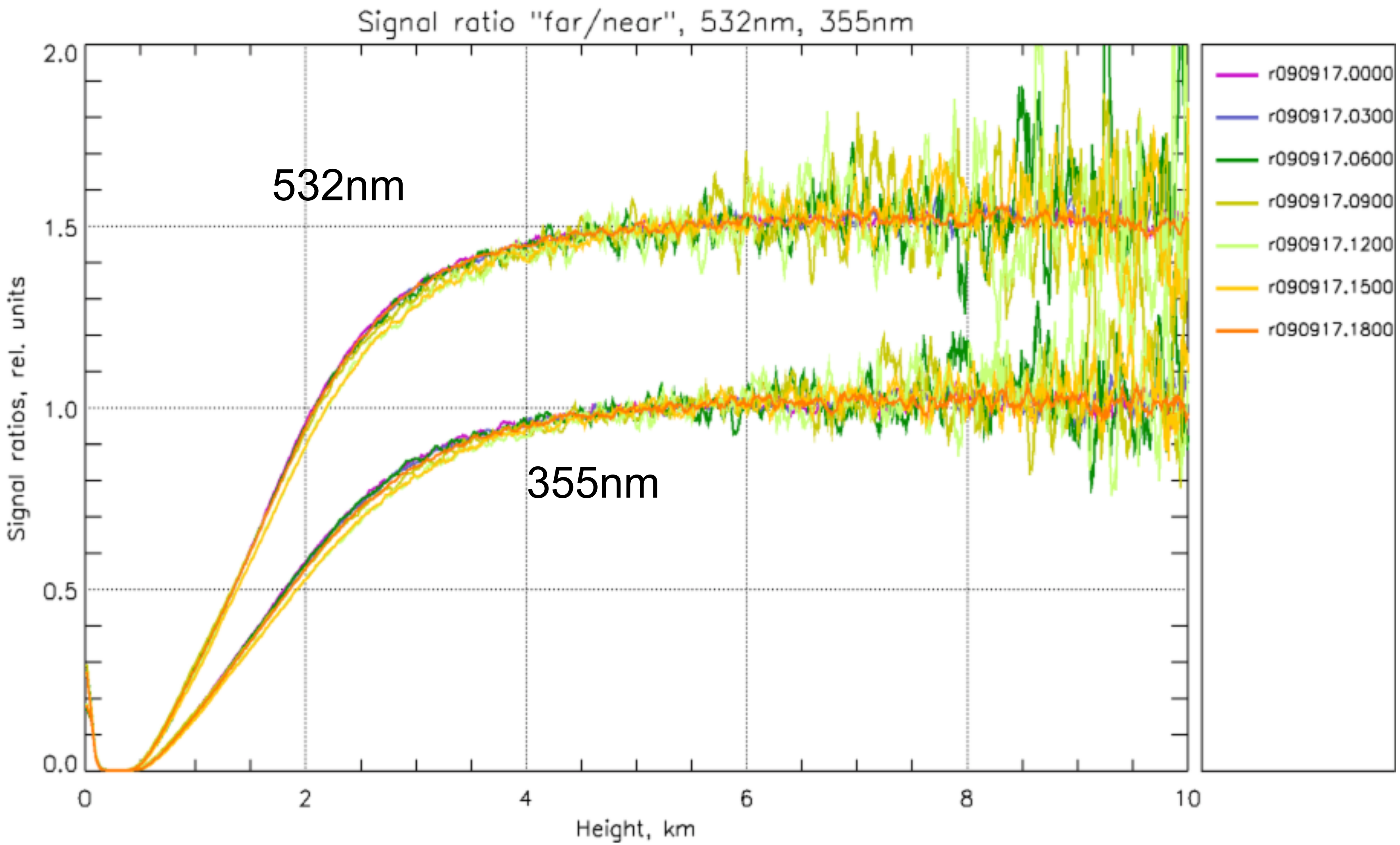

Overlap, 24h stability

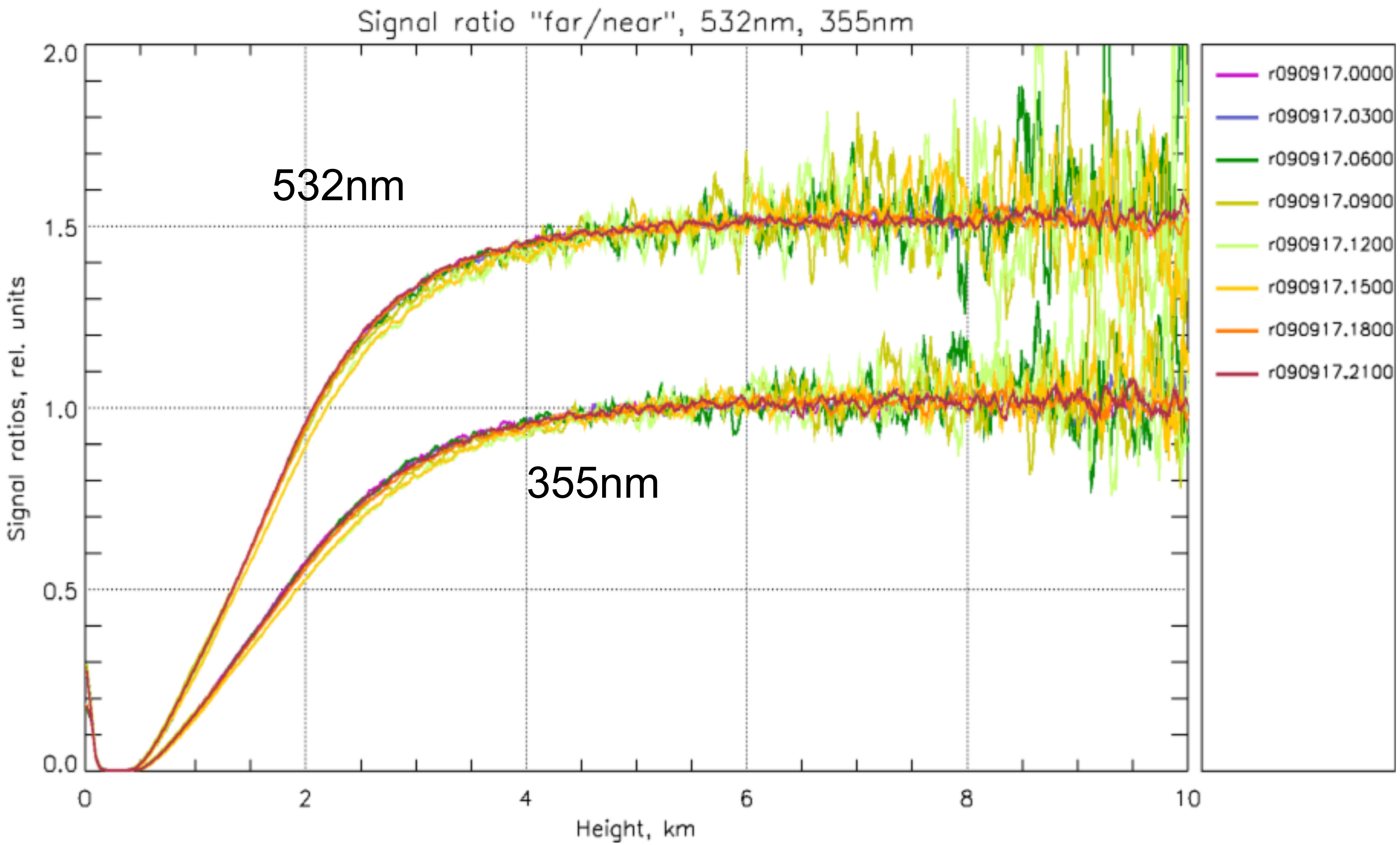

Overlap function, far range telescope, 532nm, 10.04.12

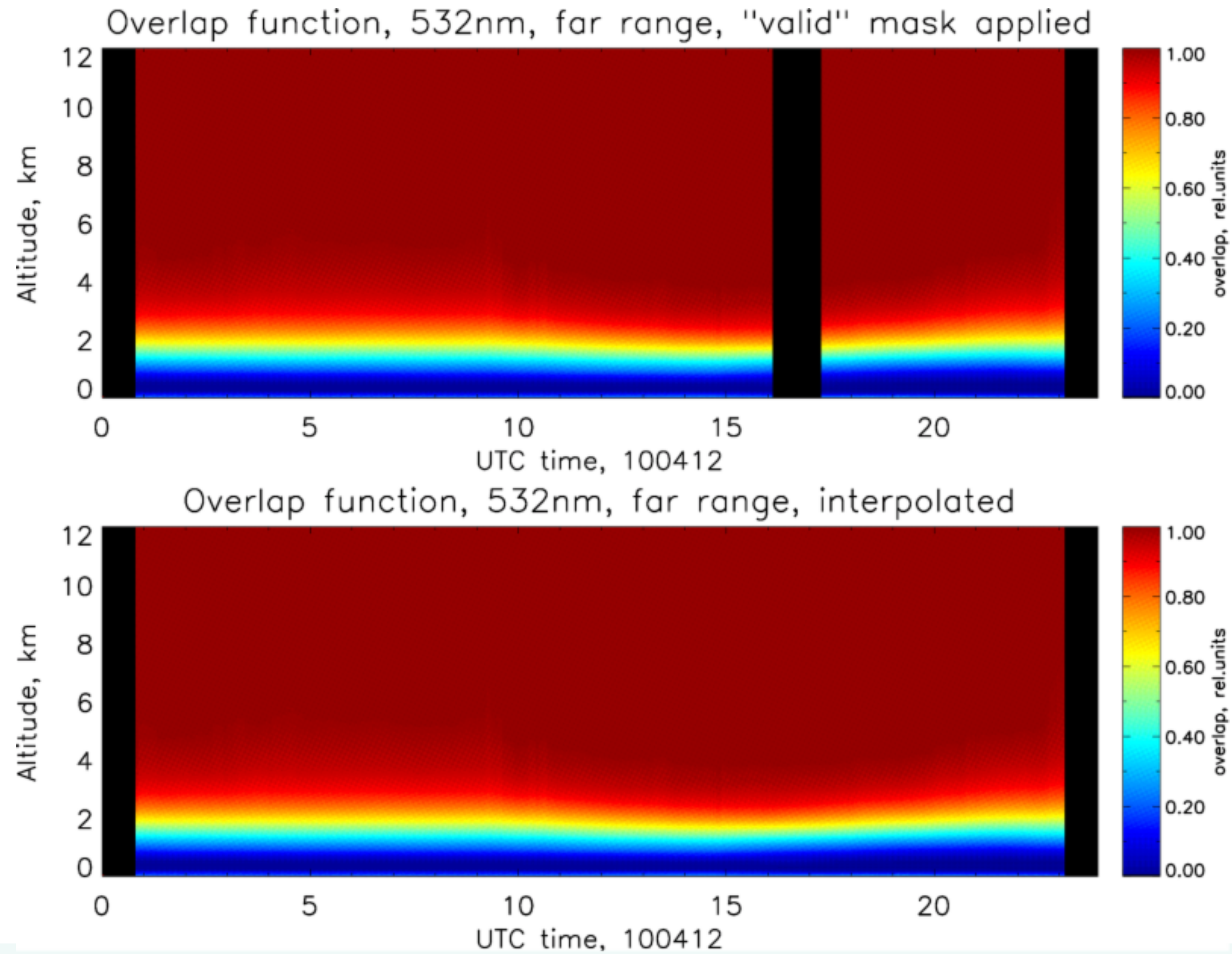

Overlap function, far range telescope, 532nm, 10.04.12

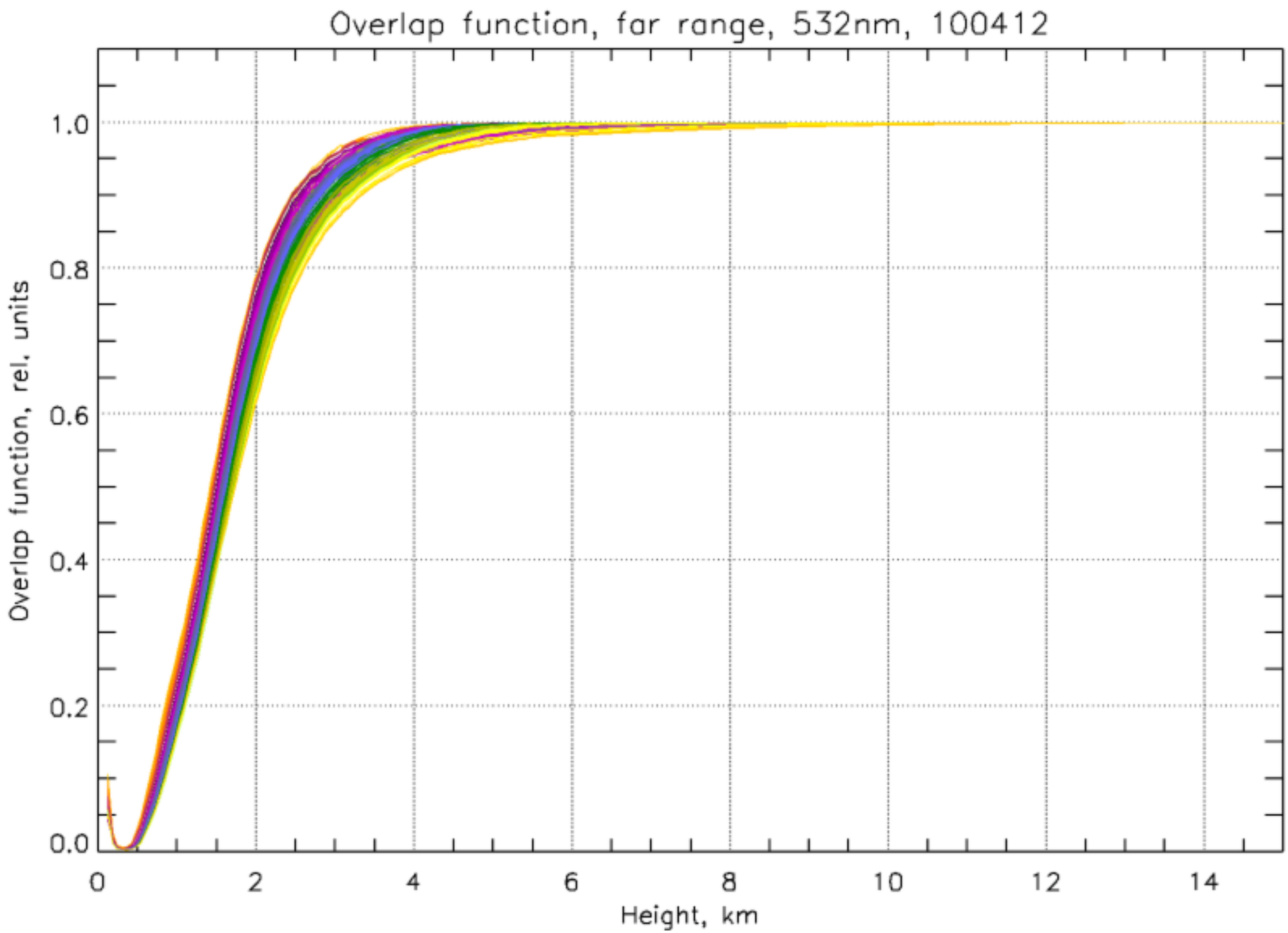

Max-Planck-Institut
für Meteorologie

resolution: 3 hours, 60m÷5km

Particle extinction, 532nm, near & far range

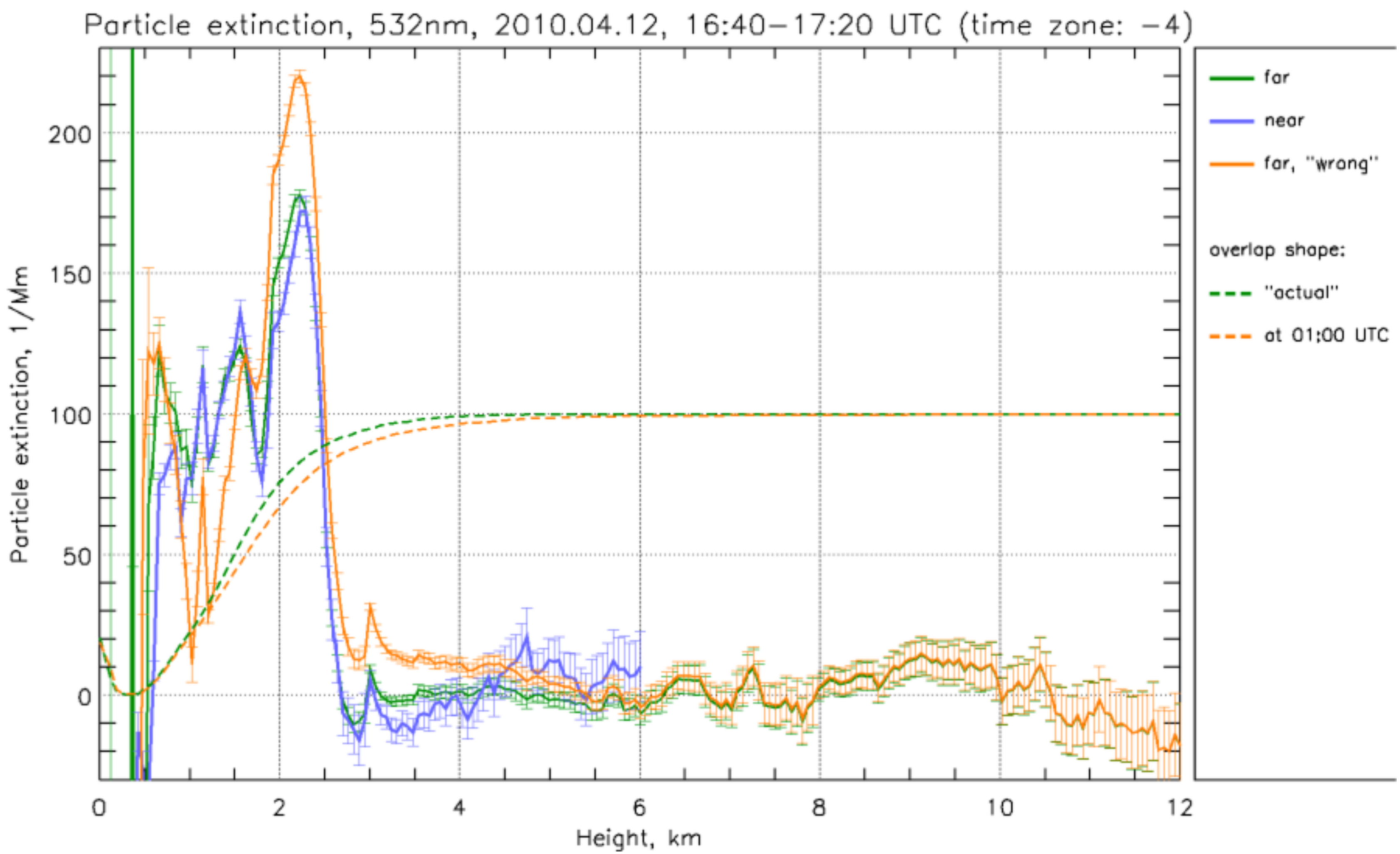

resolution: extinction: 40 minutes, 0.18÷3km
overlap: 3 hours, 60m÷5km

Particle extinction, 532nm, near & far range

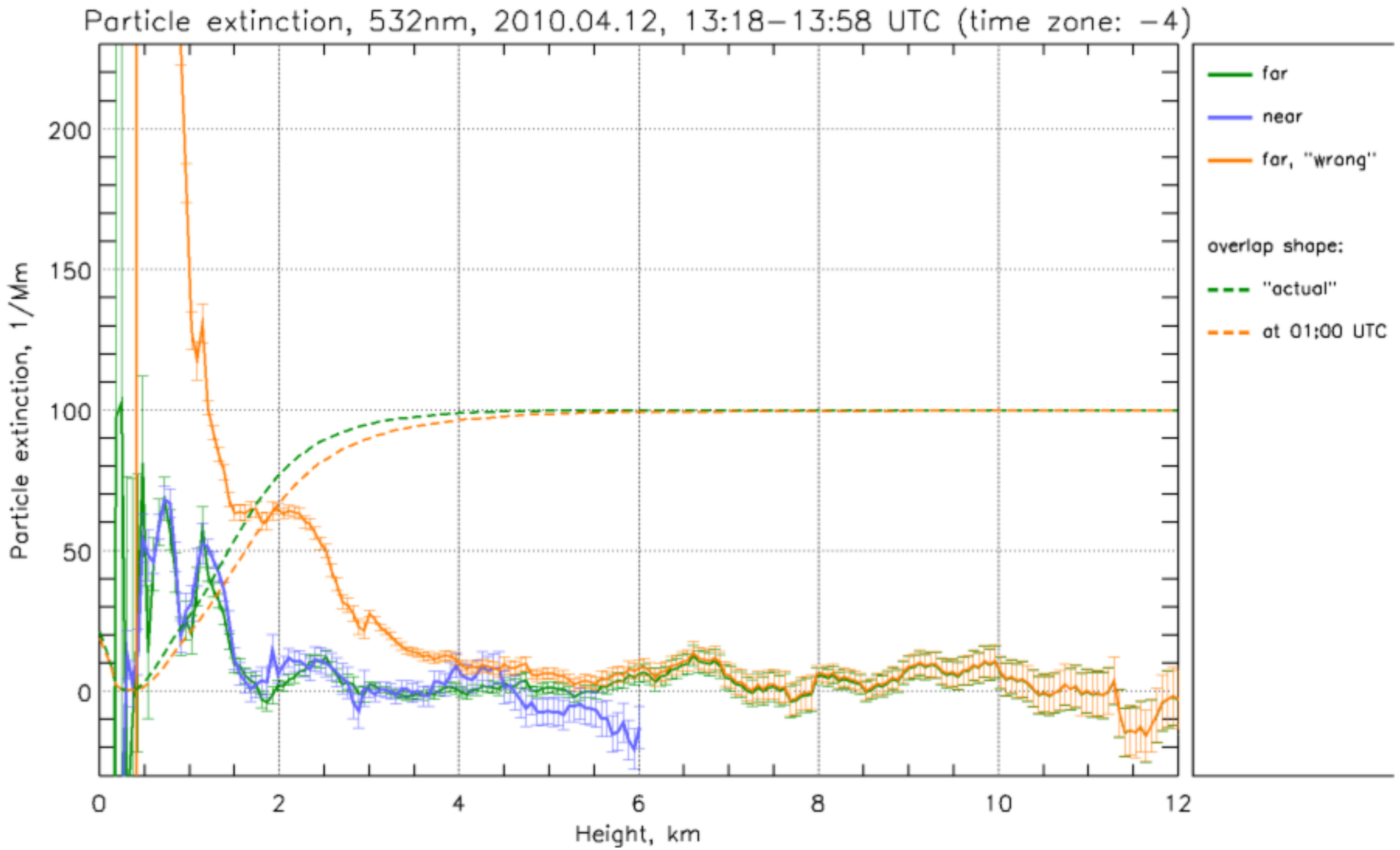

resolution: extinction: 40 minutes, 0.18÷3km
overlap: 3 hours, 60m÷5km

Overlap function, far range telescope, 532nm, 10.07.15

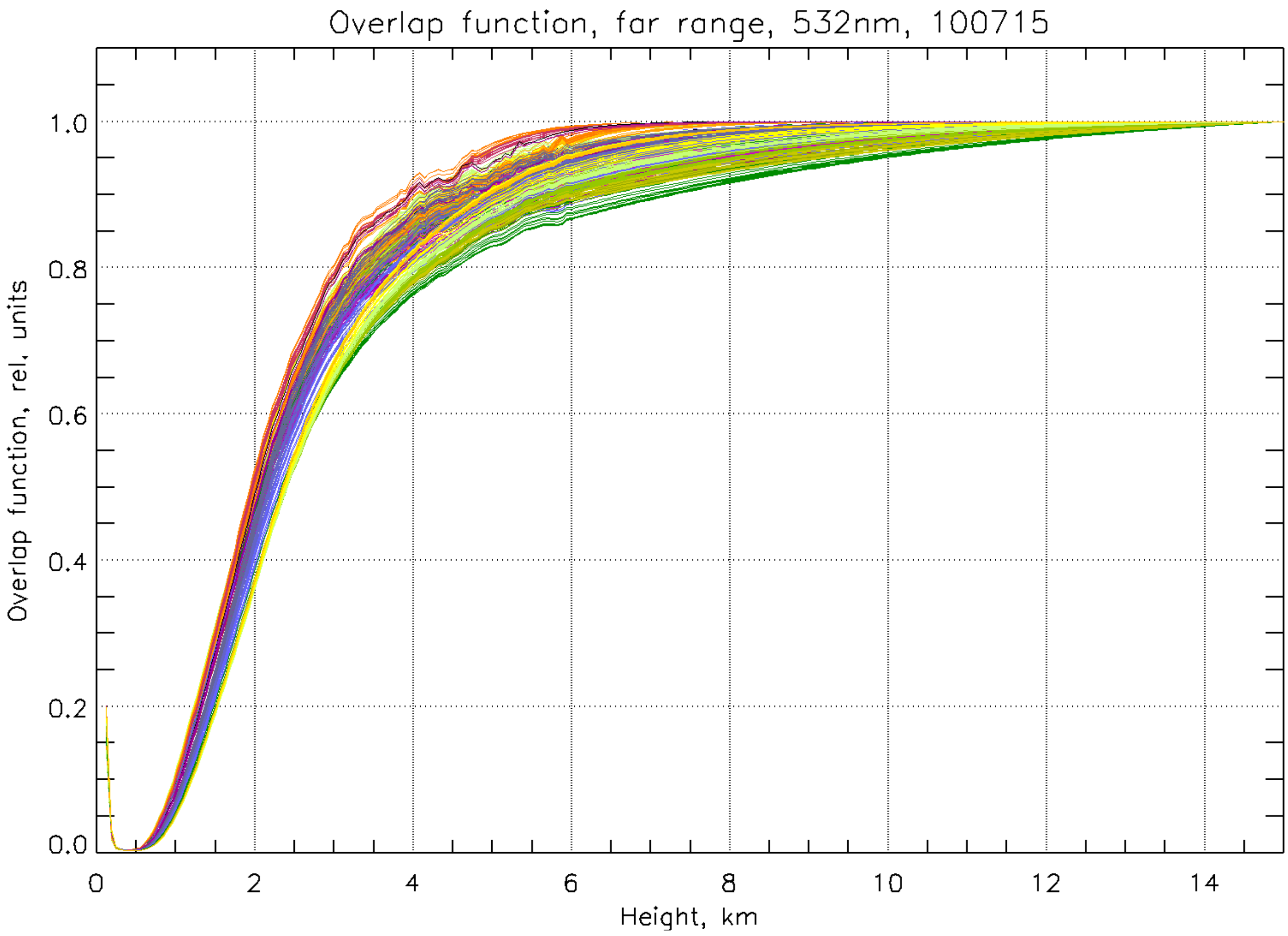

resolution: 3 hours, 60m÷5km

Raman lidar returns, 532nm, near & far range

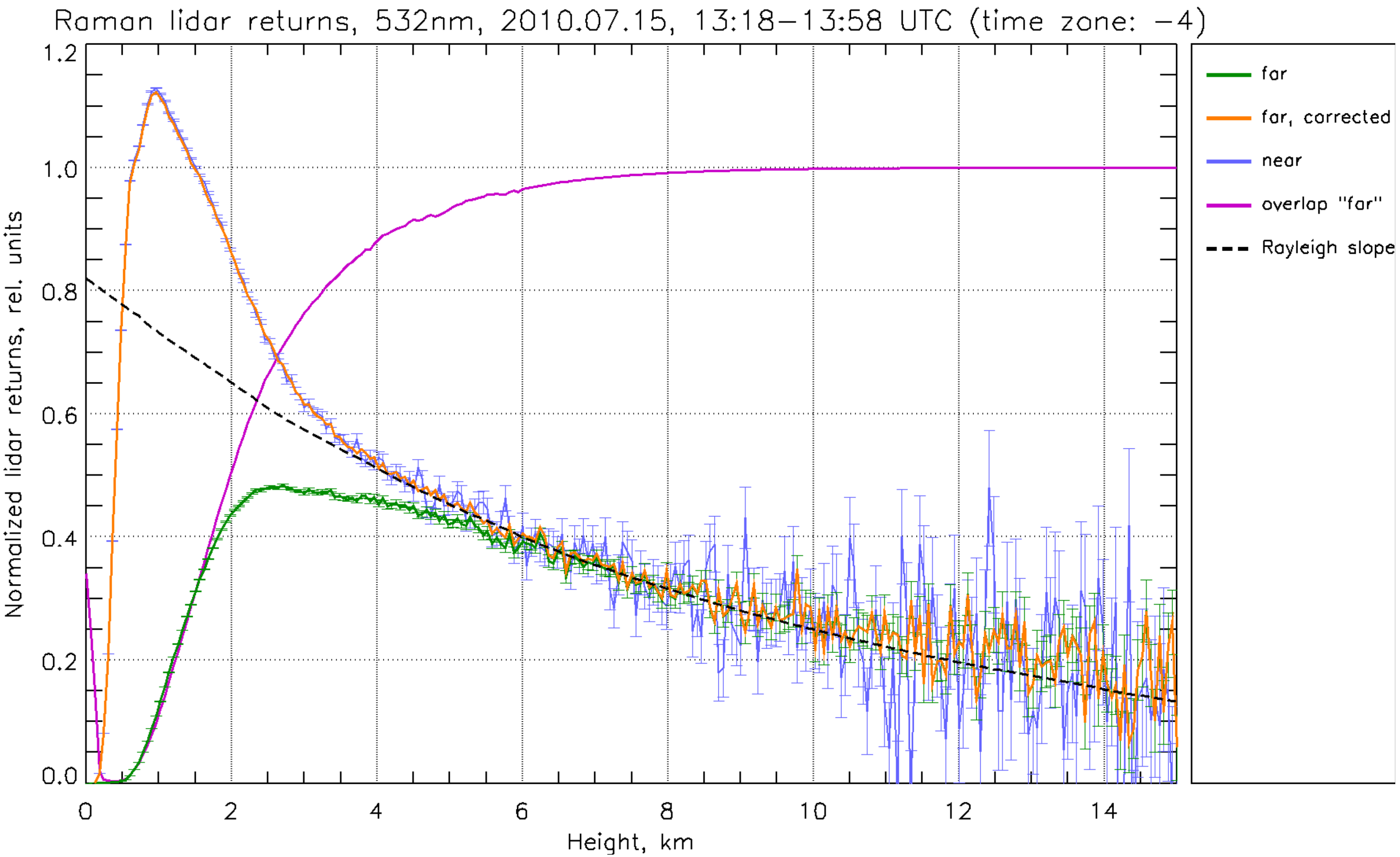

resolution: signals: 40 minutes, 60m

overlap: 3 hours, 60m÷5km

Particle extinction, 532nm, near & far range

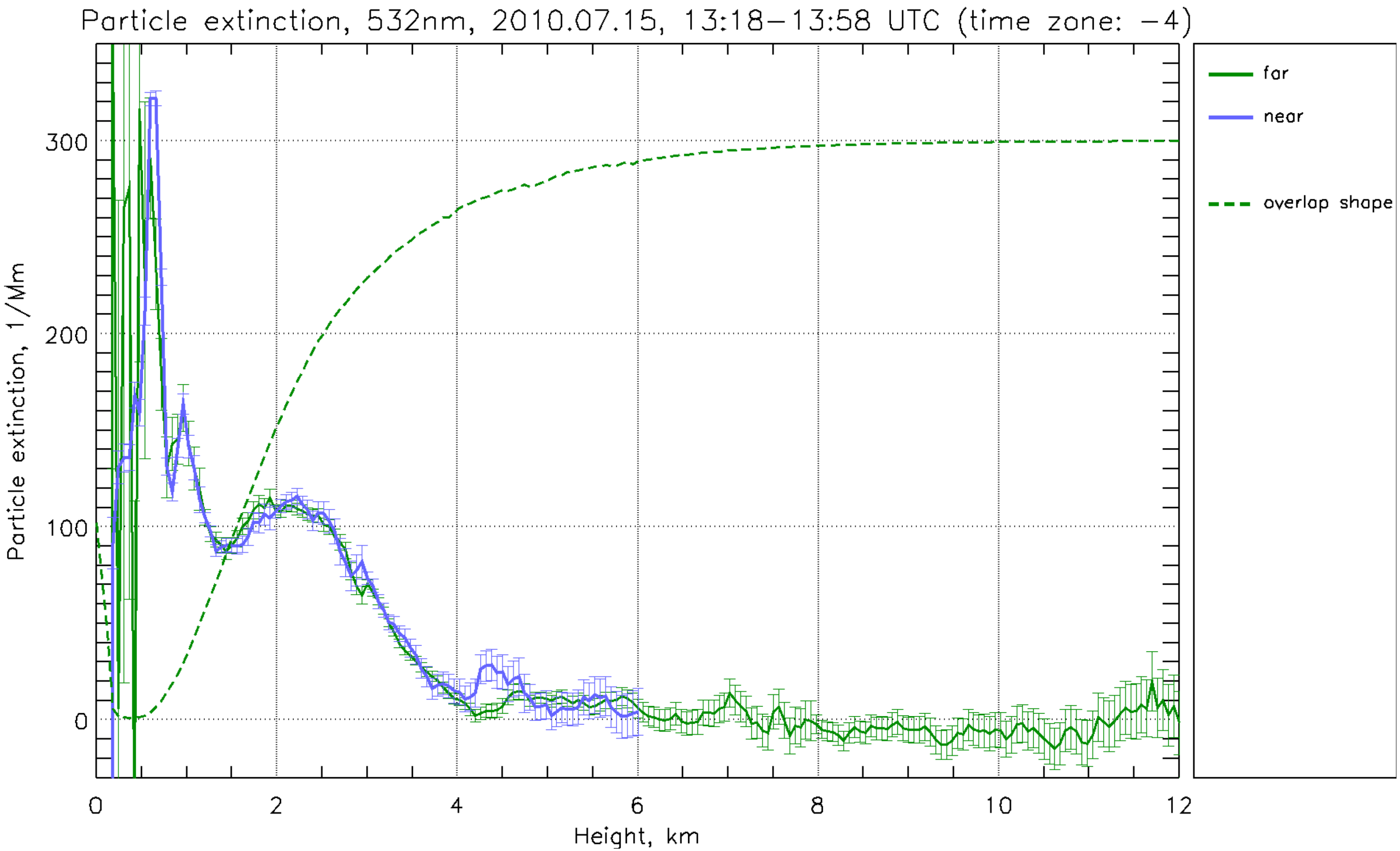

resolution: extinction: 40 minutes, 0.18÷3km

overlap: 3 hours, 60m÷5km

Particle extinction, 355nm, near & far range

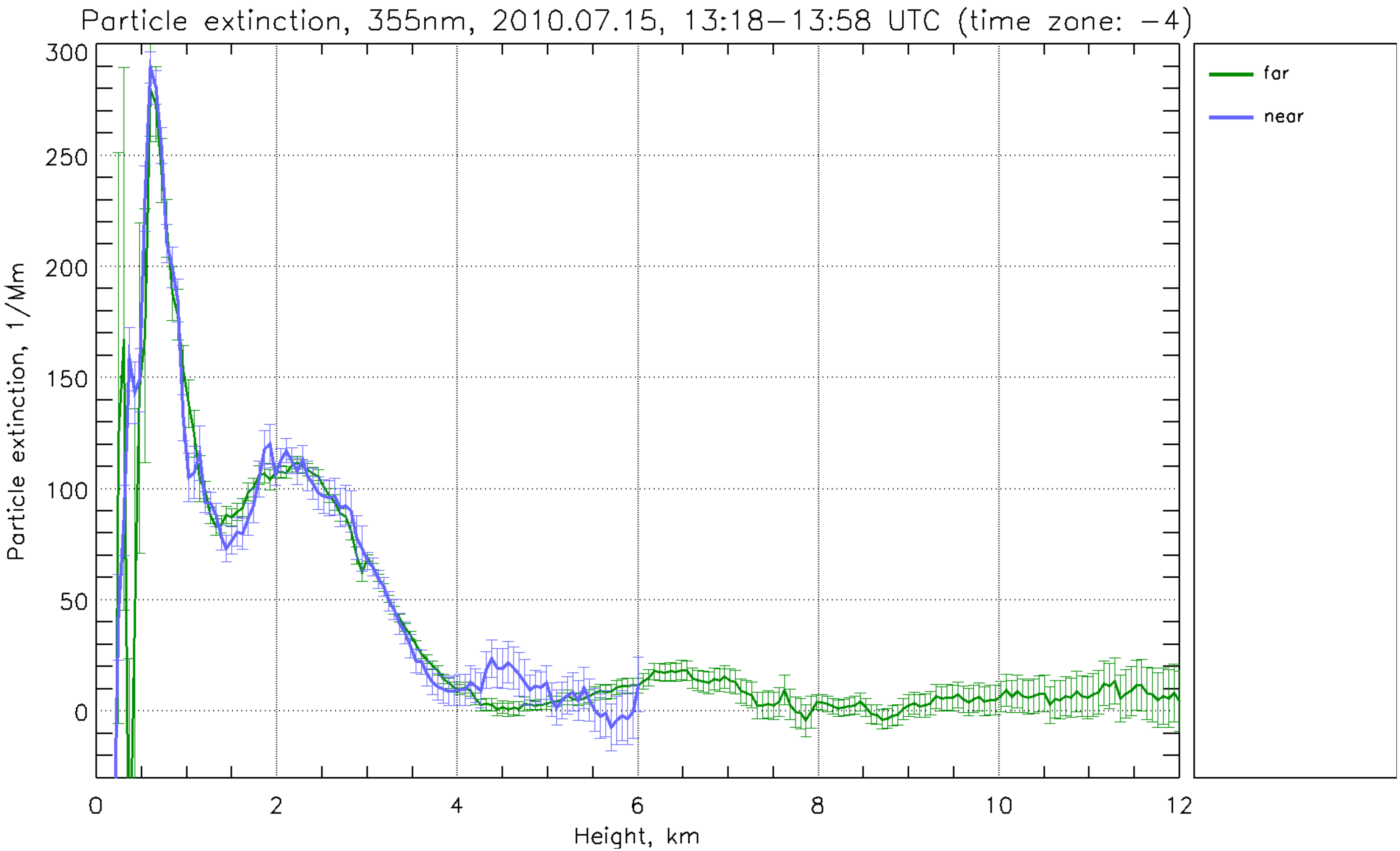

resolution: 40 minutes, 0.18÷3km

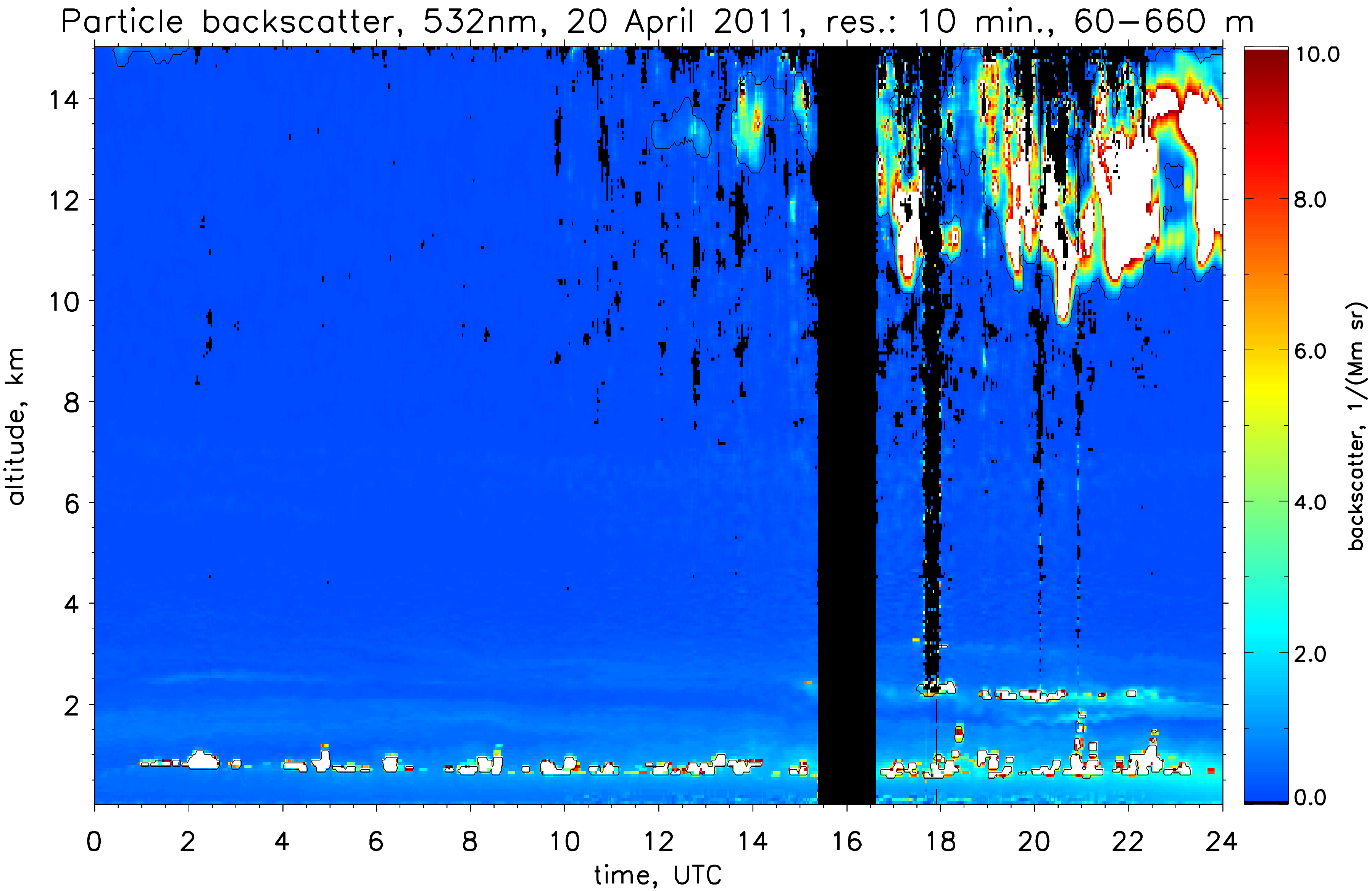
Particle backscatter, 532nm, 20 April 2011, res.: 10 min., 60–660 m
altitude, km
time, UTC
backscatter, 1/(Mm sr)
0 2 4 6 8 10 12 14 16 18 20 22 24
2 4 6 8 10 12 14
0.0 2.0 4.0 6.0 8.0 10.0

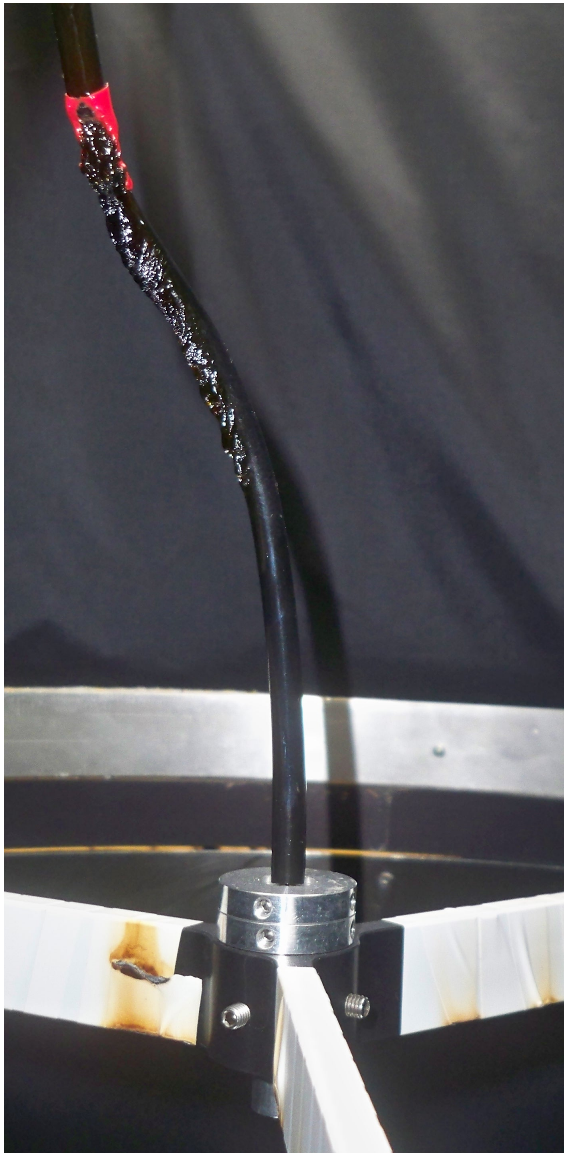

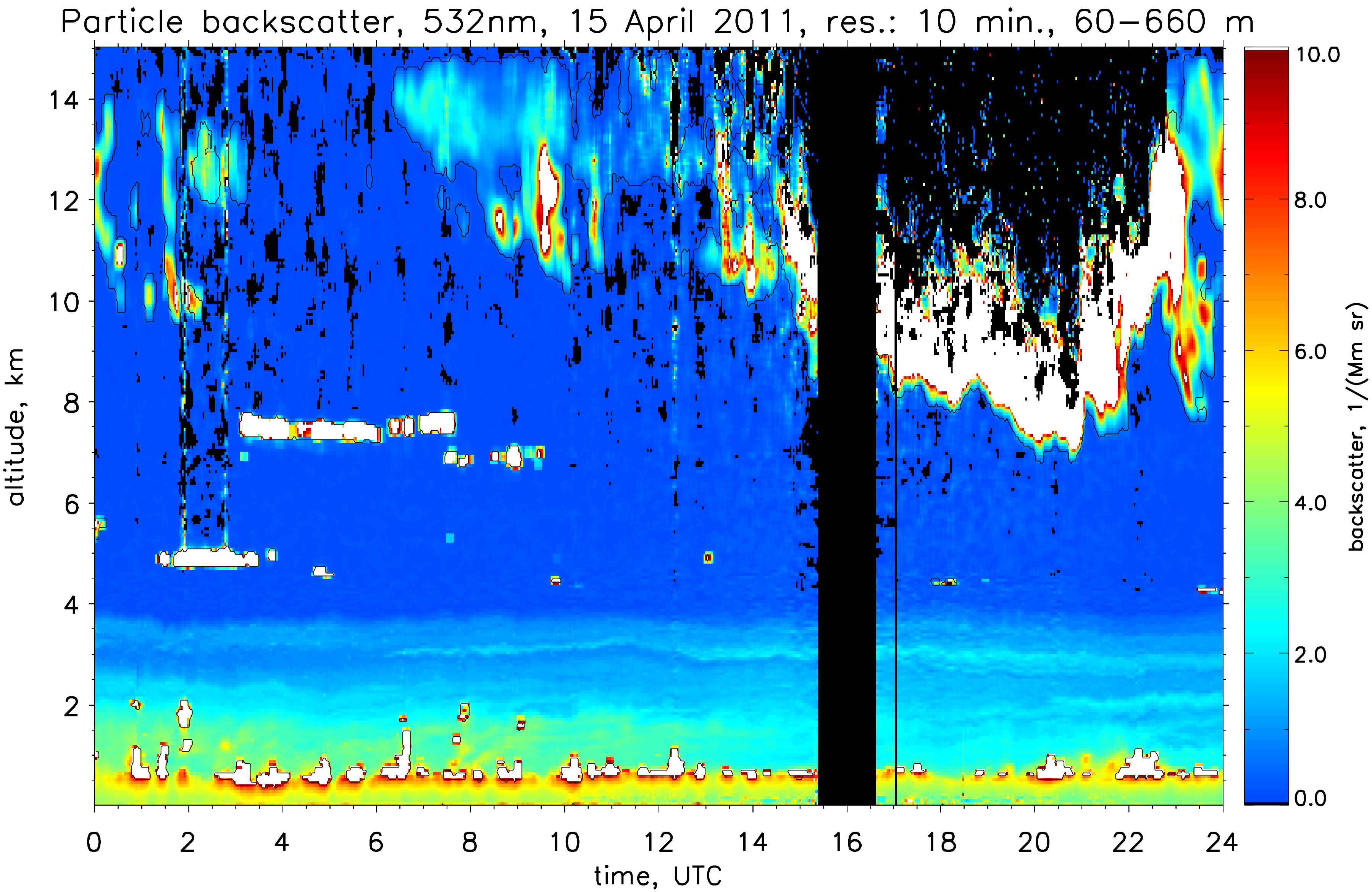
Particle backscatter, 532nm, 15 April 2011, res.: 10 min., 60–660 m
altitude, km
time, UTC
backscatter, 1/(Mm sr)
0 2 4 6 8 10 12 14 16 18 20 22 24
2 4 6 8 10 12 14
0.0 2.0 4.0 6.0 8.0 10.0

Particle backscatter, 355nm, 15 April 2011, res.: 10 min., 60–660 m

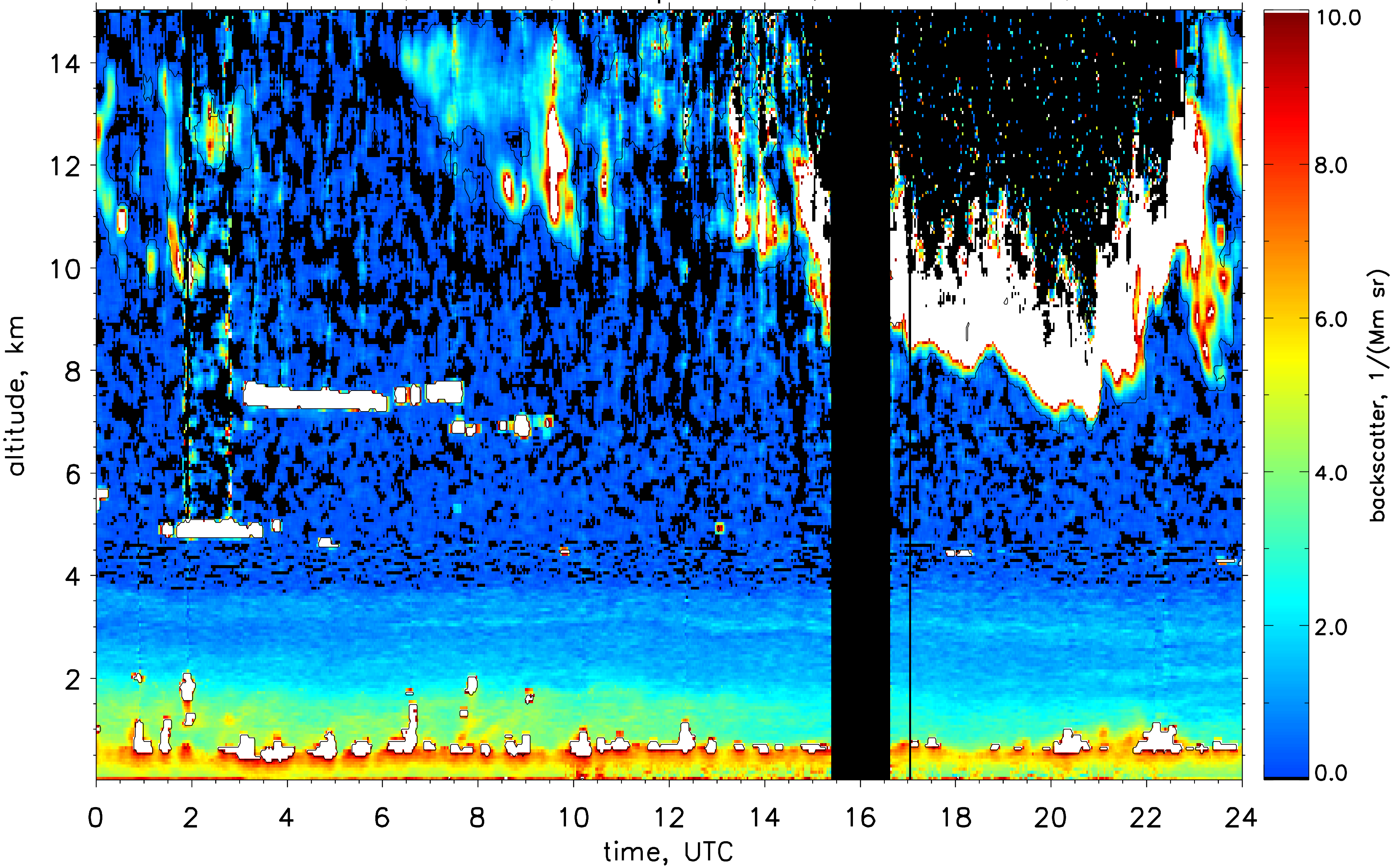

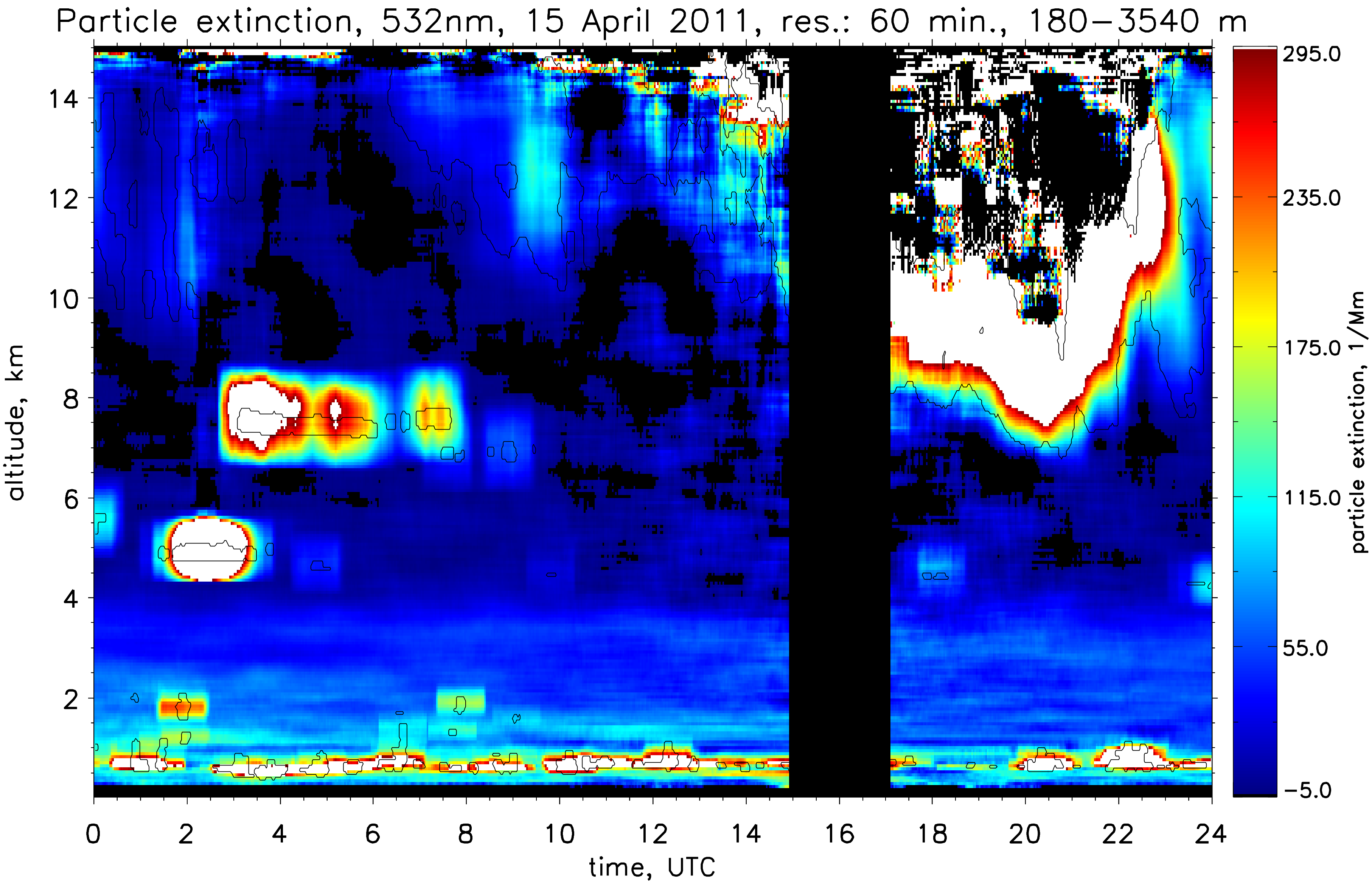

Max-Planck-Institut
für Meteorologie

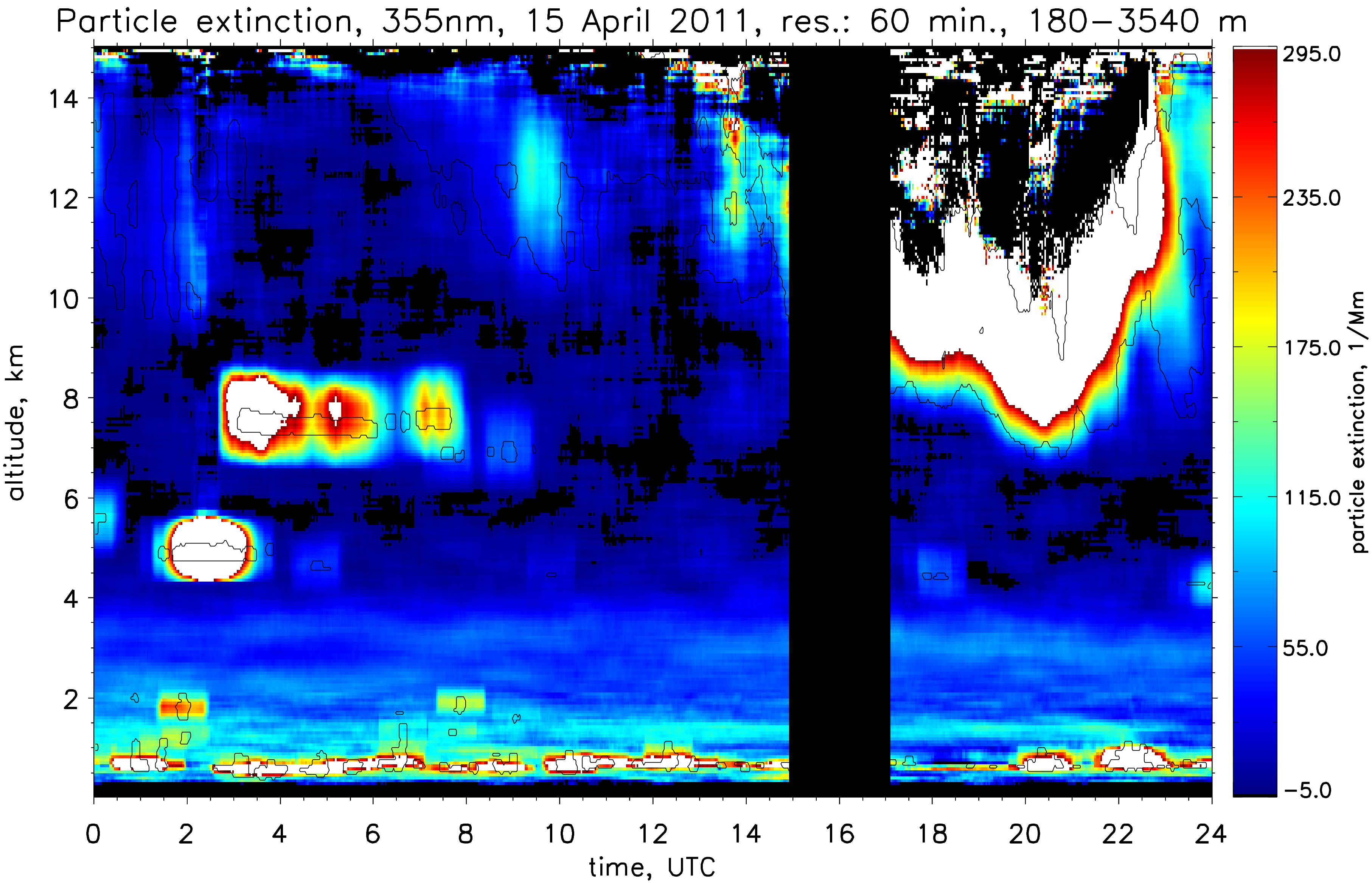
Particle extinction, 355nm, 15 April 2011, res.: 60 min., 180−3540 m
altitude, km
14
12
10
8
6
4
2
0
2
4
6
8
10
12
14
16
18
20
22
24
time, UTC
295.0
235.0
175.0
115.0
55.0
−5.0
particle extinction, 1/Mm

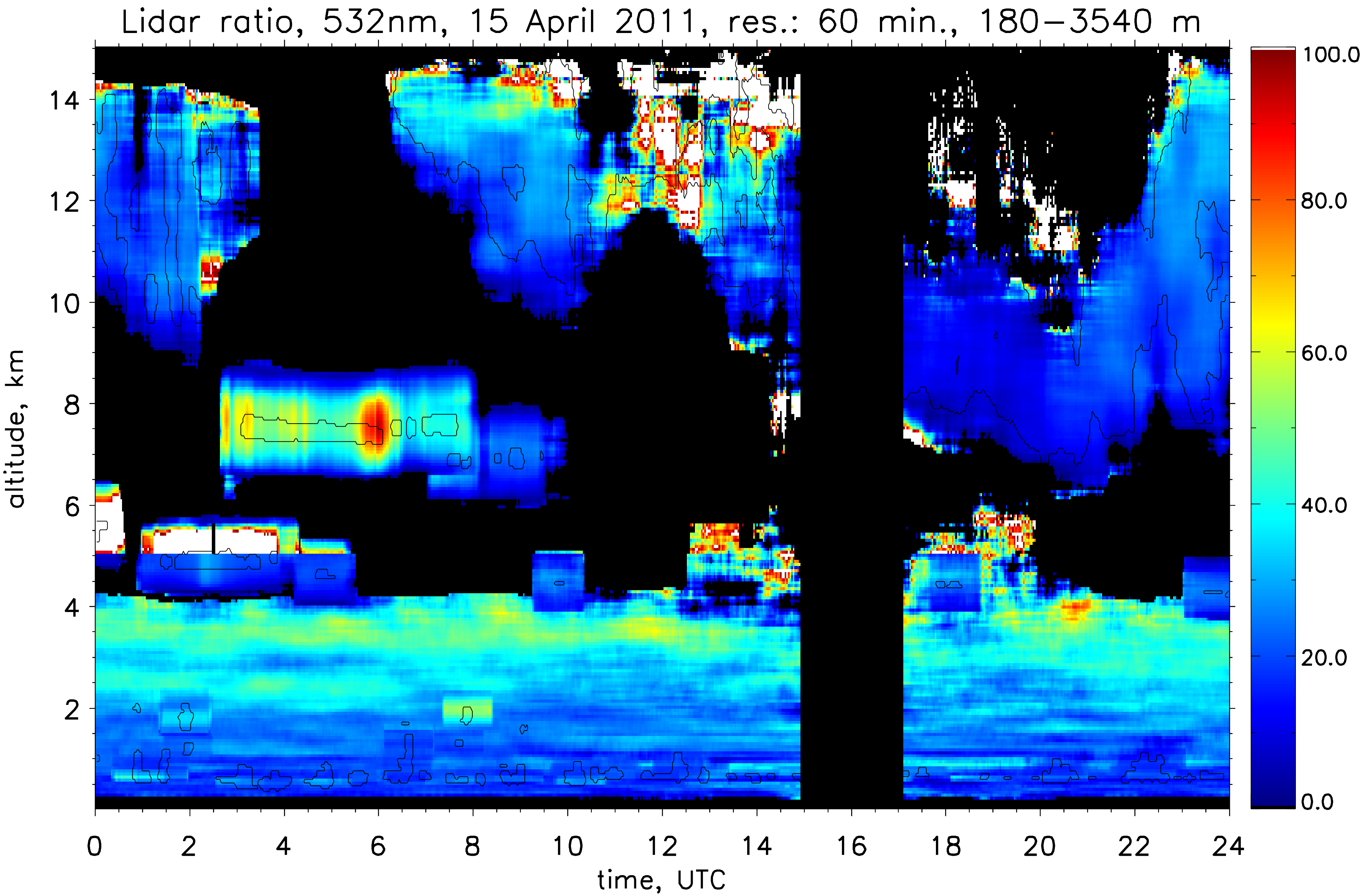

Lidar ratio, 532nm, 15 April 2011, res.: 60 min., 180−3540 m
altitude, km
time, UTC
lidar ratio, sr
0 2 4 6 8 10 12 14 16 18 20 22 24
2 4 6 8 10 12 14
0.0 20.0 40.0 60.0 80.0 100.0

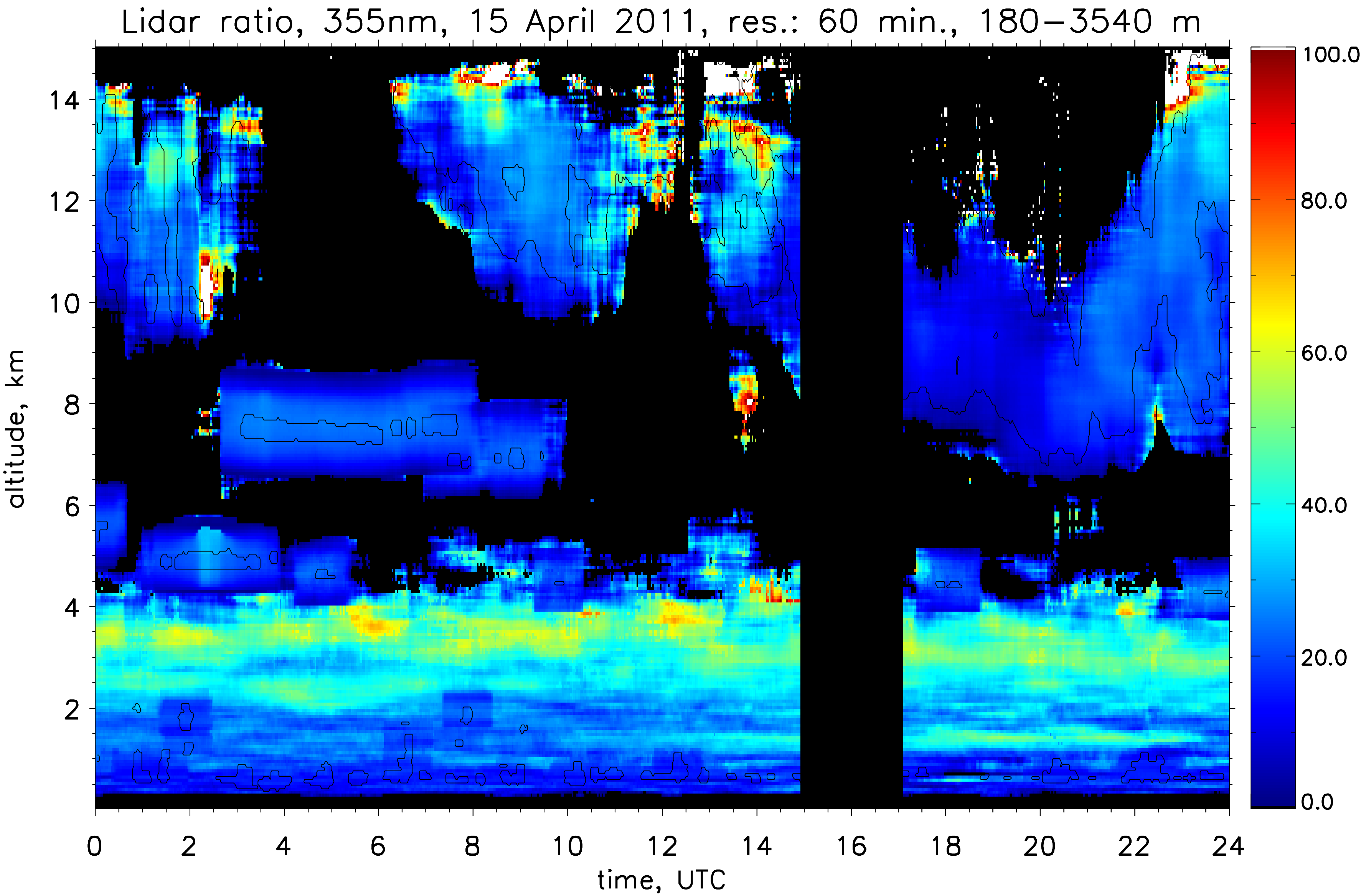
Lidar ratio, 355nm, 15 April 2011, res.: 60 min., 180−3540 m
altitude, km
time, UTC
lidar ratio, sr
0 2 4 6 8 10 12 14 16 18 20 22 24
2 4 6 8 10 12 14
0.0 20.0 40.0 60.0 80.0 100.0

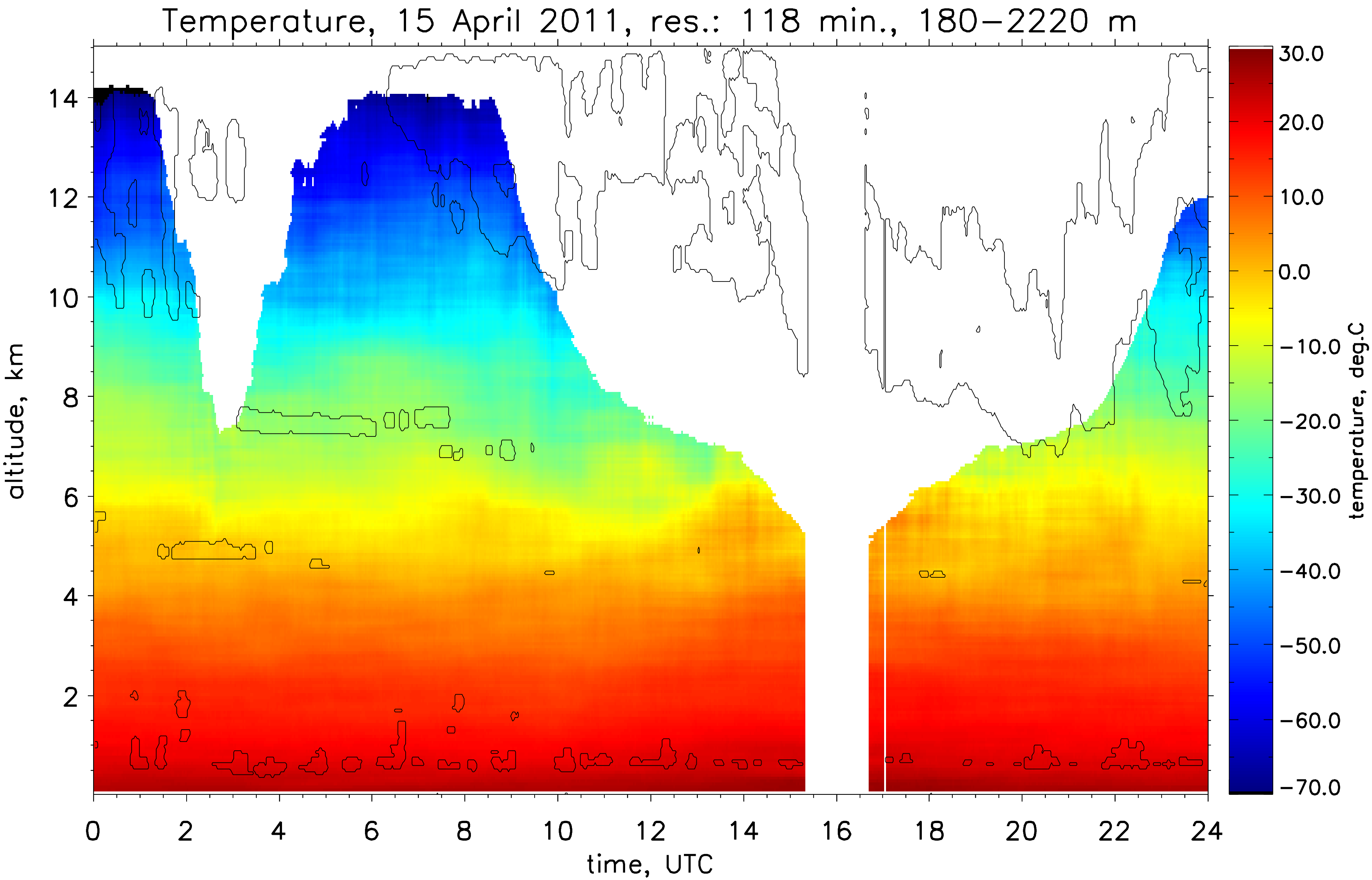
Temperature, 15 April 2011, res.: 118 min., 180−2220 m
altitude, km
14
12
10
8
6
4
2
0
2
4
6
8
10
12
14
16
18
20
22
24
time, UTC
30.0
20.0
10.0
0.0
−10.0
−20.0
−30.0
−40.0
−50.0
−60.0
−70.0
temperature, deg.C

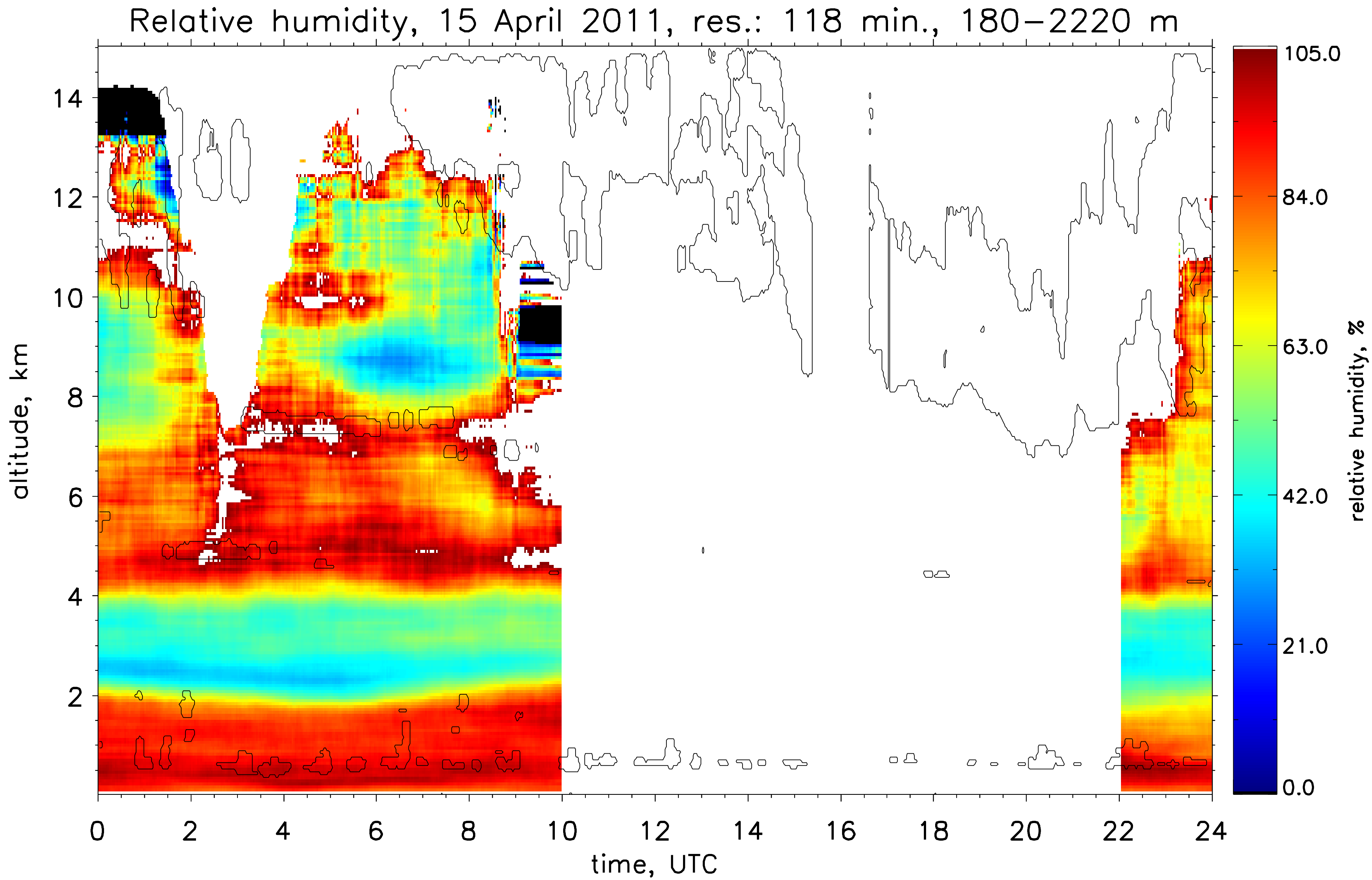

Max-Planck-Institut
für Meteorologie

Thank you!